

**PRELIMINARY UPDATED GROUNDWATER FLOW AND  
TRANSPORT MODELING REPORT FOR ROXBORO STEAM  
ELECTRIC PLANT, SEMORA, NC**

**November 2018**

Revised January 2019

Prepared for  
Duke Energy Progress, LLC

Investigators

Lawrence C. Murdoch, Ph.D. – FRx, Inc.

Rong Yu, Ph.D. – SynTerra Corporation

Regina Graziano, M.S. – SynTerra Corporation

Ronald W. Falta, Ph.D. – Falta Environmental LLC

## TABLE OF CONTENTS

<b>EXECUTIVE SUMMARY .....</b>	<b>ES-1</b>
<b>1.0 INTRODUCTION.....</b>	<b>1</b>
1.1 General Setting and Background .....	1
1.2 Objectives .....	3
<b>2.0 CONCEPTUAL MODEL.....</b>	<b>5</b>
2.1 Aquifer System Framework .....	5
2.2 Groundwater Flow System .....	6
2.3 Hydrologic Boundaries .....	10
2.4 Hydraulic Boundaries .....	10
2.5 Sources and Sinks .....	10
2.6 Water Budget .....	11
2.7 Modeled Constituents of Interest .....	12
2.8 Constituent Transport.....	12
<b>3.0 COMPUTER MODEL .....</b>	<b>14</b>
3.1 Model Selection .....	14
3.2 Model Description .....	14
<b>4.0 GROUNDWATER FLOW AND TRANSPORT MODEL CONSTRUCTION.....</b>	<b>15</b>
4.1 Model Domain and Grid .....	15
4.2 Hydraulic Parameters.....	17
4.3 Flow Model Boundary Conditions.....	17
4.4 Flow Model Sources and Sinks.....	18
4.5 Flow Model Calibration Targets.....	21
4.6 Transport Model Parameters.....	22
4.7 Transport Model Boundary Conditions .....	24
4.8 Transport Model Sources and Sinks .....	24
4.9 Transport Model Calibration Targets.....	25
<b>5.0 MODEL CALIBRATION TO CURRENT CONDITIONS.....</b>	<b>26</b>
5.1 Flow Model.....	26
5.2 Flow Model Sensitivity Analysis.....	29
5.3 Potential Receptor Wells and the Ambient Groundwater Flow System.....	30
5.4 Transport Model Calibration.....	30
5.5 Transport Model Sensitivity .....	31
5.6 Result of the Transport Simulation.....	32

**6.0 PREDICTIVE SIMULATIONS OF CLOSURE ACTION SCENARIOS ..... 37**

6.1 Interim Period with Ash Basin Pond Decanted ..... 39

6.2 Excavation Scenarios ..... 40

6.3 Final Cover Scenario..... 47

6.4 Hybrid Design Scenario ..... 50

6.5 Conclusions..... 53

**7.0 REFERENCES ..... 60**

**LIST OF TABLES**

- Table 1. Comparison of observed and computed heads (in ft.) for the calibrated flow model.
- Table 2. Calibrated hydraulic parameters.
- Table 3. Recharge in different zones in the model.
- Table 4. Flow parameter sensitivity analysis.
- Table 5. Comparison of observed and simulated boron concentrations in monitoring wells.
- Table 6. Distribution coefficients for boron.
- Table 7. Sensitivity of the simulated boron concentration to different values of  $K_d$ .

## LIST OF FIGURES

- Figure ES-1. Simulated Boron Concentrations East Ash Basin – Fractured Bedrock - Complete Excavation, Final Cover System, and Hybrid Simulations
- Figure ES-2. Simulated Boron Concentrations West Ash Basin – Fractured Bedrock - Complete Excavation, Final Cover System, and Hybrid Simulations
- Figure ES-3. Boron Time vs. Concentration Plots East Ash Basin – Fractured Bedrock - Excavation, Final Cover System, and Hybrid Simulations
- Figure ES-4. Boron Time vs. Concentration Plots West Ash Basin – Fractured Bedrock - Excavation, Final Cover System, and Hybrid Simulations
- Figure 1. Site location map of the Roxboro Steam Electric Plant, Person County, NC.
- Figure 2. Air photo of the Roxboro Steam Electric Plant showing ash basins (orange) and hydrologic features and boundary of model region (yellow).
- Figure 3. Fence diagram of the 3D hydrostratigraphic model (Solids) used to generate hydrostratigraphy.
- Figure 4. Computational grid used in the model, showing the ash basin.
- Figure 5 (a-d). Hydraulic conductivity (ft./d) distribution.
- Figure 6 (a-d). Distribution of recharge flux used in the model during 1966-2020.
- Figure 7. Surface water features in the vicinity of the Roxboro Plant.
- Figure 8. Assumed distribution of concentration of boron ( $\mu\text{g/L}$ ) in 2017.
- Figure 9. Boron sources created by concentrations ( $\mu\text{g/L}$ ) in recharge.
- Figure 10. Hydraulic conductivity of the dam in the West Ash Basin and East Ash Basin.
- Figure 11. Comparison of observed and computed heads from the calibrated steady state flow model.
- Figure 12. Simulated steady state hydraulic head distribution in the vicinity of the ash basins in the Transition Zone (layer 13).

Figure 13. Simulated local groundwater flow systems showing hydraulic heads in the vicinity of the East Ash Basin and West Ash Basin.

Figure 14. Hydraulic conductivity measurements from slug tests in ash from ash basins in North Carolina, and from the Roxboro site.

Figure 15. Simulated steady state hydraulic head distribution (feet above NAVD88) in the Transition Zone (layer 13) with inferred groundwater flow directions (orange arrows).

Figure 16. Water balance for East Ash Basin (EAB) and West Ash Basin (WAB).

Figure 17. Simulated current boron distribution (700 and 4000  $\mu\text{g/L}$ ) in the Transition Zone (layer 13) and shallow rock (layer 15) in 2017.

Figure 18: Simulated hydraulic head distribution (feet above NAVD88) in the transition zone (layer 13) during the interim period.

Figure 19. Simulated boron concentrations ( $\mu\text{g/L}$ ) during the interim period 2020-2027 in shallow fractured rock (layer 15).

Figure 20. Configuration of features used to represent the Excavation with Landfill scenario in the model (a) and simulated hydraulic heads (b).

Figure 21. Distribution of boron concentrations ( $\mu\text{g/L}$ ) during the Excavation with Landfill scenario at representative times in the Transition Zone (layer 13).

Figure 22. Distribution of boron concentrations ( $\mu\text{g/L}$ ) during the Excavation with Landfill scenario at representative times in the Shallow Rock Zone (layer 15).

Figure 23. Observation points for time series plots.

Figure 24. Times series of boron concentrations at six representative locations in the EAB and WAB during the Excavation with Landfill scenario.

Figure 25. Configuration of features used to represent the Complete Excavation scenario in the model (a) and simulated hydraulic heads (b).

Figure 26. Distribution of boron concentrations ( $\mu\text{g/L}$ ) during Complete Excavation scenario at representative times in the Transition Zone (layer 13).

Figure 27. Distribution of boron concentrations ( $\mu\text{g/L}$ ) during Complete Excavation scenario at representative times in the Shallow Rock Zone (layer 15).

Figure 28. Time series of boron concentrations at six representative locations in the EAB and WAB during the Excavation with Landfill and Complete Excavation scenarios.

Figure 29. Configuration of features used to represent the Final Cover scenario in the model (a) and simulated hydraulic heads (b).

Figure 30. Distribution of boron concentrations ( $\mu\text{g/L}$ ) during the Final Cover scenario at representative times in the Transition Zone (layer 13).

Figure 31. Distribution of boron concentrations ( $\mu\text{g/L}$ ) during the Final Cover scenario at representative times in the Shallow Rock Zone (layer 15).

Figure 32. Times series of boron concentrations at six representative locations in the EAB and WAB during the Final Cover scenario.

Figure 33. Configuration of features used to represent the Hybrid scenario in the model (a) and simulated hydraulic heads (b).

Figure 34. Distribution of boron concentrations ( $\mu\text{g/L}$ ) during the Hybrid scenario at representative times in the Transition Zone (layer 13).

Figure 35. Distribution of boron concentrations ( $\mu\text{g/L}$ ) during the Hybrid scenario at representative times in the Shallow Rock Zone (layer 15).

Figure 36. Times series of boron concentrations at six representative locations in the EAB and WAB during the Hybrid scenario.

Figure 37. Comparison of simulated boron concentrations ( $\mu\text{g/L}$ ) in the Transition Zone (left) and in the top of bedrock (right) around year 2240 for the Complete Excavation, Final Cover, and Hybrid scenarios.

Figure 38. Comparison of simulated boron concentrations ( $\mu\text{g/L}$ ) in the Transition Zone (left) and in the top of bedrock (right) around year 3040 for the Complete Excavation, Final Cover, and Hybrid scenarios.

Figure 39. Comparison of boron time series at six representative locations in the EAB and WAB for the Excavation, Final Cover, and Hybrid scenarios.

Figure 40. Comparison of closure options for the transition flow zone, model years 2020 and 2100.

Figure 41. Comparison of closure options for the transition flow zone model years 2330/2350 and 3030/3040.

Figure 42. Comparison of closure options for the upper bedrock flow zone, model years 2020 and 2100.

Figure 43. Comparison of closure options for the upper bedrock flow zone, model years 2330/2350 and 3030/3040.

## EXECUTIVE SUMMARY

Duke Energy Progress, LLC. (Duke Energy) owns and operates the Roxboro Steam Electric Plant (Roxboro Plant, Plant, Site) located at 1700 Dunnaway Road in Semora, Person County, North Carolina. The Roxboro Plant began operations in the 1960s and continued to add capacity through the 1980s. Currently, the Plant operates four coal-fired units. Coal combustion residuals (CCRs) have historically been managed at the Plant's on-site ash basins: the East Ash Basin (EAB) and the West Ash Basin (WAB). Inorganic compounds from ash within the basins have leached out into the groundwater, and have then been transported by groundwater flow within the vicinity of the ash basins.

Preliminary numerical simulations of groundwater flow and transport have been calibrated to current conditions and used to evaluate different scenarios being considered as options for closure of the ash basins. The predictive simulations presented herein are not intended to represent a final detailed closure design. These simulations use conceptual designs that are subject to change as the closure plans are finalized. The simulations are intended to show the key characteristics of groundwater flow and mobile constituent transport that are expected to result from the closure actions. It should be noted that, for groundwater modeling purposes, a reasonable assumption was made for initiation dates for each of the closure options. The assumed dates were based on information that is currently evolving and may vary from dates provided in contemporary documents. The potential variance in closure dates presented in the preliminary groundwater model is inconsequential to the results of the model as it does not produce substantial changes in the modeled scenarios. This preliminary model report is intended to provide basic model development information and simulations of conceptual basin closure designs. A more detailed model report is planned for inclusion in the groundwater corrective action plan (CAP) scheduled for completion in December 2019.

The model simulations were developed using flow and transport models MODFLOW and MT3DMS. Boron was the constituent of interest (COI) selected to estimate the time to achieve compliance because it is common in ash but rare in natural settings in the vicinity of Roxboro. It is unreactive and highly mobile, so boron is a good indicator of the maximum extent of plumes originating in ash. The less mobile, more reactive constituents (i.e. arsenic, selenium, chromium,

etc.) will follow the same flow path as boron; however, they generally are not present at concentrations greater than 2L beyond the compliance boundary.

The calibrated model was adjusted to represent conditions that would occur during four closure scenarios, termed Excavation with Landfill, Complete Excavation, Final Cover, and Hybrid. The Complete Excavation closure option is based on discussions with Duke Energy engineers, and the other designs are based on closure options analyses (Wood, Plc). The Complete Excavation scenario was analyzed after the other three scenarios were modeled and reported in November 2018. A description of the Complete Excavation scenario was added to this revised report. The analyses were conducted to simulate 1,000 years into the future, and the results describing the distribution of boron concentrations were used to evaluate the performance of the four closure scenarios<sup>1</sup>. Three closure-specific compliance boundaries<sup>2</sup> were used to evaluate the results:

- Final Cover scenario is evaluated using a compliance boundary that is 500 ft. from the current waste boundary.
- Excavation scenarios are evaluated using a compliance boundary that is 250 ft. from the current waste boundary.
- Hybrid scenario is evaluated using a compliance boundary 250 ft. from the final waste boundary.

The distribution of boron in the saprolite/transition zone and bedrock adjacent to the ash basins resulted from hydrologic and mass loading conditions during operation of the ash basins. These conditions will change during the interim period and during closure because of decanting operations and as ash is regraded, removed or covered. In the model, these changes cause the

---

<sup>1</sup> It is noted that these modeled scenarios do not include any active form of groundwater remediation. The relative benefits of various groundwater remediation alternatives will be addressed in the groundwater CAP. However, preliminary modeling of corrective action (e.g., groundwater extraction) indicates that the relative effectiveness and timeframes required to achieve the applicable standards at the compliance boundaries will not be significantly different between the four closure scenarios considered with those corrective actions, therefore, the comparison of the performance of the closure scenarios via the groundwater modeling presented in this report (without corrective actions) is valid.

<sup>2</sup> These compliance boundaries are based upon retention of the NPDES permit for the Final Cover scenario and the proposed North Carolina CCR Rules for the Excavation and Hybrid scenarios. However, for comparison purposes, Section 6.5 and Figures 40-43 utilize the existing 500-foot compliance boundary for all four scenarios.

hydraulic head to drop and the direction of groundwater flow to change in some areas. The modeled hydraulic head changes are more significant in the WAB than the EAB.

During closure scenario simulations, the extent of the boron distribution is lesser in the upper bedrock compared to the overlying saprolite/transition zone. The upper bedrock is largely below the water table and the boron is more mobile than in the saprolite/transition zone which is unsaturated in most upland areas. As a result, the distribution of boron in the upper bedrock is more representative of concentrations in groundwater than distributions in the saprolite/transition zone.

Boron concentrations at the beginning of the interim period (year 2020) exceed the 2L standard of 700 µg/L in the upper bedrock at the existing 500-ft. compliance boundary at five locations around the EAB, and at no areas around the WAB (Figures ES-1 and ES-2), according to the simulations. The existence of the boron source material outside the waste boundary is inferred based on calibrating the model to observed concentrations, and it is consistent with the known occurrence of the unlined portion of the industrial landfill and landfill base grade structural fill around the periphery of the EAB, in an area called the “halo zone.”

Decanting operations and subsequent closure scenarios alter the groundwater flow in and around EAB and WAB, resulting in reductions in boron concentrations and the extent of regions with concentrations greater than the 2L standard. By year 2330, compliance with the closure-specific boundaries has been reached in the EAB for the Excavation and Final Cover scenarios (Figure ES-1). For these scenarios, the extent of boron concentrations above the 2L standard is within or at the compliance boundaries. By year 2330, the Hybrid scenario has not yet reached compliance and boron concentrations greater than the 2L standard extend beyond the northern edge of the EAB compliance boundary (Figure ES-1). Simulation results indicate the Hybrid scenario will reach compliance in year 3030.

By year 2330, compliance with the closure-specific boundaries has been reached in the WAB for all closure scenarios and the extent of boron concentrations above the 2L standard is within or at the compliance boundaries (Figure ES-2).

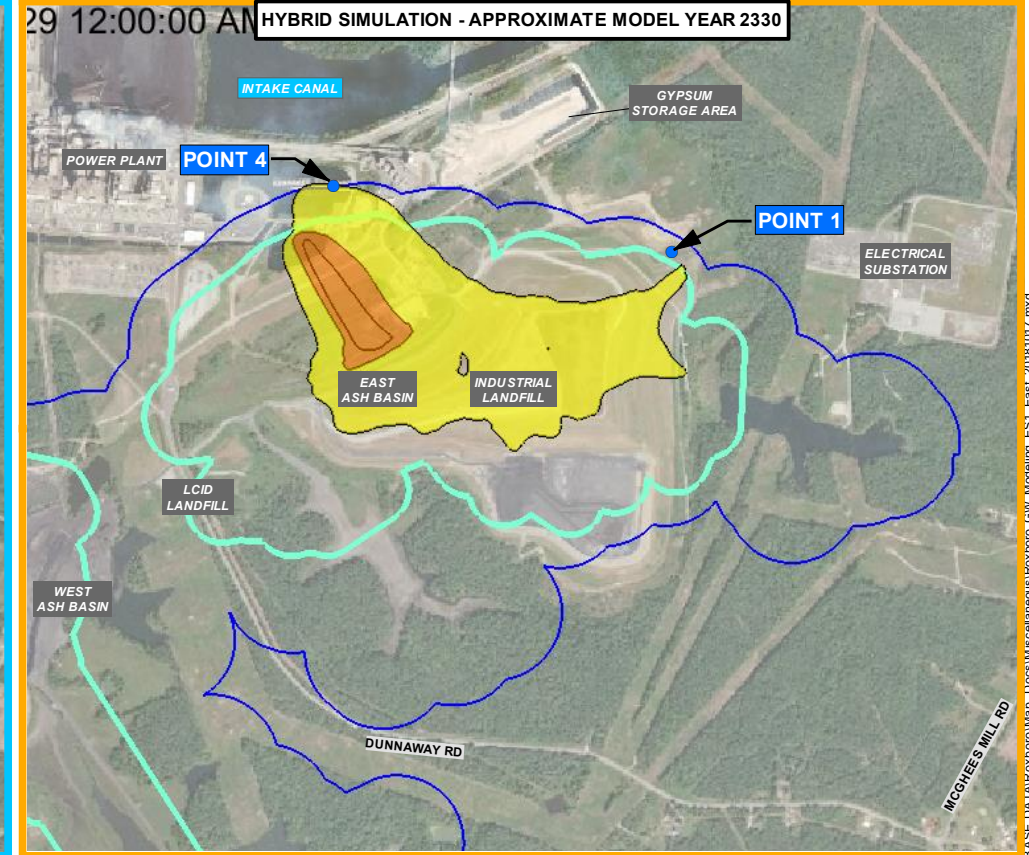
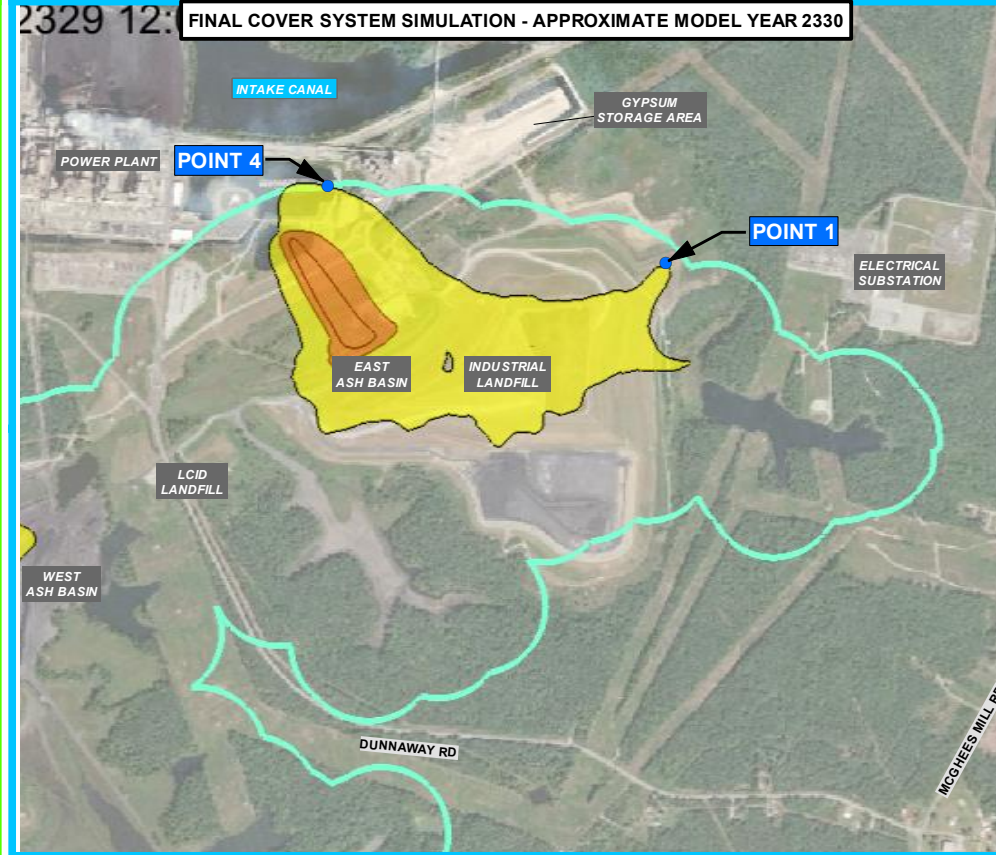
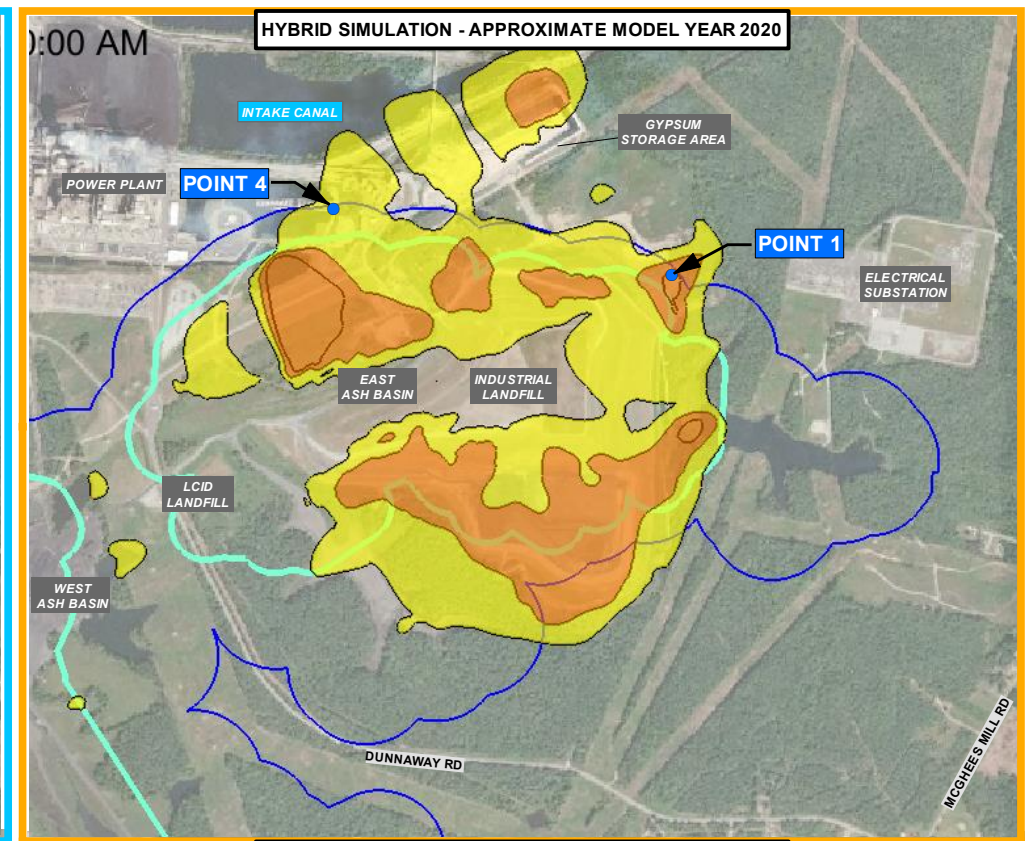
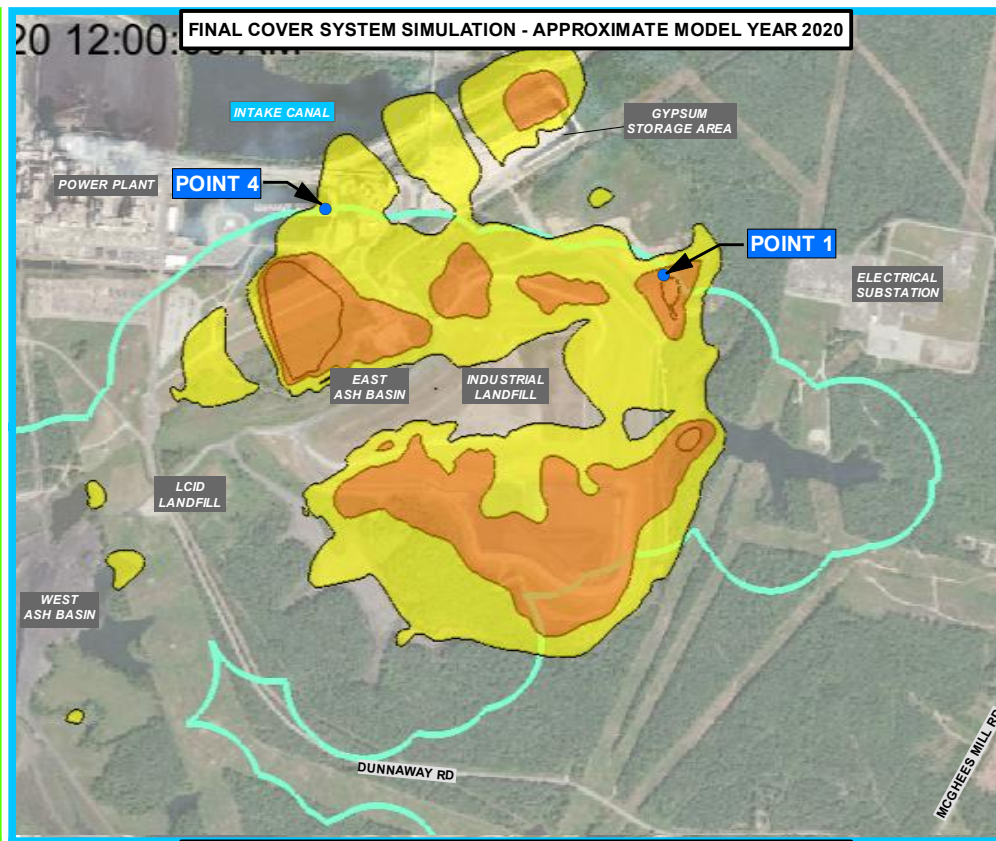
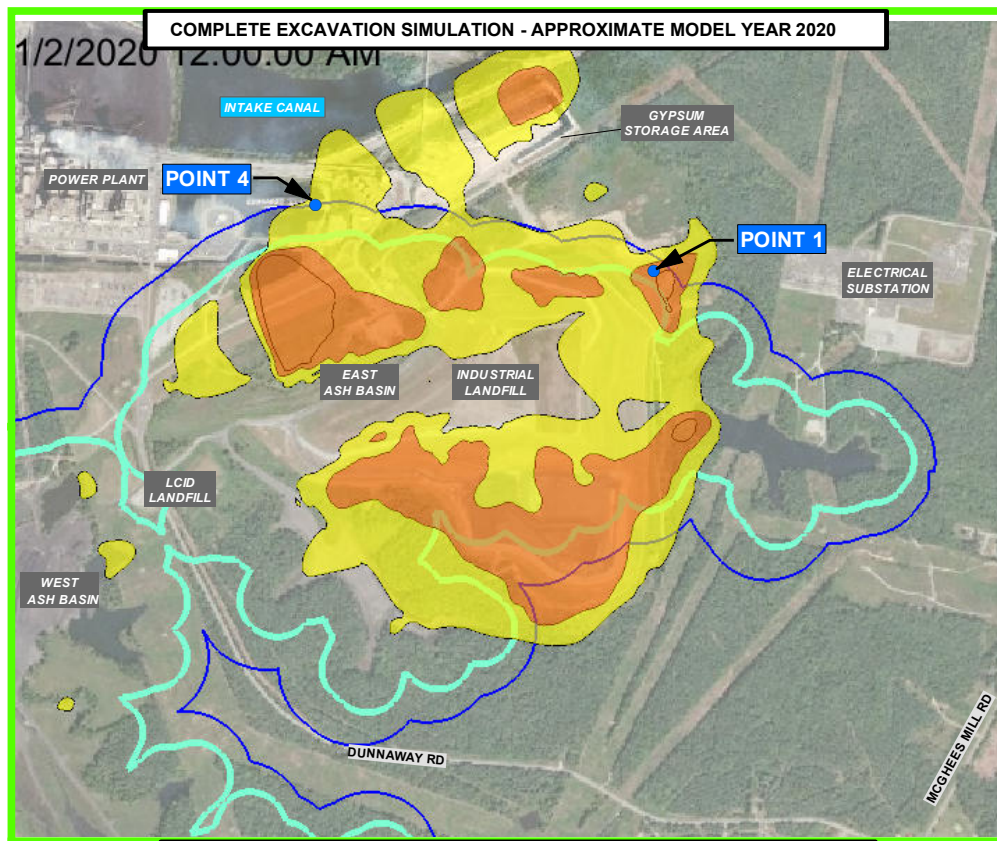
Reference points on or near compliance boundaries around the EAB and WAB were selected to evaluate changes in boron concentrations with time for the closure designs. At

certain locations, the response for the scenarios is similar. For example, at Point 1 in the EAB, boron concentrations decrease to 2L in approximately year 2150 for all four scenarios (Figure ES-3). In other locations, there are distinct variations between scenarios that result from changes to the flow system during closure. At Point 4 (EAB), for example, the boron concentration decreases to below the 2L standard by around year 2060 for both Excavation scenarios, but it takes approximately another 100 years to reach the 2L standard in the Final Cover and Hybrid scenarios (Figure ES-3). The effect of removing the industrial landfill (Complete Excavation) from the EAB was compared to leaving the landfill in place but excavating the vicinity of the landfill (Excavation with Landfill). The modeling results were mixed in that removing the landfill decreases the concentrations within the EAB, but it increases the time to reach the 2L standard at reference Points 3 and 6.

At Point 9 in the WAB, the time for boron concentrations to reach 2L is similar for the Excavation and Hybrid scenarios (approximately year 2060), and it occurs roughly 100 years later for the Final Cover scenario (Figure ES-4). For the location with the highest concentrations, Point 10, the boron concentrations decrease to the 2L standard between years 2350 and 2430 for the different scenarios (Figure ES-4).

Boron concentrations greater than 2L occur in the simulations at depths below the shallow fractured rock represented by grid layer 15. Details of the distribution of boron in the deeper rock are uncertain because only a few wells in the deeper rock are available at Roxboro. Additional deeper wells are planned and data from those wells will be used to refine the constraints on the distribution of boron. These results will be included in a later report.

The simulations indicate that there are no exposure pathways between the groundwater flow through the ash basins and the pumping wells used for water supply in the vicinity of the Roxboro site. Domestic and public water supply wells are outside, or upgradient of the groundwater flow system containing the ash basins. Domestic and public water supply wells are not affected by constituents released from the ash basins or by the different closure options, according to the simulations.



**NOTES:**  
 THE MODELED TIME TO RETURN TO COMPLIANCE WITH 2L GROUNDWATER STANDARDS IS APPROXIMATELY 300 YEARS FOR BOTH THE EXCAVATION AND FINAL COVER SYSTEM OPTIONS USING BORON IN FRACTURED BEDROCK AS THE BASIS FOR THE ESTIMATE.  
 FRACTURED BEDROCK RESULTS SHOWN SINCE THIS REPRESENTS THE MOST TRANSMISSIVE ZONE.  
 THE THREE MODEL SIMULATIONS ARE BASED ON THE COMPLETION DATES FOR THOSE ACTIVITIES. THESE DATES ARE: EXCAVATION - YEAR 2040, FINAL COVER SYSTEM - YEAR 2030, HYBRID - YEAR 2030.  
 SEE FIGURE 3 FOR TIME VS. CONCENTRATION PLOTS OF BORON AT POINT 1.  
 HYBRID WASTE BOUNDARY PROVIDED BY WOOD PLC.  
 POTENTIAL COMPLIANCE BOUNDARY ASSOCIATED WITH CLOSURE IS 250 FEET FROM WASTE BOUNDARY OR 50 FEET WITHIN THE PROPERTY BOUNDARY, WHICHEVER IS CLOSER TO THE WASTE.  
 AERIAL PHOTOGRAPHY OBTAINED FROM GOOGLE EARTH PRO ON AUGUST 17, 2017. IMAGE COLLECTED ON JUNE 13, 2016.  
 DRAWING HAS BEEN SET WITH A PROJECTION OF NORTH CAROLINA STATE PLANE COORDINATE SYSTEM FIPS 3200 (NAD83).

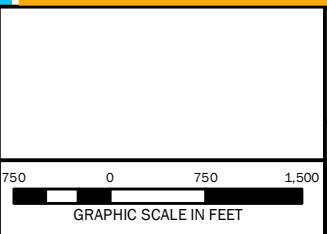
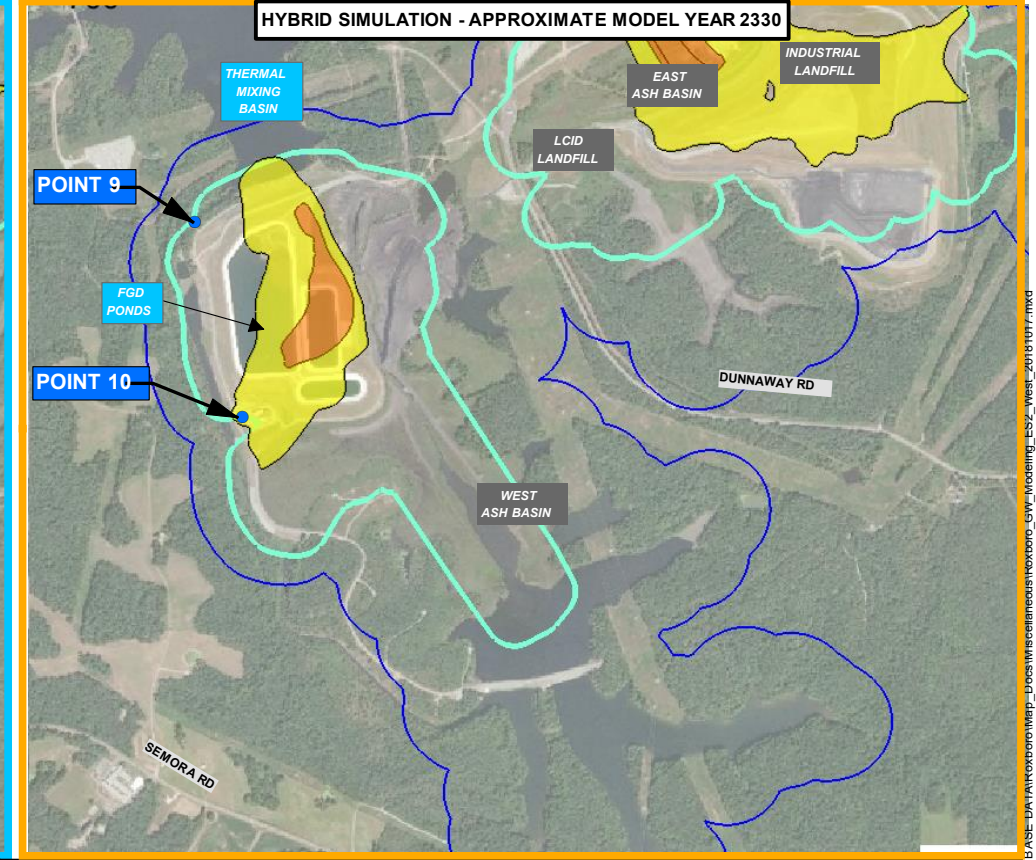
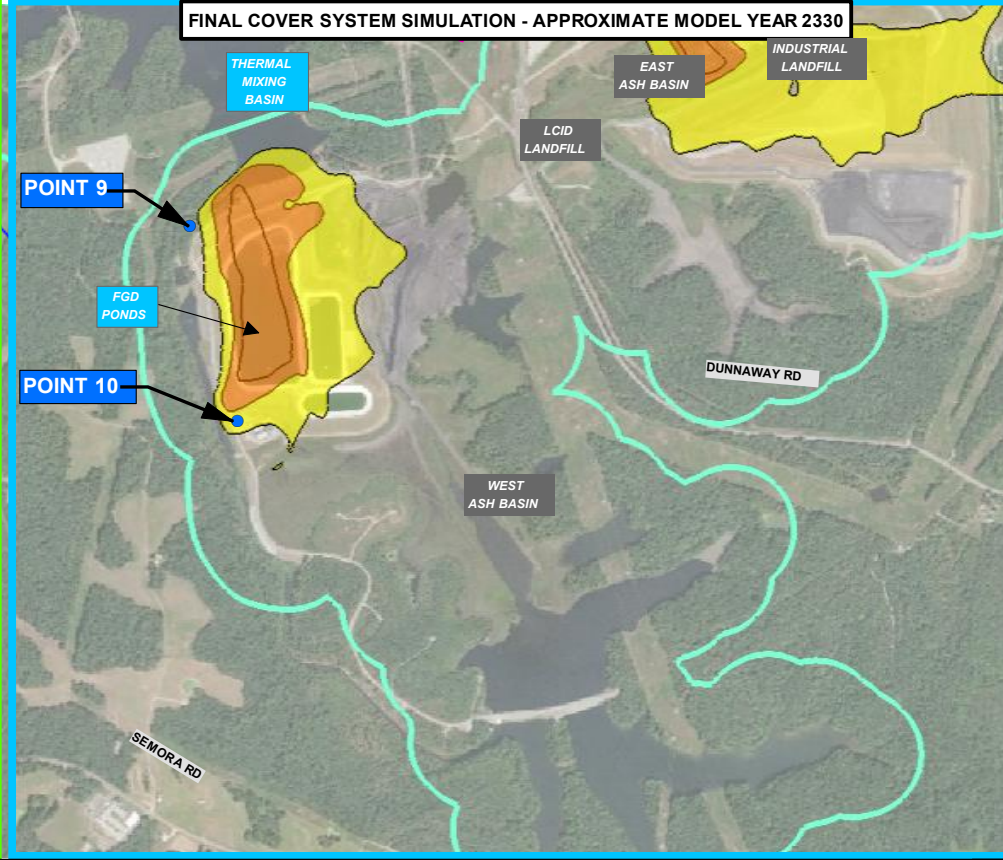
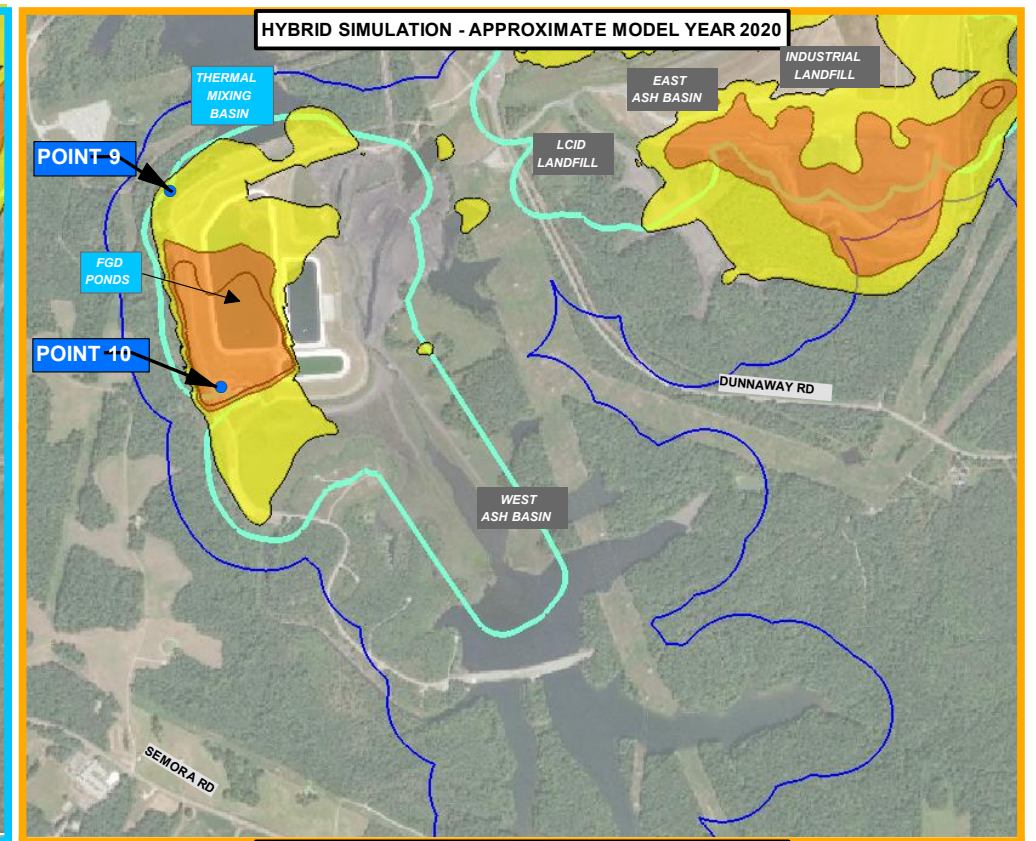
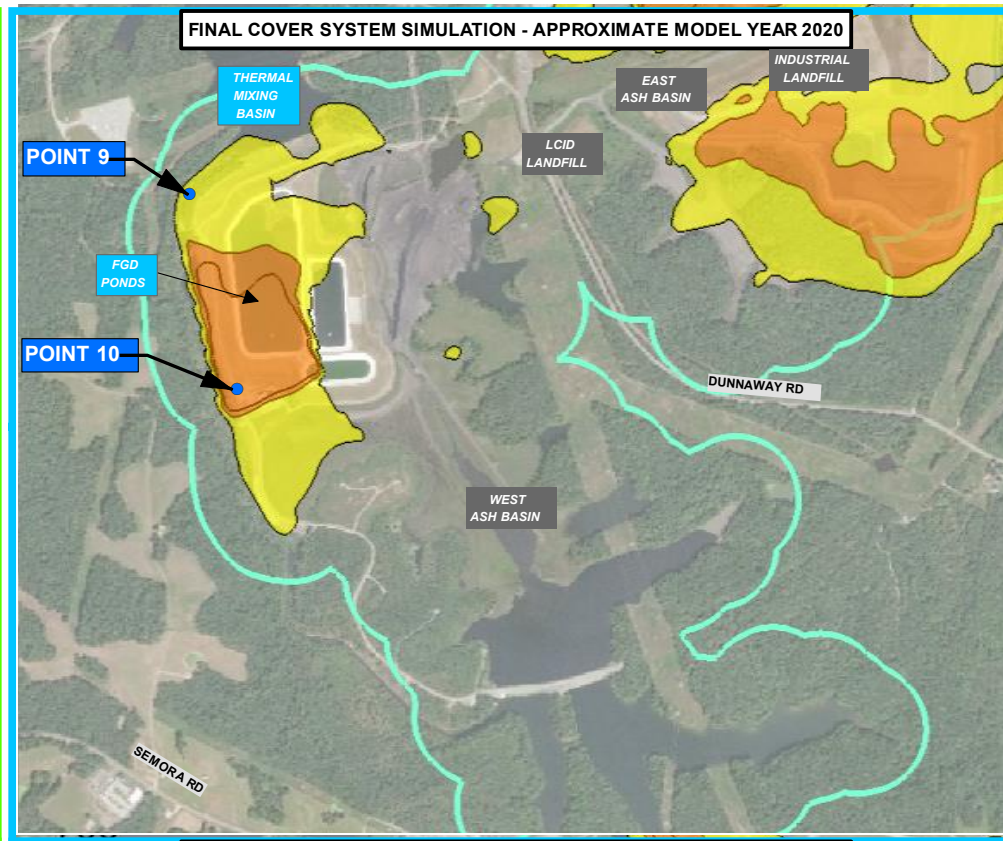
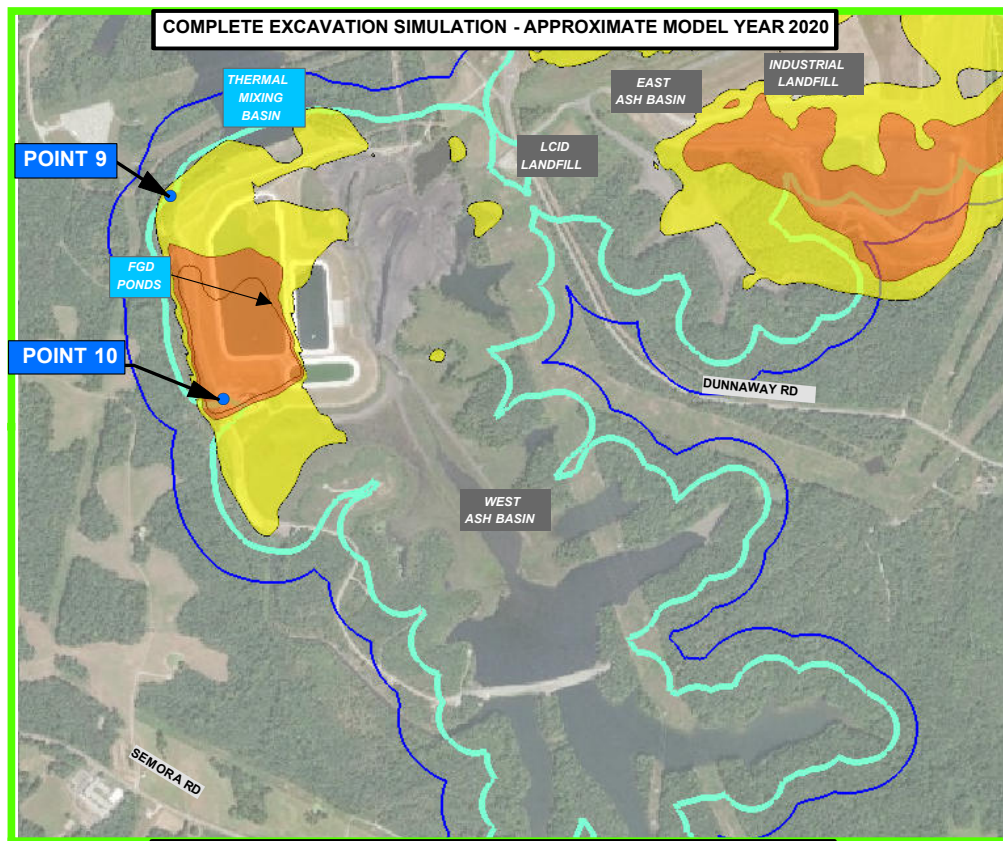


**FIGURE ES-1**  
**SIMULATED BORON CONCENTRATIONS**  
**EAST ASH BASIN - FRACTURED BEDROCK**  
**COMPLETE EXCAVATION, FINAL COVER**  
**SYSTEM, AND HYBRID SIMULATIONS**  
**ROXBORO STEAM ELECTRIC PLANT**  
**DUKE ENERGY PROGRESS, LLC**  
**SEMORA, NORTH CAROLINA**

P:\Duke\_Energy\_Progress\1026300 GIS BASE\DATA\ROXBORO\_Map\_Docs\Miscellaneous\ROXBORO\_CW\_Modeling\_ES1\_East\_20181017.mxd



**LEGEND**

- BORON CONCENTRATION RANGE (>4,000 µg/L)
- BORON CONCENTRATION RANGE (700 - 4,000 µg/L)
- ASH BASIN COMPLIANCE BOUNDARY (CURRENT)
- POTENTIAL COMPLIANCE BOUNDARY ASSOCIATED WITH EXCAVATION OR HYBRID OPTION
- TIME-SERIES PLOT POINT

**NOTES:**

THE MODELED TIME TO RETURN TO COMPLIANCE WITH 2L GROUNDWATER STANDARDS IS APPROXIMATELY 300 YEARS FOR BOTH THE EXCAVATION AND FINAL COVER SYSTEM OPTIONS USING BORON IN FRACTURED BEDROCK AS THE BASIS FOR THE ESTIMATE.

FRACTURED BEDROCK RESULTS SHOWN SINCE THIS REPRESENTS THE MOST TRANSMISSIVE ZONE.

THE THREE MODEL SIMULATIONS ARE BASED ON THE COMPLETION DATES FOR THOSE ACTIVITIES. THESE DATES ARE: EXCAVATION - YEAR 2040, FINAL COVER SYSTEM - YEAR 2030, HYBRID - YEAR 2030.

SEE FIGURE 3 FOR TIME VS. CONCENTRATION PLOTS OF BORON AT POINT 1.

HYBRID WASTE BOUNDARY PROVIDED BY WOOD PLC.

POTENTIAL COMPLIANCE BOUNDARY ASSOCIATED WITH CLOSURE IS 250 FEET FROM WASTE BOUNDARY OR 50 FEET WITHIN THE PROPERTY BOUNDARY, WHICHEVER IS CLOSER TO THE WASTE.

AERIAL PHOTOGRAPHY OBTAINED FROM GOOGLE EARTH PRO ON AUGUST 17, 2017. IMAGE COLLECTED ON JUNE 13, 2016.

DRAWING HAS BEEN SET WITH A PROJECTION OF NORTH CAROLINA STATE PLANE COORDINATE SYSTEM FIPS 3200 (NAD83).

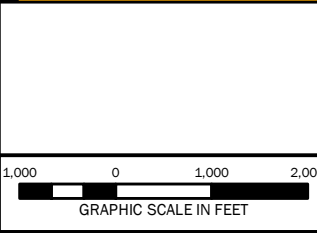
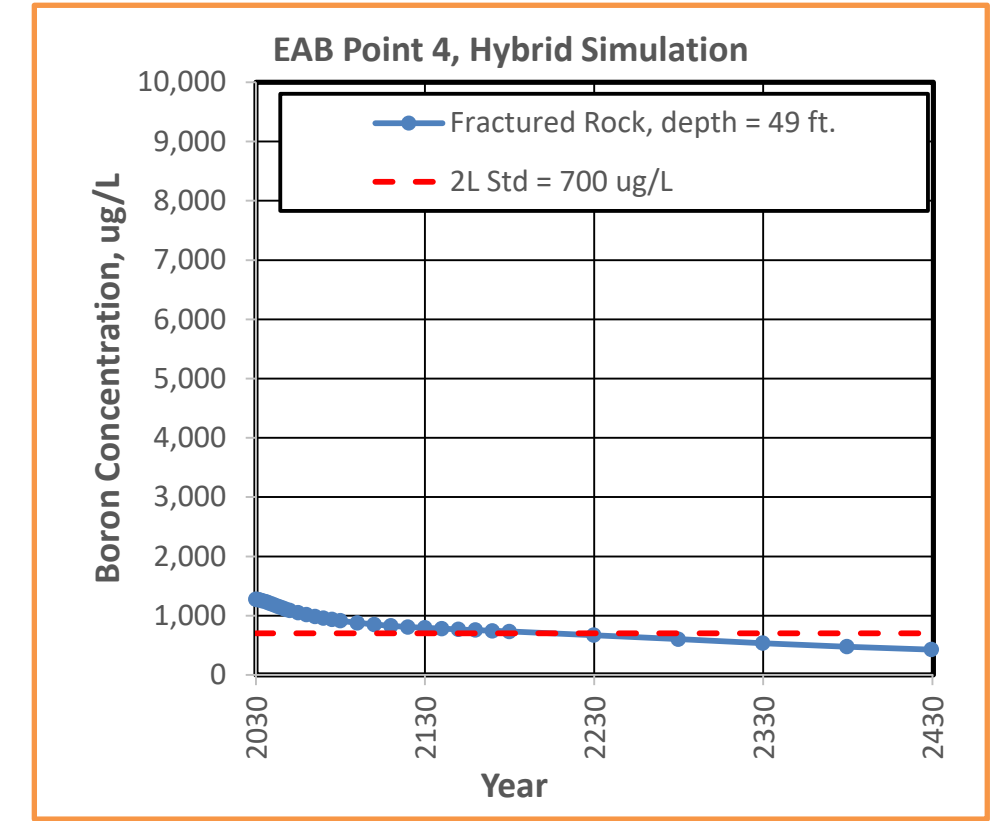
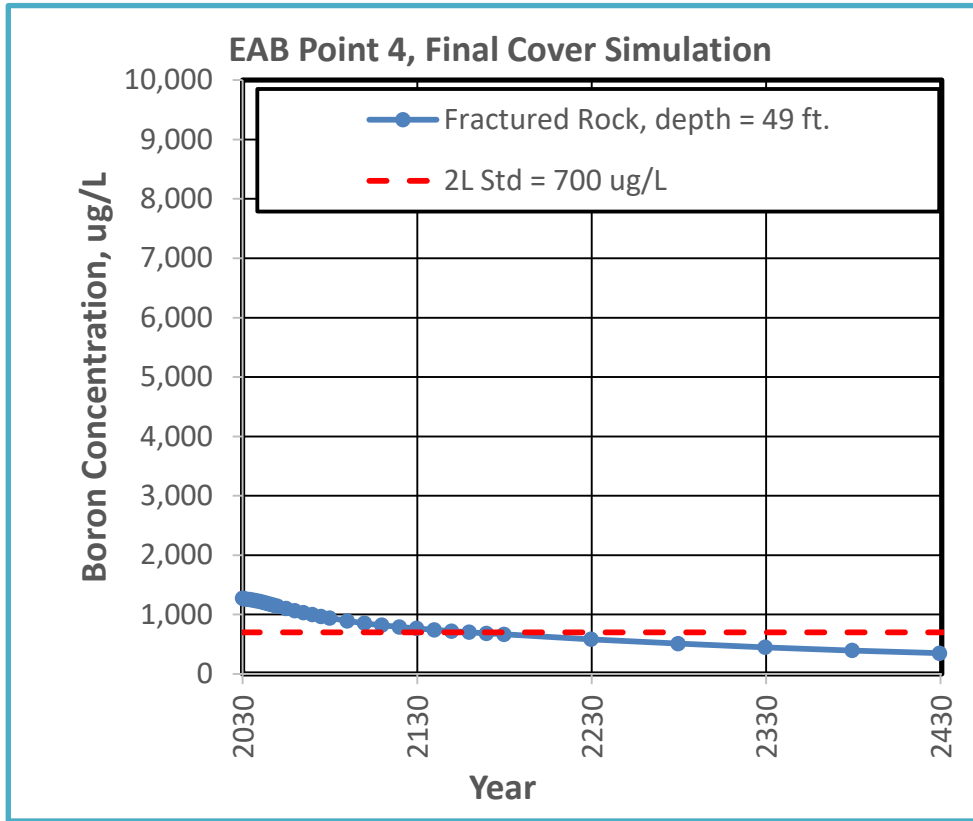
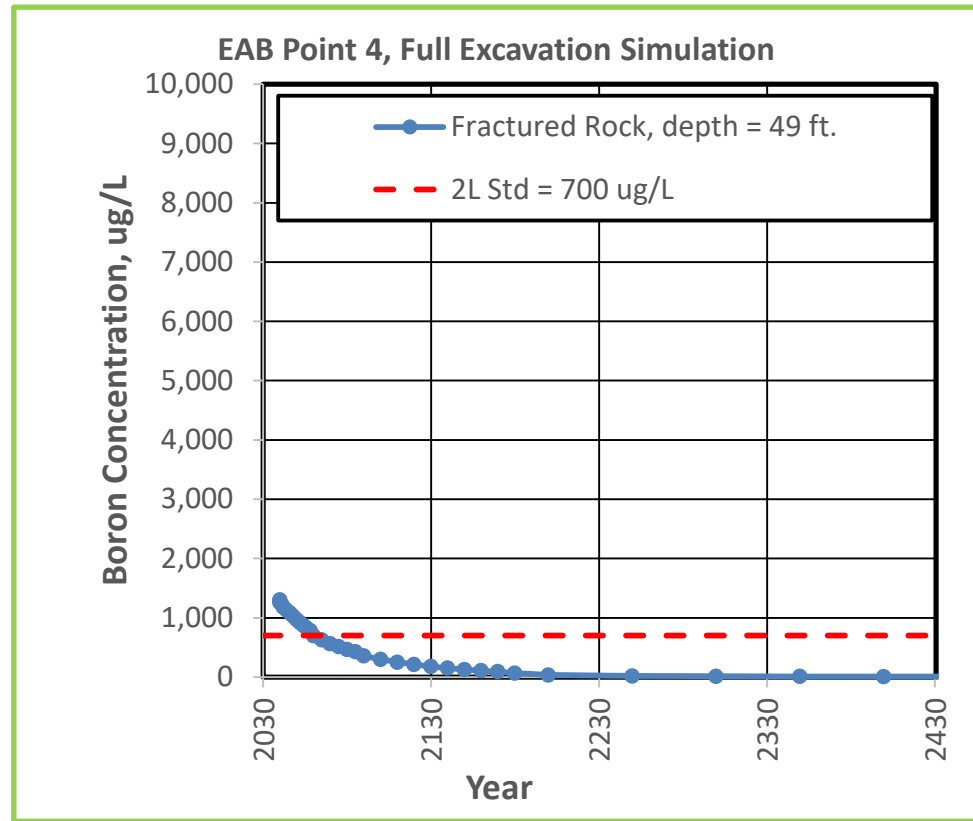
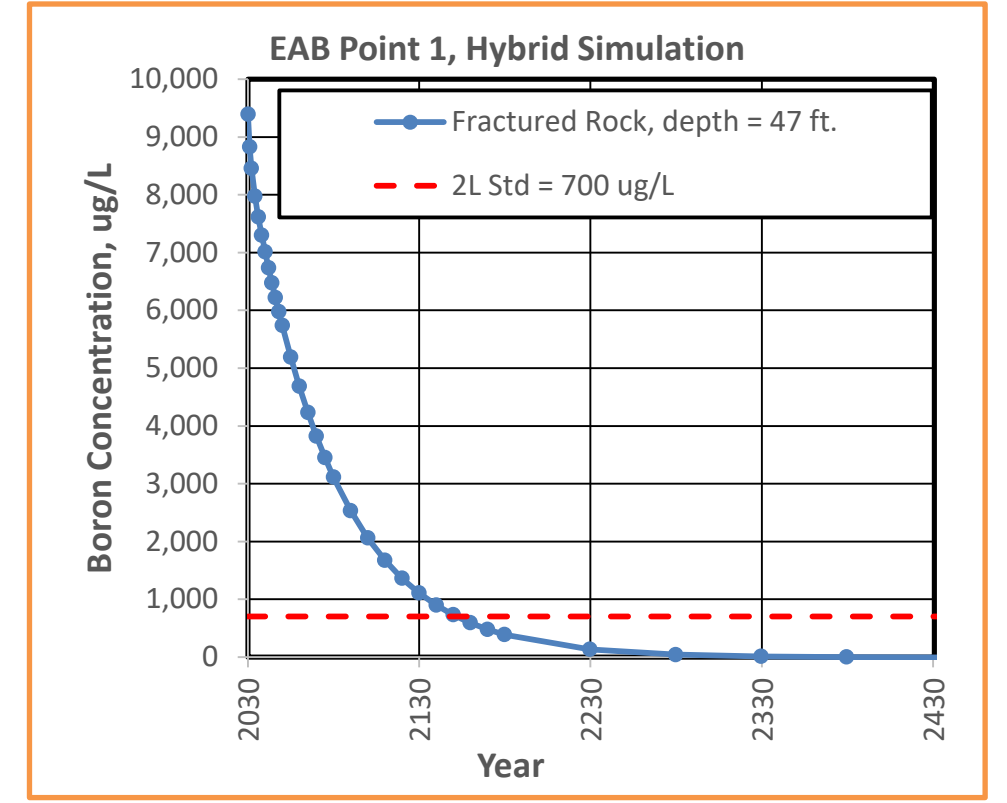
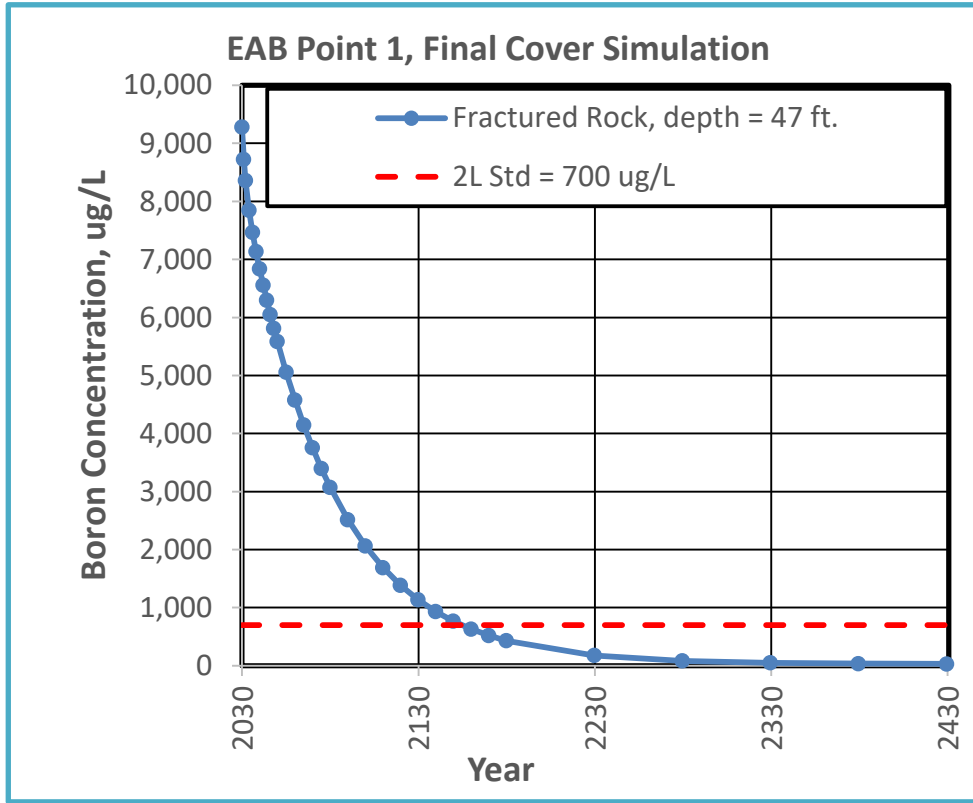
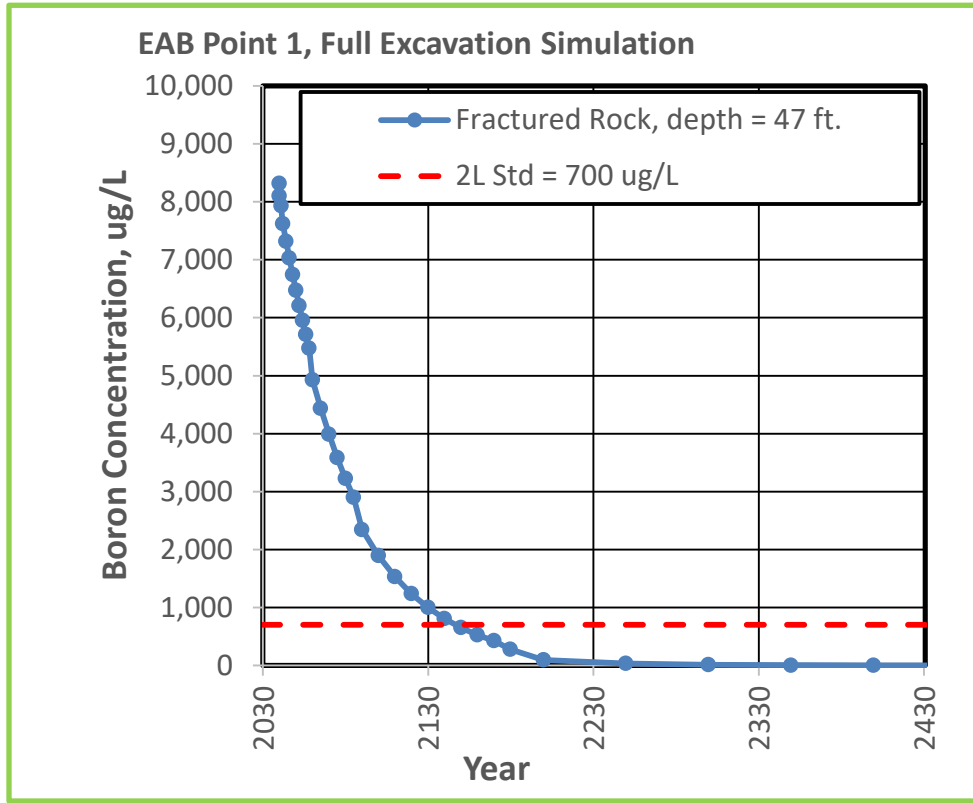


**FIGURE ES-2**  
**SIMULATED BORON CONCENTRATIONS**  
**WEST ASH BASIN - FRACTURED BEDROCK**  
**SYSTEM, EXCAVATION, FINAL COVER**  
**SYSTEM, AND HYBRID SIMULATIONS**  
**ROXBORO STEAM ELECTRIC PLANT**  
**DUKE ENERGY PROGRESS, LLC**  
**SEMORA, NORTH CAROLINA**

P:\Duke\_Energy\_Progress\1026300\_GIS\_Base\DATA\Knoxboro\Map\_Docs\Miscellaneous\Knoxboro\_GW\_Modeling\_SS2\_West\_2018\1017.mxd

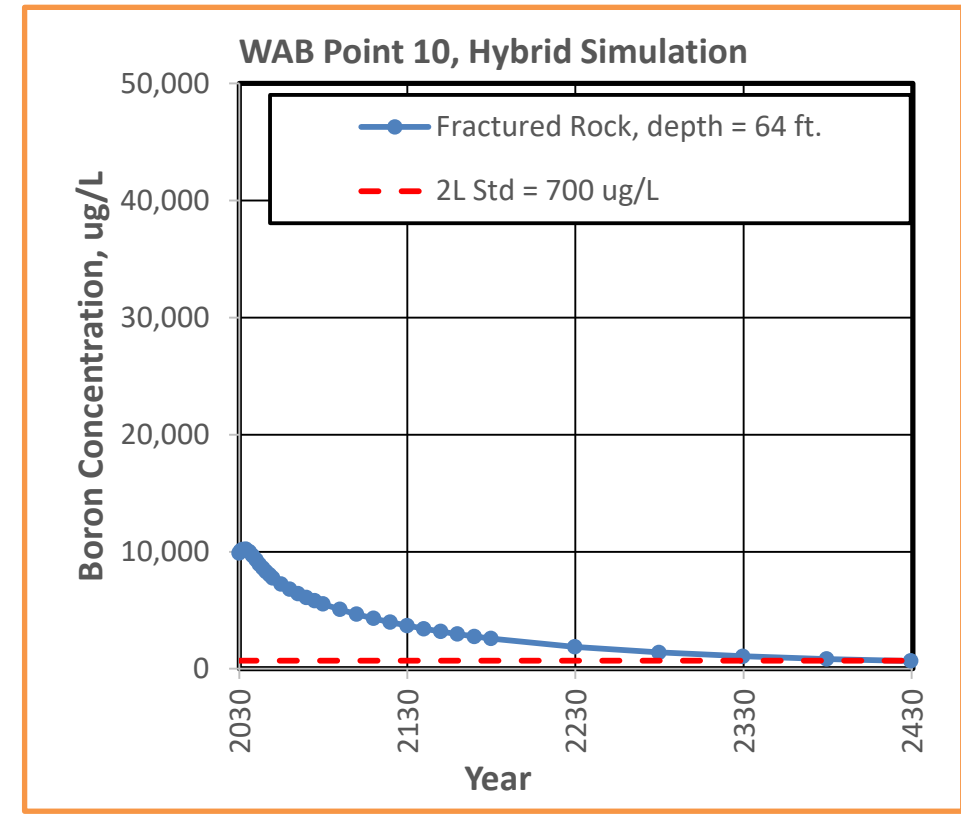
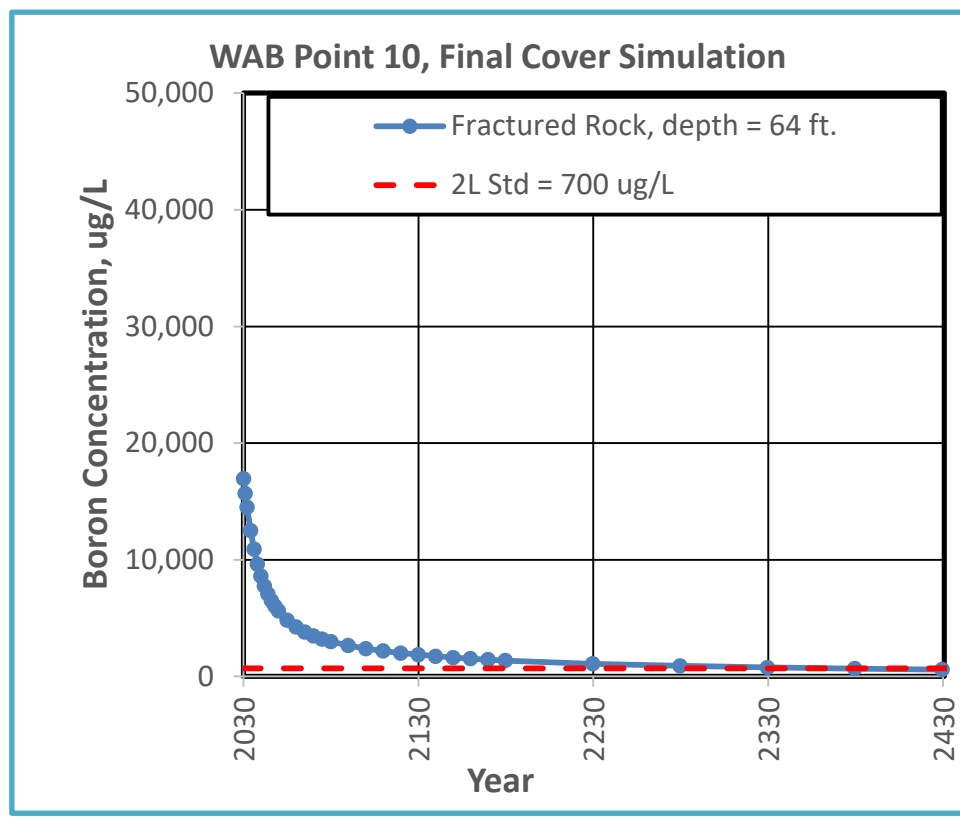
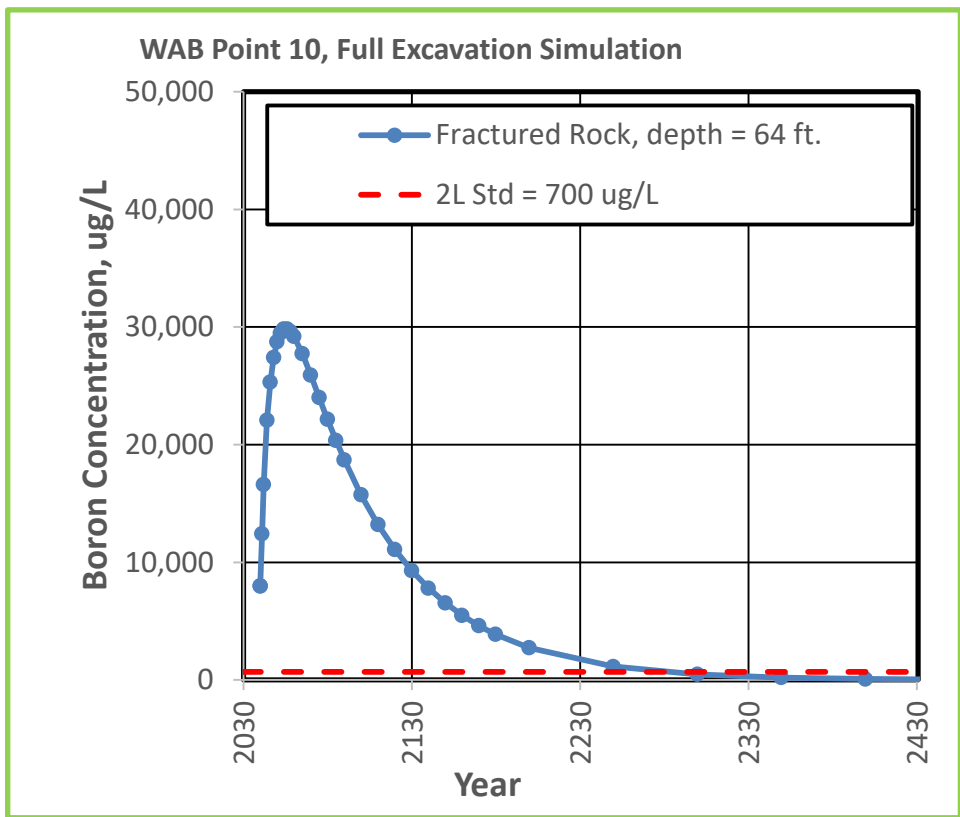
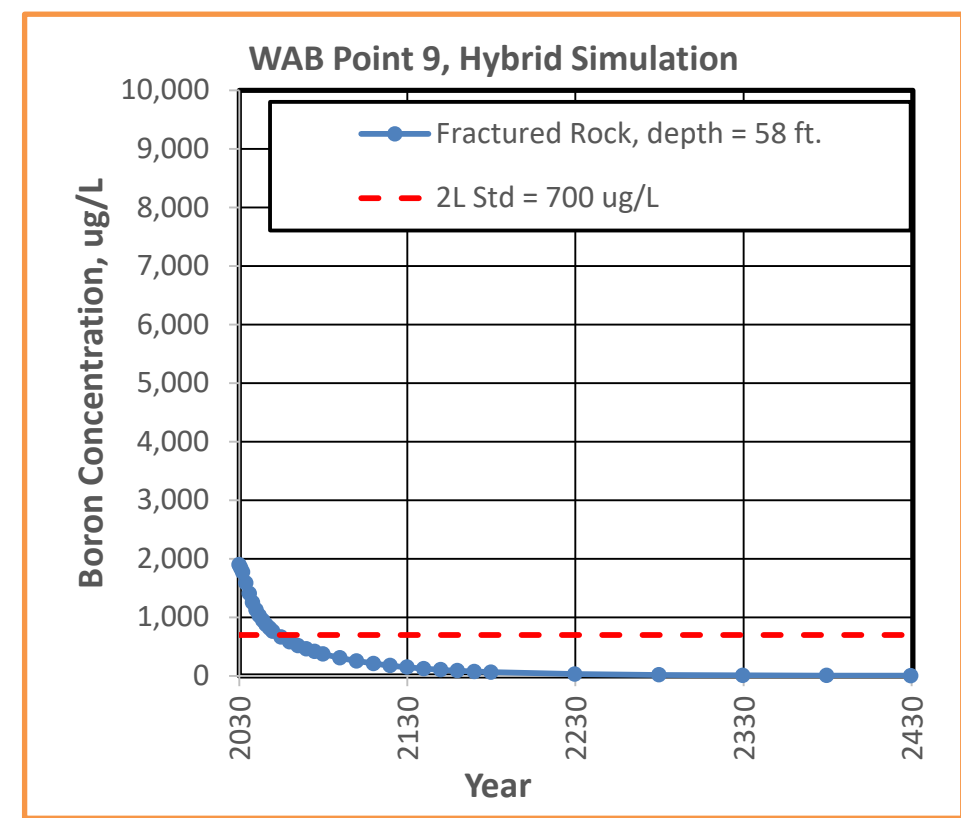
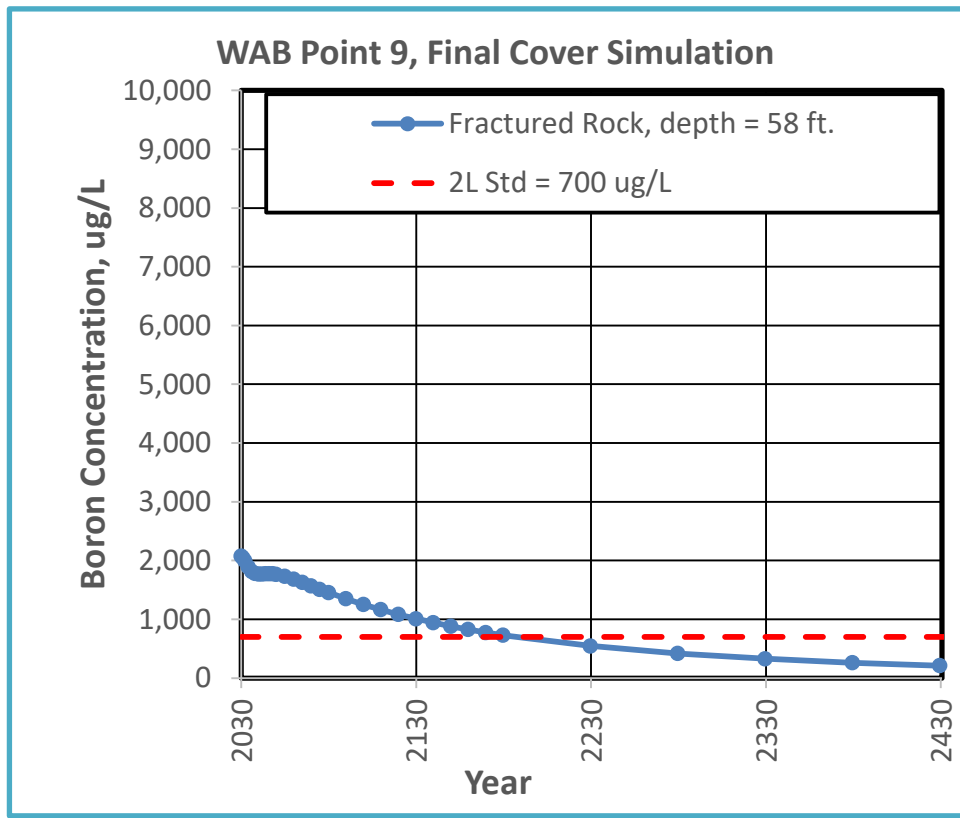
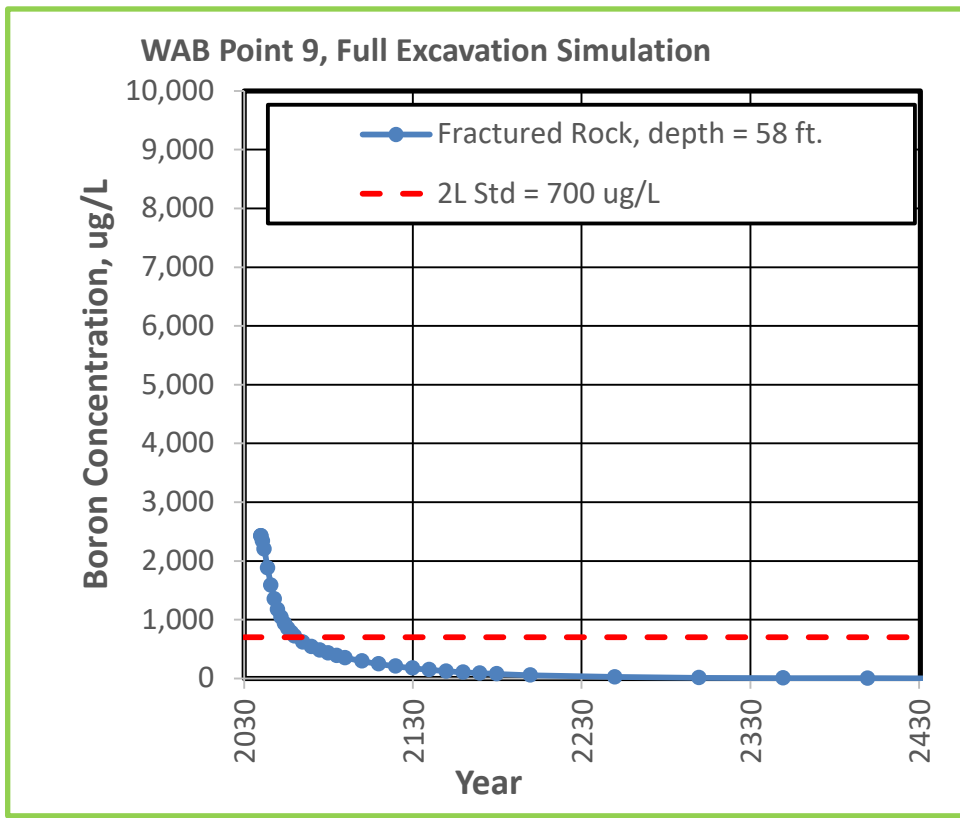


**NOTES:**  
 THE START DATES FOR THE THREE MODEL SCENARIOS ARE BASED ON THE COMPLETION DATES FOR THOSE ACTIVITIES.  
 THESE DATES ARE:

- COMPLETES EXCAVATION – YEAR 2040
- FINAL COVER SYSTEM – YEAR 2030
- HYBRID – YEAR 2030

FRACTURED BEDROCK ZONE RESULTS SHOWN REPRESENTING THE MOST TRANSMISSIVE ZONE.

**FIGURE ES-3**  
**BORON TIME VS. CONCENTRATION PLOTS**  
**EAST ASH BASIN – FRACTURED BEDROCK**  
**COMPLETES EXCAVATION, FINAL COVER SYSTEM, AND HYBRID SIMULATIONS**  
**ROXBORO STEAM ELECTRIC PLANT**  
**DUKE ENERGY PROGRESS, LLC**  
**SEMORA, NORTH CAROLINA**



**NOTES:**  
 THE START DATES FOR THE THREE MODEL SCENARIOS ARE BASED ON THE COMPLETION DATES FOR THOSE ACTIVITIES.  
 THESE DATES ARE:

- COMPLETES EXCAVATION – YEAR 2040
- FINAL COVER SYSTEM – YEAR 2030
- HYBRID – YEAR 2030

FRACTURED BEDROCK ZONE RESULTS SHOWN REPRESENTING THE MOST TRANSMISSIVE ZONE.

**FIGURE ES-4**  
**BORON TIME VS. CONCENTRATION PLOTS**  
**WEST ASH BASIN – FRACTURED BEDROCK**  
**COMPLETES EXCAVATION, FINAL COVER SYSTEM, AND HYBRID SIMULATIONS**  
**ROXBORO STEAM ELECTRIC PLANT**  
**DUKE ENERGY PROGRESS, LLC**  
**SEMORA, NORTH CAROLINA**

## 1.0 INTRODUCTION

Duke Energy Progress, LLC (Duke Energy) owns and operates the Roxboro Steam Electric Plant (Roxboro Plant, Plant, Site) located at 1700 Dunnaway Road in Semora, Person County, North Carolina. The Roxboro Plant began operations in the 1960s and continued to add capacity through the 1980s. Currently, the Plant operates four coal-fired units. Coal combustion residuals (CCRs) have historically been managed at the Plant's on-site ash basins: the East Ash Basin (EAB) and the West Ash Basin (WAB). The two ash basins are approximately one half mile to the southeast and southwest of the Plant, respectively. Inorganic compounds from ash within the basins have leached out into the groundwater, which then have been transported by groundwater flow within the vicinity of the ash basins. Preliminary numerical simulations of groundwater flow and transport have been calibrated to current conditions and used to evaluate different scenarios being considered as options for closure of the ash basins. The methods and results of those simulations are described in this report.

### 1.1 General Setting and Background

The Roxboro Plant is built next to Hyco Lake, which provides water for Plant operations and also serves as the local hydrogeologic discharge point (Figure 1). The ash basins were created by building dams on north/northwestward-flowing streams that discharged into Hyco Lake. The dams created impoundments that were used to store ash. The EAB was the first basin to be constructed and started receiving ash in the mid-1960s. Construction of the WAB followed and became active in the early 1970s (Figure 1 and Figure 2). An unlined industrial landfill was constructed on top of a portion of the EAB in the late 1980s. In 2002, Roxboro began constructing landfill phases with engineered liner systems. Operation of the lined landfill phases began in 2004 and continues today. Dry fly ash was placed in the unlined portion of the landfill, which is above the water table in the EAB. To allow development of the overlying industrial landfill, an earthen separator dike was constructed in the eastern portion of the EAB which formed a barrier separating the EAB from a portion of the former basin creating the eastern extension impoundment. For the WAB, the main dam was raised 13 feet and a series of dikes (Dikes #1 through #4) and a discharge canal were constructed in 1986. A rock filter dike (Dike

#1) was installed in the southern end of the WAB which isolated the southern end of the WAB and created the southern extension impoundment.

The Roxboro Plant is situated in the eastern Piedmont Physiographic Province, which is underlain by weathered saprolite derived from fractured metamorphic and igneous rocks (Trapp and Horn, 1997). Topography consists of rounded hills and rolling ridges cut by small streams and drainages. Elevations in the vicinity of the Plant range from 410 feet<sup>3</sup> during full pool at Hyco Lake to 570 feet southeast of the Plant. The area is underlain by metamorphic rock, which is fractured and weathered at shallow depths. The upper 10 to 30 feet consists of friable, highly weathered saprolite. The degree of weathering decreases with depth, with a transition zone of up to 30 feet, between the highly weathered saprolite and the underlying fractured rock (SynTerra, 2015). Groundwater within the Site area exists under unconfined, or water table, conditions within the saprolite, transition zone and in fractures and joints of the underlying bedrock. The shallow water table and bedrock water-bearing zones are interconnected. The saprolite, where the saturated thickness is sufficient, acts as a reservoir for supplying groundwater to the fractures and joints in the bedrock. Shallow groundwater generally flows from local recharge zones in topographically high areas, such as ridges, toward groundwater discharge zones, such as stream valleys.

The groundwater flow and transport model for the Roxboro site has been under development since 2015. The development process began with a steady-state groundwater flow model and a transient model of constituent transport that were calibrated to field observations resulting from an intensive drilling campaign in early and mid-2015. The first set of simulations were completed in November 2015 (SynTerra, 2015b) and revised in February 2016 (SynTerra, 2016). Since then, additional assessment activities, including the installation of additional groundwater monitoring wells and multiple groundwater sampling events, has resulted in a significant increase in the data describing hydraulic head and contaminant distribution. These additional data have further improved the predictive capability and reduce uncertainty in the model results. To take advantage of this potential, the model was recalibrated using data from both the new and existing groundwater wells.

---

<sup>3</sup> The datum for all elevation information presented in the report is NAVD88.

The following data sources were used during calibration of the revised groundwater flow and fate and transport model:

- Average site-wide water levels measured in CAMA/CCR/Compliance groundwater monitoring wells through November 2017.
- Groundwater quality data obtained from CAMA/CCR/Compliance sampling events conducted in November 2017.
- Concentration sources in solid waste landfill cells and in an extension impoundment area of the EAB.
- Surface water elevations as described in the CAP2 report (SynTerra, 2016).
- Estimated recharge, as described in CAP2 report (SynTerra, 2016).

The model revision consisted of three activities: development of a calibrated steady-state flow model of historical average conditions through 2017; development of a historical transient model of constituent transport that is calibrated to 2017 conditions; and simulations that predict the response of four closure scenarios:

1. Excavation with Landfill scenario assumes that ash is excavated in both basins while leaving the industrial landfill in place within the EAB.
2. Complete Excavation scenario assumes all ash is removed and dams are breached in both EAB and WAB. This scenario was included in a revision completed in January 2019.
3. Final Cover scenario assumes the ash in both basins is covered a low permeability cap.
4. Hybrid scenario assumes ash is excavated and moved from selected locations within basins where it is covered with a low permeability cap.

In all four scenarios, the extension portions of the EAB and WAB will be dredged.

## **1.2 Objectives**

The overall objective of the groundwater flow and transport modeling effort is to predict the performance of four closure scenarios. The goal is for these predictions to guide decisions

during the selection of closure actions. The flow and transport models have been undergoing a process of continuous improvement and refinement by including new field data. The continuous improvement process is designed to increase the accuracy and reliability of the performance predictions.

The objective of this model is to describe a subset of the overall results of simulations of boron transport in saprolite, the transition zone, and the underlying fractured rock. The predictive simulations shown here are not intended to represent a final detailed closure design. These simulations use conceptual designs that are subject to change as the closure plans are finalized. The simulations are intended to show the key characteristics of groundwater flow and mobile constituent transport that are expected to result from the closure actions.

## 2.0 CONCEPTUAL MODEL

The site conceptual model for the Roxboro Plant is primarily based on the Comprehensive Site Assessment Report (CSA report) (SynTerra, 2015), the CSA Supplement Report (SynTerra, 2016) and the CSA Update (SynTerra, 2017). The CSA report contains extensive detail and data related to most aspects of the site conceptual model.

### 2.1 Aquifer System Framework

The aquifer system at the Site is unconfined and includes three main hydrostratigraphic units consisting of a saprolite/transition zone, upper bedrock, and lower bedrock (Legrand, 1988). The saprolite/transition zone consists of partially to thoroughly weathered rock that ranges in thickness from 10 ft. to 30 ft. at the Site (SynTerra, 2015). The saprolite/transition zone is underlain by fractured metamorphic rock. The degree of fracturing is spatially variable and generally decreases downward. Vertical and horizontal fracture zones can cause localized zones of high permeability within the rock (Legrand, 1988; Miller, 1990). The permeability of the rock intersected by many of the bedrock wells is moderate, and it is inferred that the fracture density and hydraulic conductivity decrease downward (Legrand, 1988).

The saprolite/transition zone is saturated in the vicinity of streams and lakes where groundwater is discharging, but it is unsaturated in most upland areas. The water table occurs in the fractured bedrock in most upland areas. Ash is saturated within most portions of the ash basins and in these portions the localized pore water is connected to the local aquifer system. The ash material fills the three alluvial valleys (one valley for the WAB and two valleys for the EAB (eastern and western lobes)) with maximum thicknesses of approximately 80 ft.

Hydraulic conductivity values were determined in the field using slug tests. The hydraulic conductivity of the saprolite ranged from 2.9 feet/day (ft/d) to 3.5 ft/d with a geometric mean of 3.2 ft/d (SynTerra, 2015). The transition zone was tighter than the saprolite, ranging from 0.06 ft/d to 0.6 ft/d with a geometric mean of 0.2 ft/d (SynTerra, 2015). This difference may be affected by the small sample size with one slug test conducted in a saprolite well and four tests conducted in wells in the transition zone. The small sample size occurred because the saprolite and transition zone were saturated in only a few locations adjacent to the Plant NPDES treatment water bodies and areas associated with Hyco Lake.

The hydraulic conductivity of the bedrock spanned approximately 4 orders of magnitude ranging from 0.004 ft/d to 25 ft/d, according to the results from 44 slug tests. The 25% percentile is 0.1 ft/d, the 50% percentile is 3 ft/d and the 75% is 4 ft/d. It is inferred that the low end of the range characterizes the lower bedrock. The high values were probably measured at wells that intersect significant fractures zones in the shallow rock.

The hydraulic conductivity of the ash was measured by conducting a total of 17 slug tests at 7 wells completed in the ash. Hydraulic conductivity spanned 4 orders of magnitude, from 0.09 ft/d to 300 ft/d, with a geometric mean of 2 ft/d.

## **2.2 Groundwater Flow System**

The groundwater system is recharged by rain water and from water that infiltrates through the bottom of the ash basins. The average value of recharge was estimated from the map of recharge in North Carolina by Haven (2003) and from analyzing stream hydrographs. A shapefile of the recharge map by Haven (2003) was enlarged and features of the Site were superimposed. Colors on the map were compared to colors on the legend because quantitative data were unavailable from the file. This indicated that recharge was in the range of 6-10 inch/yr. in the watershed draining into the ash basins.

The stream flow in Hyco Creek was obtained from measurements made at the gauging station USGS 02077200 near Leasburg, NC. The gauging station is in Caswell County, approximately 10 mi SW of the Site, and measures flow from a watershed covering approximately 45.9 mi<sup>2</sup> to the south. Hyco Creek flows into Hyco Lake, which borders the Site. The analysis was conducted on 11 years of data starting in January 2002. The hydrograph was analyzed by separating stormflow and baseflow from the hydrograph using the method described by the Institute of Hydrology (1980). This method of hydrograph separation is widely used by the USGS and others. The separated hydrograph was analyzed using methods described by Mau and Winter (1997), and Rutledge and Mesko (1996) to estimate the recharge required to produce the observed baseflow. Recharge was estimated on a monthly basis and then averaged over the time period of the dataset. This resulted in an estimate of recharge that ranges from 3 to 7 inch/yr., depending on how the recharge is assumed to occur between baseflow turning points.

Recharge estimated using the hydrograph from Hyco Creek was generally less than that shown on from the map by Haven (2003), although the ranges from the two methods overlap. Both of these methods of estimating recharge have advantages and disadvantages, so it was assumed that the recharge to the upland areas was the average of the end members of the two methods, 0.0018 ft/d (approximately 7.9 inch/yr.). Further, it was assumed that recharge was negligible in the vicinity of the Plant, the lined phases of the industrial landfill, the FGD ponds, the lined gypsum storage area, and the low permeability dams. Recharge higher than the regional average was assumed on the unvegetated ash basins. Specific values assumed for the recharge are provided later in Section 4.4.

The EAB was originally developed in 1964 with the construction of an earthen dam, approximately 50 feet in height with a crest width of 15 feet, which impounded two creeks and created two lobes (eastern and western) within the basin. CCRs were deposited in the EAB by hydraulic sluicing operations in 1966. In 1973, the East Ash Basin dam was raised 20 feet to its present configuration. By 1983, hydraulic sluicing to the EAB was discontinued with the majority of the eastern lobe filled by the late 1980s. In 1986, the Roxboro facility converted to dry fly ash (DFA) handling resulting in the construction of the industrial landfill (Permit 7302), which was constructed partially in the waste boundary of the EAB. To allow development of the overlying industrial landfill, an earthen separator dike was constructed in the eastern portion of the EAB which formed a barrier separating the EAB from a portion of the former basin creating the eastern extension impoundment. The original landfill was unlined with subsequent synthetic lined phases constructed over the unlined area beginning around 2002 and in operation by 2004. The western lobe of the EAB was partly filled with ash and water in 1990. Presently, the western lobe is unvegetated and filled with ash to an elevation of approximately 470 ft., whereas the landfill on the eastern lobe rises to approximately 530 ft. The elevation of the top of the dam at the EAB is approximately 475 ft. A topographic map from the USGS Geospatial Database, and shown in the CSA, indicates the ground surface was between 390 and 400 ft. below the dam in the EAB.

The WAB was created in 1973 with the construction of an earthen dam (main dam) in the Sargents Creek stream channel. The main dam is an earth fill embankment with a central earth core constructed between two cofferdams over a prepared rock foundation with a central core

keyway excavated 10 feet into rock. In 1986, the main dam was raised 13 feet and a series of dikes (Dikes #1 through #4) and a discharge canal were constructed. A rock filter dike (Dike #1), constructed of rock fill with a sand filter blanket, was installed in the southern end of the WAB to enhance settling and retention time. The rock filter dike isolated the southern end of the WAB and created the southern extension impoundment. The distance measured within the basin from the main dam to the rock filter dike is approximately 4,700 ft. long. Water and ash enter the WAB at the northeast end of the basin near the Plant, and then the water flows to the south. A series of lined lagoons (FGD Ponds) were constructed on top of the northwestern corner of the WAB and are used to settle wastewater and solids formed during the desulfurization of flue gas.

Surface water runoff from the EAB is hydraulically connected to the WAB. Surface water flows to the north toward the dam of the EAB. The surface water is routed to the west where it enters the northeastern end of the WAB. Water carrying bottom ash also discharges to the northern end of the WAB. The process water flows to the south and through the rock filter dike to the southern end of the WAB, then into the western discharge canal. Flow is controlled by the spillway on the filter dike to keep the head in the south end of the basin lower than at the northern end. Process water flowing through the western discharge canal, positioned along the western side of the ash basin, discharges to the heated water discharge canal, which ultimately flows into Hyco Lake through NPDES Outfall 003 (Figure 1).

The surface of the WAB slopes gently to the southeast, where the elevation is approximately 465 ft. The ground surface elevation was between 390 ft. and 410 ft. along Sargents Creek prior to construction of the WAB dam.

The recharge in the ash basins is expected to be highly variable, ranging from essentially zero beneath the lined portions of the landfill to values greater than the regional average where the ash is flat and unvegetated. For example, the western lobe of the EAB and the WAB are unvegetated and the recharge there is expected to be between the 0.0018 ft/d (7.9 inch/yr.) and the average rainfall rate of 0.01 ft/d (45 inch/yr.). Recharge was estimated to be 0.004 ft/d in the ash basins.

Average water level elevations in four wells completed within ash of the EAB were remarkably consistent, ranging from 467 ft. to 469 ft. during baseline measurements. Three

wells are completed in ash of WAB with water level elevation from 463 to 464 ft. during baseline measurement. The stage of the EAB impoundment area east of the industrial landfill is approximately 465 ft.

Hydraulic heads were measured below the ash basins in nine locations. The heads in the underlying bedrock are similar, to slightly lower than the heads in the basins. This indicates that the ash and underlying bedrock are part of a continuous hydrologic system, and a component of downward flow from ash to bedrock occurs in some locations.

The hydraulic head in the ash basins is bordered regionally by heads of 500 ft. or higher in upland areas to the south with heads of approximately 410 ft. to the north at Hyco Lake (full pool is 410 ft.). On a more local scale, the hydraulic head between the ash basins and along a topographic ridge that trends toward the eastern lobe of the EAB is higher than within the ash basins themselves. The head is lower than the ash basins in a discharge canal that drains north from the EAB extension impoundment on the east side and a discharge canal on the west side of the WAB (Figure 1).

The distribution of observed hydraulic head indicates a general pattern of groundwater flow that differs between the two lobes of the EAB and the WAB. It is inferred, from the head measurements, that groundwater flow into the eastern lobe of the EAB is from uplands to the south and east, and flows north toward the cooling water intake canal on Hyco Lake and northeast to the discharge canal draining the extension impoundment to the east. Groundwater is inferred to flow into the western lobe of the EAB from the west, south, and east. Groundwater flow from the western lobe is inferred to occur to the north toward the Plant.

The distribution of observed hydraulic head indicates that groundwater flows into the WAB from upland areas located to the southeast. It is inferred from the head distribution that groundwater flows from the WAB to the north through and around the dam, as well as to the discharge canal to the west of the WAB. It is also inferred that flow occurs from the primary WAB through and beneath the filter dike in the south central end of the WAB because of elevated heads within the primary WAB.

### **2.3 Hydrologic Boundaries**

The major discharging locations for the shallow water system serve as hydrologic boundaries to the shallow groundwater system. These include lakes and streams.

### **2.4 Hydraulic Boundaries**

The shallow groundwater system does not appear to contain impermeable barriers or boundaries in the study area, but it does include hydraulic boundaries between zones of different hydraulic conductivity. The degree of fracturing, and thus the hydraulic conductivity, is expected to decrease with depth in metamorphic rock. This will result in blocks of unfractured rock where the hydraulic conductivity is quite low to negligible. However, isolated fractures may occur that result in large local hydraulic conductivities, and the locations of these fractures is difficult to predict or to comprehensively map. It was assumed that the rock was impermeable below the depth of the bottom modeled layer, and a no-flow boundary was used to represent this condition.

### **2.5 Sources and Sinks**

Recharge is the major source of water in the uplands and ash basins. Most of the groundwater discharges to streams and lakes, as previously discussed. Groundwater discharges into the ash basins and flows as pore water through the ash basins, which act as both a source of, and sink for, groundwater. Surface water occurs in both ash basins and comes from sluicing and wastewater inflows, groundwater discharge, and surface water runoff. Some surface water may infiltrate to recharge groundwater flowing under the dams at the northern ends of the ash basins.

Approximately 63 water supply wells have been identified in the vicinity of the Roxboro Plant (SynTerra, 2014), included as sinks in the groundwater model. Screen elevations and pumping rates from most of these wells are unknown. Woodland Elementary School has two wells to the southwest of the Plant, one of the wells is currently used for water supply. The model assumes both are active because the second may become active in the future and this is more conservative when considering potential receptors. Woodland Elementary School wells are the only public supply wells in the area. Another water supply well is used by CertainTeed Building Products Plant, a building materials manufacturing facility that makes drywall located to the northeast of the Roxboro Plant. The remaining wells are assumed to be domestic wells

that supply water to single family residences, largely in the upland areas southwest and southeast of the Plant. Water from some domestic wells was sampled by North Carolina Department of Environmental Quality (NCDEQ, formerly NCDNER) and used for chemical analysis. These data were consistent with ambient groundwater composition and there was no evidence of impact from ash basins. The wells are situated in distinct drainage basins/slope-aquifer systems separate and/or upgradient relative to groundwater flow from the Plant area and the ash basins.

Measurement data on the discharge rate from the water supply wells was unavailable, so an average discharge rate was used in the model. The average daily water use in North Carolina is 60 gallons (gals) to 70 gals per person (Treece et. al. 1990); therefore, a well providing water for a family of four people would be pumped at approximately 280 gal/day.

Residential sanitary waste water is disposed of through septic systems in the vicinity of the Roxboro site, which causes much of the water that is pumped from the aquifer to infiltrate into the vadose zone through septic drain fields. Radcliffe et al. (2006) studied septic drain fields in the southeast and found that 91% of the water used by a household was discharged to the septic drain field. This corresponds to a consumptive use of 9%. This is consistent with the data presented by Treece et al. (1990), who conclude that consumptive use is less than 6%. Daniels et al. (1997) developed a groundwater model of the Indian Creek watershed in North Carolina, which used the analysis of Treece et al. (1990) to characterize pumping and septic return rates. Septic systems were considered a source of water in the model.

## **2.6 Water Budget**

The long-term average rate of water inflow to the study area is equal to the rate of water outflow from the study area. Water enters the groundwater system through recharge, typically derived from rain but also including septic return, and leaves by discharge of surface water and water supply wells. The magnitude of components of the water budget are difficult to constrain using field data at the Site, but water budget details are derived from the groundwater model and will be provided in Sections 5.0 and 6.0.

## **2.7 Modeled Constituents of Interest**

Antimony, boron, chromium (total and hexavalent), cobalt, iron, manganese, molybdenum, pH, selenium, strontium, sulfate, total dissolved solids (TDS), uranium and vanadium were detected in the ash basin (pore) water at concentrations greater than 2L standards or IMAC values. These compounds are recognized as the constituents of interest (COIs) at the Roxboro site. Of these constituents, boron is the most prevalent in groundwater. Boron is present at relatively high concentrations in both ash basins and it was identified in groundwater outside of the ash basins at concentrations in excess of the 2L standard. Boron is rare in background samples from the vicinity of Roxboro, and it is unreactive and highly mobile. As a result, we infer that boron is a good indicator of the maximum extent of contaminants with a source in ash. For this reason, the following preliminary report will focus on boron. Other constituents have been evaluated using transport simulations and geochemical models. These results will be presented later.

The remaining constituents were not considered for the modeling exercise for one or more of the following reasons: 1) concentrations in the ash pore water do not greatly exceed background levels; and 2) there is no discernable plume of the constituent extending downgradient from the ash basins.

Many of the COIs identified from sampling the ash basin water were also identified in background wells including antimony, chromium (total and hexavalent), cobalt, iron, manganese, TDS, and vanadium. These constituents are commonly detected in groundwater in the Piedmont of North Carolina. Site background concentration ranges for these constituents are available from routine monitoring of the upgradient compliance boundary monitoring wells and background wells. These constituents did not form plumes that could be distinguished from background concentrations. Other constituents, like arsenic, are reactive and readily sorb, so their mobility is low.

## **2.8 Constituent Transport**

The COIs that are present in the coal ash dissolve into the ash pore water. As water infiltrates past the bottom of the basins, water containing COIs can enter the groundwater system. Once in the groundwater system, the COIs are transported by advection and dispersion,

subject to retardation due to adsorption to solids. During transport, dilution occurs as infiltrated pore water merges with the groundwater system. As the COIs reach surface water, they are no longer present in the groundwater system.

## **3.0 COMPUTER MODEL**

### **3.1 Model Selection**

The numerical groundwater flow model was developed using MODFLOW (McDonald and Harbaugh, 1988), a three-dimensional (3D) finite difference groundwater model created by the United States Geological Survey (USGS). The chemical transport model is the Modular 3-D Transport Multi-Species (MT3DMS) model (Zheng and Wang, 1999). MODFLOW and MT3DMS are widely used in industry and government, and are considered to be industry standards. The models were assembled using the Aquaveo GMS 10.3.2 graphical user interface (<http://www.aquaveo.com/>).

### **3.2 Model Description**

MODFLOW uses Darcy's law and the conservation of mass to derive water balance equations for each finite difference cell. MODFLOW considers 3D transient groundwater flow in confined and unconfined heterogeneous systems, and it can include dynamic interaction with pumping wells, recharge, evapotranspiration, rivers, streams, springs, lakes, and swamps.

This study uses the MODFLOW-NWT version (Niswonger, et al., 2011). The NWT version of MODFLOW provides improved numerical stability and accuracy for modeling problems with variable water tables. The improved capability is helpful in the present work where the position of the water table in the ash basin can fluctuate depending on the conditions under which the basin is operated and on the closure action activities.

MT3DMS uses the groundwater flow field from MODFLOW to simulate 3D advection and dispersion of the dissolved COIs including the effects of retardation due to COI adsorption to the soil matrix.

## 4.0 GROUNDWATER FLOW AND TRANSPORT MODEL CONSTRUCTION

The flow and transport model for this site was built through a series of steps.

- Step 1: Build a 3D model of the site hydrostratigraphy based on field data.
- Step 2: Determine the model domain and construction of the numerical grid.
- Step 3: Populate the numerical grid with flow parameters
- Step 4: Calibrate the steady-state flow model with adjustments of the numerical grid
- Step 5: Develop a transient model of historical flow to provide time-dependent constituent transport development.
- Step 6: Calibrate round 2 to ensure the flow model matched the observed heads and the transient model reproduced the observed plumes.

The current model is a revised version of a previous model. The process of revising the model involved using the original model as a starting point and following an iterative process of adjusting parameters until the model adequately predicted the observed heads and concentrations.

### 4.1 Model Domain and Grid

The initial steps in the model grid generation process were the determination of the model domain, and the construction of a 3D hydrostratigraphic model (Figure 3). The model has dimensions of approximately 4 miles by 3 miles, and with the long dimension trending N30E. This trend is parallel to the axis of Hyco Lake. The NW corner of this region was underlain by Hyco Lake and the model was set as inactive to the west of the approximate center of the lake. Portions of the model that were set as inactive are excluded from the numerical simulation. This configuration was selected so that most of the NW and SW sides of the model were bounded by Hyco Lake. The distance to the SE and NE boundaries of the model were made large relative to the area of interest in order to minimize the influence of outer model boundary conditions.

The ground surface of the model was interpolated from USGS NED n37w079 1/3 arc-sec 2013 1 degree IMG dataset obtained from <http://viewer.nationalmap.gov/viewer/>. The elevations for the top of the ash basin were modified using more recent surveying data from the WSP USA Aerial Topographic Survey from May, 2015.

The hydrostratigraphic model consists of seven units: Ash from the EAB, Ash from the WAB, Saprolite, Transition Zone, Upper Bedrock, Middle Bedrock, and Lower Bedrock. The hydrostratigraphic model was developed using “Solids” in GMS (Figure 3). Four solids were created and then subdivided after the computational mesh was developed. The solids include: ash, saprolite/transition zone, fractured rock, and unfractured rock. The ash solid includes the EAB and WAB hydrostratigraphic units. The saprolite/transition zone solid includes the Saprolite and Transition Zone units. The fractured rock solid includes the Upper Bedrock unit and top portions of the Middle Bedrock unit. The unfractured rock solid includes the lower portions of the Middle Bedrock unit and the Lower Bedrock unit. The lower contact between the ash basin and the underlying saprolite was assumed to be the ground surface prior to construction of the ash basins. An electronic file describing this surface was created by digitizing a preconstruction topographic map. The digitized points were interpolated to create a continuous surface representing the preconstruction ground surface, and this was used as the contact between the ash and the underlying saprolite. The lateral extent of the ash was determined from aerial photographs and maps in the CSA report (SynTerra, 2015).

The saprolite and transition zone were combined into the same solids model. The contact between the transition zone and underlying bedrock was determined by interpolating data measured in borings from the CSA report and historical data. This produced an isopach map of the thickness of the weathered zone (saprolite and partially weathered rock in the transition zone). The interpolated isopach surface was subtracted from the ground surface to create the contact used in the model. The methodology outlined above for creating a geologic model was done so the interpolated contacts would approximately follow the ground surface between boreholes, which are consistent with the expectations based on the hydrogeology of the Piedmont region (e.g. LeGrand, 1988; Miller, 1990). The upper fractured zone is approximately 100 feet thick, based on general field observations and data from boring logs interpretation.

The numerical model grid consists of 23 layers representing the hydrostratigraphic units. The model grid was set up to conform to the contacts from the solids. The model grid layers correspond to the solids as follows:

<u>Hydrostratigraphic layer</u>	<u>Grid layer</u>
Ash	1-8
Saprolite	9-11
Transition zone	12-13
Upper fractured rock	14-16
Middle fractured rock	17-20
Lower Rock	21-23

The numerical grid consists of rectangular blocks arranged in columns, rows and layers. There are 267 columns, 224 rows, and 23 layers (Figure 4). The maximum width of the columns and rows is 100 ft. The size of the grid blocks is approximately 50 ft. in the vicinity of the ash basins. The horizontal dimension of some of the grid blocks is as small as 25 ft. in the vicinity of the dams. Grid layers 1-8 were set as inactive outside of the region of the ash basin as determined from aerial photos and the CSA report. Grid layers 9-23 were set as inactive in the northwest corner of the model that represented region on the far side of Hyco Lake.

#### **4.2 Hydraulic Parameters**

The horizontal hydraulic conductivity and the horizontal to vertical hydraulic conductivity anisotropy ratio (anisotropy) are the main hydraulic parameters in the model. The distribution of these parameters is based primarily on the model hydrostratigraphy, with some additional vertical variation. Most of the hydraulic parameter distributions in the model were uniform throughout a model layer (Figure 5). Initial estimates of parameters were based on literature values, results of slug and core tests, and simulations performed using a preliminary flow model. The hydraulic parameter values were adjusted during the flow model calibration process described further in Section 5.0 to provide a best fit to observed water levels in observation wells.

#### **4.3 Flow Model Boundary Conditions**

The flow model outer boundary conditions are different for the different aquifer units. The outer lateral boundary conditions for the saprolite are almost entirely constant head, with small areas of no-flow locally. Boundaries on the west and northern parts of the model include parts of Hyco Lake. The head in the upper layer of the model was set to the stage of the lake (408 ft.).

The boundaries on the south and east sides of the model are independent of a definitive hydrologic feature. A constant head boundary condition with the head set 3 feet above the top of the saprolite layer was used along these boundaries. This boundary condition forces the water table to be in the top of the saprolite along the south and east boundaries, which is a reasonable approximation of the observed and expected conditions. The constant head boundary condition extends along the upland areas, but it is terminated within a few hundred feet of the locations of streams or lakes. This is because streams or lakes that intersect the boundary are defined by their own boundary conditions (as either constant head or drain-type boundaries). This creates short intervals of no-flow conditions between streams or lakes and the uplands in the saprolite.

The constant head boundary condition was assigned to layers 9-16, which is where most of the flow occurs. The underlying layers were set to no-flow.

The model boundary on the west and north sides of the model was set to constant head where it cuts across Hyco Lake or related water bodies. The boundary condition outlined above was used along the western and northern boundaries where the model cut across upland areas.

#### **4.4 Flow Model Sources and Sinks**

The flow model sources and sinks on the interior of the model consist of recharge, lakes, wetlands, streams, and groundwater pumping.

Recharge is a key hydrologic parameter in the model (Figure 6). As described in Section 2.2, the recharge rate for upland areas of the Roxboro was assumed to be 0.0018 ft/d (7.9 inch/yr.). The recharge rate was set to zero in the regions around the lakes that serve as groundwater discharge zones. The recharge rate in the Roxboro Plant was set to 0.0001 ft/d, due to the large areas of roof and pavement, and a similar value was assumed for the gypsum storage area. The recharge rate for the lined area of the industrial landfill in and around the EAB and the area of the lined FGD ponds on the WAB was set to zero (Figure 6). Recharge on the dams was set to  $10^{-5}$  ft/d because of the low permeability of these features. Recharge on the ash was assumed to be greater than ambient conditions. The recharge on the unvegetated western lobe of the EAB and all of the exposed parts of the WAB were set to 0.004 ft/d (approximately 2x ambient). Recharge was omitted from the southern end of the WAB (Figure 6) where standing water is present in the ash basin and southern extension impoundment.

Recharge to the exposed portions of the unlined area of the industrial landfill of the EAB was set to 0.004 ft/d. It is partly vegetated and the slopes are steeper compared to the EAB western lobe and the WAB. A portion of the unlined landfill area was recently covered with an engineered capping system, the recharge rate for that area was set to zero.

Figure 6 shows the distribution of recharge zones in the model, and recharge magnitudes are given in Table 3. Recharge was not adjusted much during the initial model calibration process, but it is included in the sensitivity analysis. The reason for not including recharge as a calibration parameter is that for steady-state unconfined flow, the hydraulic heads are determined primarily by the ratio of recharge to hydraulic conductivity, so the two parameters are not independent. In situations where the groundwater discharges to a flow measuring point (for example, a gauged stream in a watershed), the flow measurement can be used to calibrate the recharge value allowing both the recharge rate and the hydraulic conductivity to be simultaneously calibrated. However, no streams were gauged at the Roxboro site, so recharge was fixed.

Recharge was adjusted slightly during the model revision. The revision included reducing the recharge for the unlined area of the industrial landfill in the EAB to simulate liner placement. Heterogeneities were used in the vicinity of GMW-07 and GMW-08 to match the observed heads in the original model. Reducing the recharge allowed the heads to be adequately explained at those wells using average hydrostratigraphic properties.

Lakes and other water bodies were represented as constant head set to their stage (Figure 7). This includes Hyco Lake and NPDES treatment water bodies within the Plant that were assumed to be at the same stage as Hyco Lake. The full pool stage of Hydro Lake is 410 ft., but the lake stage was less than full pool when the calibration water levels were made, therefore 408 ft. was used for the stage in the model. The upper two layers of the model used to represent Hyco Lake are approximately 20 ft. thick. This is consistent with the bathymetry of the lake, however, the distribution of the lake bathymetry was unavailable; therefore, the lake depth was assumed to be uniform. The stages of NPDES treatment water bodies were determined from Light Detection and Ranging (LiDAR) data.

Streams were represented as Type 3 boundary conditions, called “drains” in MODFLOW (Figure 7). The elevation of the streams is set to the ground surface elevation determined from the LiDAR to account for small amounts of incision observed in the field. The drain conductance was set to 100 ft<sup>2</sup>/day, a relatively large value that will cause negligible head loss, and was not adjusted during calibration.

The ash basins were represented by simulating the observed surface water as specified head and applying recharge based on estimates from the current land cover. This approach treats the ash basins in the same way as other hydrogeologic components in the model, and it was selected as the best approach to characterize current conditions. However, the hydrologic conditions of the ash basins in the past differ from the current conditions. The ash basins appear as open water bodies in an aerial photograph from 1977. The stage of the water in the ash basins appears to be similar to water levels observed in wells presently.

Channels through the ash basins were represented as specified (constant) head, even though streams elsewhere in the model were treated as drains. This was done to allow water to flow into or out of the channels as they flow through the ash basins. Streams were only allowed to gain water from groundwater by treating them as drains.

The hydraulic history of the ash basins was represented by assuming present conditions to reasonably approximate the conditions in the basin since they were built. One exception is the distribution of recharge on the basin. The recharge was assumed to be equal to the ambient recharge in the uplands in the regions currently covered by the lined FGD ponds in the WAB and lined areas of the industrial landfill in the EAB. The recharge was assumed to decrease to negligible values at those locations in 2004 (Figure 6). In addition, the installation of a liner on and in the vicinity of a portion of the unlined landfill was assumed to reduce the recharge at those locations in 2014.

Little information is available about the public and private wells in the model area, other than their locations, which are shown on Figure 1 and Figure 2 (from SynTerra, 2015). Most of the wells are probably open boreholes in the upper 100 feet of bedrock. However, it is common for drillers in the Piedmont to extend wells to depths of several 100s of feet in an effort to intersect permeable fractures and create more productive wells. As a result, the depth of the

wells probably ranges from 150 ft. to 600 ft. The wells are assumed to be screened in grid layer 16 in the model.

The pumping rates from the wells were unknown, therefore it was assumed that the wells were pumped at 280 gals/day, which is an average water use for a family of four (Treece et al. 1990; North Carolina Water Use, 1987, and 1995). Septic return was assumed to be 94% of the pumping rate, based on Treece et al. (1990), Daniels et al. (1997) and Radcliffe et al. (2006). The septic return was injected into layer 11 (saprolite) in the model.

The wells used for water supply at the Woodland Elementary School and at the CertainTeed Building Materials plant were assumed to be pumped at a steady rate of 500 ft<sup>3</sup>/day. Approximately 280 students and staff are at the Woodland School, according to their website (<http://woodland.person.k12.nc.us/cms/One.aspx?portalId=23434&pageId=222558>). The website was accessed in 2016, but it is no longer available. It was assumed that approximately 20 percent of daily water consumption occurred at the school, and the daily water consumption was estimated using the data outlined above of 70 gal/day (280 gal/day for a family of four). No data was available for the CertainTeed Building Materials plant well and therefore a pumping rate was assumed. This assumption will be updated in the final model if data becomes available.

#### **4.5 Flow Model Calibration Targets**

The steady state flow model calibration targets were average water level measurements from 127 groundwater monitoring wells obtained through November 2017. For comparison, the previous flow model was calibrated with data from 111 wells obtained in October 2016. The flow model calibration target wells are listed in Table 1. In general, wells with an S designation at the end of the name are screened in the saprolite, wells with a D designation at the end of the name are screened in the transition zone, and whereas those with a BR designation are screened in the upper bedrock and a BRL designation are screened in the lower bedrock. Wells with ABMW are screened in ash.

The water levels used for calibration were determined by taking the average value for head data. Water levels are expected to vary on an annual period due to seasonal changes in recharge. These fluctuations in water level are not simulated because the flow model is steady state. The average water level values are the best available estimates of the steady state

hydraulic heads, so they were used for calibration. This approach differs from previous calibrations of the model where the most recent water level measurements were used. Water level data has been recorded during quarterly (seasonal) monitoring over the last three years which now allow calculation of statistically meaningful average water levels for most of the wells.

One exception was noted with the observed hydraulic heads considerably below the simulated hydraulic head (greater than 14 feet) in two locations (BG-01BRL and MW-23BRR (a replacement well for MW-23BR)). The hydraulic heads in these wells are extremely slow to respond after development and sampling, because the wells were completed in unfractured crystalline rock with a low permeability. The anomalously low water level measurement occurred because the wells had not equilibrated with the ambient heads when the water level was measured. These wells were not used in the calibration and are not included in Table 1.

#### **4.6 Transport Model Parameters**

The transport model uses a transient MODFLOW simulation to provide the time-dependent groundwater velocity field. The transient MODFLOW simulation was started January 1966, and continued through November 2017. The Roxboro Plant began operations in 1966, and the EAB was the first basin to receive ash. The history of the EAB is complex and included building a separator dike in the upstream end of the eastern lobe; creation of an industrial landfill; and development of a lined landfill. However, it is reasonable that the hydraulic head remained roughly similar from the time the basin was filled with water until present day. The implication is that the groundwater exchanged between the ash basins and the natural aquifer materials today is approximately the same as it was during sluicing operations. The flow model assumes that the ash basins fill with water quickly and the heads are maintained at the same level as they are today. As a result, a steady state calibration to the current conditions was used to simulate water flow during transport.

The key transport model parameters (besides the flow field) are the constituent source concentration in the ash basins, and the constituent soil-water distribution coefficients ( $K_d$ ). Secondary parameters are the longitudinal, transverse, and vertical dispersivity, and the effective

porosity. The constituent source concentrations were estimated from recently measured ash pore water concentrations in monitoring wells (SynTerra, 2015).

Ash leaching tests were performed on 2 samples from the EAB and 3 samples from the WAB using US EPA (LEAF) Method 1316. The leaching data were analyzed to develop a  $K_d$  (partition coefficient) value for boron in the coal ash.  $K_d$  of boron in ash in laboratory data ranged from 0.1 mL/g to 0.5 mL/g with a geometric mean value of 0.24 mL/g. A value of 0.4 mL/g was determined during calibration to field data. This value is within the range determined from the leaching data and is used in the model. The modeling approach for the predictive simulations of future boron transport allows the boron concentration in the ash to vary with time in response to flushing by groundwater. Using the  $K_d$  value that is derived from ash leaching tests ensures that the model response of the boron in the ash to groundwater flushing is realistic.

Linear adsorption  $K_d$  values for boron were measured in the laboratory using samples from the coal ash and native aquifer materials obtained from the Site (Langley and Oza, 2015). In general, the measured  $K_d$  values are highly variable, and the variability within a given material type was larger than the variability between different materials.

In light of the variability of the measured  $K_d$  values, it was decided that a conservative approach would be used for the  $K_d$  value in the model. The calibration process involved starting with the lowest value of  $K_d$  measured in the laboratory and then evaluating other values based comparisons to field data. In general, the  $K_d$  values that were ultimately selected were on the low end of the range that resulted in acceptable representation of the observed data. For example, the initial value for boron used in calibration was 5 mL/g, which is the summary value measured by Langley and Oza (2015). This value was adjusted from 0.02 to 1.0 mL/g during calibration for boron (Table 6).  $K_d$  values used in the original model were unchanged during model revision.

The longitudinal dispersivity was assigned a value of 20 ft., the transverse dispersivity was set to 2 ft., and the vertical dispersivity was set to 2 ft. The effective porosity was assumed to decrease with depth based on the hydrogeologic conceptual model, from 0.3 in the ash, saprolite and transition zone to 0.001 in the deep rock. It was assumed the effective porosity was uniform within a grid layer and was distributed according to:

<b>Layer</b>	<b>Effective porosity</b>
1-8	0.3
9-11	0.2
12-13	0.2
14-16	0.05
17-20	0.01
21-23	0.001

The dry bulk density of the porous media was assumed to be 1.6 g/mL. Dispersivity, porosity and bulk density were poorly constrained by the available field data, so the assumed values were fixed during the calibration process.

#### **4.7 Transport Model Boundary Conditions**

The transport model boundary conditions are no flow on the exterior edges of the model except where constant head boundaries exist, where they are specified a fixed concentration of zero. As water containing dissolved constituents enters these zones, the dissolved mass is removed from the model. The infiltrating rainwater is assumed to lack contaminants in most locations, and it enters from the upper active layer of the model.

The initial condition for the current conditions transport model (in 1966) is zero concentration of COIs in groundwater. No background concentrations are considered. The concentrations in the EAB are assumed to be at the observed concentrations at the start of the simulation. The concentrations in the WAB are zero at the start of the simulation and they increase to the observed concentrations in 1974 when the ash basin is created.

#### **4.8 Transport Model Sources and Sinks**

The ash basins are the primary source of boron in the model. These sources are simulated by holding the boron concentration constant in cells located inside the ash basins. Figure 8 gives the assumed distribution of boron concentrations in ash in 2017. This allows infiltrating water to carry dissolved constituents from the ash into the groundwater system. With the MODFLOW/MT3DMS modeling approach, it is critical that this source zone is placed in cells that contain water (not “dry cells”). Some of the cells in the ash basin were dry, so the specified concentration condition was placed in all 8 layers representing the ash. Soil as a secondary source is considered in the model.

Chemical analyses from seven wells were used to characterize the distribution of boron concentration within the ash basins. The concentration observed in the wells was assumed to represent the concentration in the vicinity of the well throughout the simulation. This resulted in a patch-like distribution of concentration within the ash basins (Figure 8).

During the model revision, the concentrations of COIs in the ash was subdivided into additional patches. This was necessary to explain the variation of concentrations observed in the wells installed along the periphery of the basins for compliance with the CCR rule.

The concentration of boron was specified in recharge parts of the model underlain by the unlined landfill between the eastern and western lobes of the EAB (Figure 8). The ash is above the water table in this area, so it was assumed the boron was dissolved as water flowed through ash in the vadose zone. The concentration of boron was specified in the recharge in this area to account for the overlying vadose zone source. Concentrations were adjusted to match observed concentrations during the calibration process.

Concentrations of boron beneath the gypsum storage area (Figure 8 and Figure 9) were specified to simulate observations in wells MW-03BR, GPMW-01S, GPMW-01D, GPMW-01BR, GPMW-02BR, and GPMW-03D. Assessments within the area were inconclusive as to the source of the boron in the gypsum storage area. Potential sources of the boron include dry fly ash used as structural fill beneath the gypsum storage area, the industrial landfill, or the adjacent ash basin. The recharge rate at the gypsum storage area was assumed to be approximately 0.5% of the average regional recharge, to account for a liner beneath the gypsum storage area.

The transport model sinks are the constant head lakes and streams. As groundwater enters these features, it is removed along with any dissolved constituent mass.

#### **4.9 Transport Model Calibration Targets**

The transport model calibration targets are boron concentrations measured in 124 monitoring wells in November 2017.

## 5.0 MODEL CALIBRATION TO CURRENT CONDITIONS

### 5.1 Flow Model

The flow model was calibrated in stages starting with a model that assumed homogeneous conditions in most hydrostratigraphic layers. In general, calibration was done by seeking the simplest configuration of parameters that matched the observed hydrogeologic conditions and the assumed or observed geologic conditions. The layer properties are homogeneous in many locations through the model domain. Several heterogeneities were assumed to improve the fit between the simulated and observed heads and concentrations (Figure 5).

The calibration was initiated using the geologic model to define the geometry of hydrogeologic units and assigning hydraulic conductivities typical of the region. The parameter estimation software PEST was then used to minimize the residual between predicted and observed heads during calibration of the original model. This resulted in reasonably close matches, however, there were several wells where the simulation significantly over- or under-predicted the heads.

#### Heterogeneities

The next step was to infer heterogeneities that could reduce the residuals. The model over-predicted the heads at several wells. It was inferred that these wells intersected or were near zones of relatively high permeability that were broad enough to extend toward a nearby stream or lake. This configuration reduced the head in the well, and the hydraulic conductivity of the zone was increased until either the head was reduced sufficiently, or an upper limit of hydraulic conductivity was reached (Figure 5).

As the calibration effort continued, some formations were given different properties in different layers. Many of model layer properties were homogeneous, except for discontinuities in the dams and in the Upper Rock hydrostratigraphic layer (Figure 5 and Figure 10). Flat-lying zones of interconnected fractures several hundred feet or more across were described in crystalline rock at the USGS Mirror Lake research site (e.g. Tiedeman et al. 2001), and similar fracture zones have been recognized at other fractured rock sites. Information about the fracture

zones at the Site was unavailable, so it was assumed that the fractures were shaped like flat-lying layers several hundred feet in maximum dimension, similar to those described by Tiedeman et al. (2001). Some of the inferred zones of high hydraulic conductivity are elongate and these are interpreted to be vertical fracture zones.

Volume balance and residuals

The final revised calibrated flow model has the following volume balance for the entire flow model:

<b>Volume balance in steady state model in ft<sup>3</sup>/d</b>		
<b>Feature</b>	<b>Input</b>	<b>Output</b>
Constant Head	43412	194140
Recharge	442703	0
Wells	0	3094
Septic field	1971	0
Drains (streams)	0	290852
Total	488086	488086

The difference between the input and output is less than 0.05 ft<sup>3</sup>/d, which is a volume balance error of less than 10<sup>-5</sup> consistent with the model constraint setup to assure inflow is equal to outflow. The major input to the model is from recharge with a lesser amount from constant head boundaries. The constant head boundaries creating input to the model are where groundwater is flowing into the model from the constant head boundaries around the periphery. The output is split between groundwater discharging to constant head boundaries and drains. The major constant head boundary is the Hyco Lake, and the drains represent streams. Less than 1 percent of the water input is removed through domestic wells, according to the model. The volume of water supplied by septic fields is slightly less than the water removed by the domestic wells.

The revised calibrated flow model has a mean head residual of -0.89 ft. and a root mean squared head residual of 4.73 ft. The total span of historical average head ranged over 123 ft, from 408 ft. to 531 ft. Using this range to normalize the residual gives a normalized root mean square error of 3.9%. A comparison of the observed and simulated water levels is listed in Table

1, and the observed and simulated levels are cross-plotted in Figure 11. Table 2 lists the best-fit average hydraulic parameters from the calibration effort. Most of the residuals between predicted and observed heads are less than 7 ft, and 18 residuals are between 7 ft and 14 ft (Figure 12). Cross-sections along the long axis of the ash basins show a water table that is near the ground surface in the ash basins and in the saprolite and transition zone in much of the uplands (Figure 13). The water table is in the upper fractured rock in some of the uplands near the ash basins, and this will play a role in the transport analyses.

#### Hydraulic conductivity

The hydraulic conductivity of the ash used in the model is 2 ft/d for both ash basins (Table 2), which is the approximate geometric mean of all the slug test values for ash (Figure 14). The sensitivity to these conductivities is low (Table 4). The highest calibrated hydraulic conductivity occurred in the ash and it progressively decreased with depth. The calibrated conductivity of the saprolite and transition zones is 1 ft/d. The hydraulic conductivity of the upper fracture rock is 0.3 ft/d and decreased to 0.005 ft/d and 0.002 ft/d with depth.

The calibrated values of hydraulic conductivity are consistent with values from the slug tests conducted in the ash, transition zone, and upper fractured rock. No tests were conducted below the upper fractured rock hydrostratigraphic unit, and testing in the saprolite was limited to one well.

#### Hydraulic head distribution

The computed heads in the transition zone (layer 13) show a high at the south end and a regional low at Hyco Lake (Figure 15). Ridges of high hydraulic head separate the two lobes of the EAB and western lobe of the EAB from the WAB.

#### Water budget

A water budget for the vicinity of the ash basins was determined from the results of the calibrated model. The water budget analysis identified a local groundwater flow system in the vicinity of the ash basins. This means that groundwater flows from the aquifer into a basin in some areas and it flows out of the basin and recharges the aquifer in other places. Groundwater flows into the WAB on the east side of the basin, and it flows out on the north and west sides,

and through the filter dike on the south side (Figure 15). The flow pattern associated with the EAB is variable, but in general groundwater flows into the EAB from the southeast and it leaves by flowing out to the northwest or by discharging to surface water. The local flow system is assumed to be bounded by a groundwater divide that extends from one end of the dam and wraps around the watershed to the other end of the dam (Figure 16). This definition implies that groundwater cannot enter the local ash basin flow system, but it can leave the system by flowing through or beneath the dam. The local groundwater flow system is assumed to be bounded by divides in the uplands and to extend beneath the ash basins and terminate upgradient from the dams (Figure 16). The dams were also used as a component of the water balance. This required recognizing flows into the dams or out from the dam areas into groundwater in areas peripheral to the dams. Zones were defined within GMS and the Zone Budget tool in MODLFOW was used to determine components of the water balance. The results were edited slightly to be consistent with the definition of the flow system.

Results indicate that for the WAB, the major inflow into the system is from surface water (133 gpm) and the secondary inflows are groundwater (74 gpm) and direct recharge (63 gpm). The major outflows from the system are to surface water (117 gpm) and groundwater (108 gpm) with minor losses through the dam (10 gpm) and filter dam (34 gpm). The major inflows into the EAB system are from direct recharge (35 gpm) and groundwater (27 gpm) with minor contributions from surface water (4 gpm). The major outflow from the system is to surface water (41 gpm) with minor outflows to groundwater (15 gpm), the dam (5 gpm), and the filter dam (5 gpm). The water balance for current conditions is summarized in Figure 16.

## **5.2 Flow Model Sensitivity Analysis**

A parameter sensitivity analysis was performed on the calibrated model by systematically increasing and decreasing the main parameters by factors of either 2 or 0.5 from their calibrated values. Table 5 shows the results of the analysis, expressed in terms of the normalized root mean square error (NRMSE) for each simulation. The NRMSE is calculated by taking the square root of the mean of the squared residuals between the predicted and observed values and dividing by the maximum difference in observed hydraulic head. The NRMSE for the calibrated flow model is 0.0385.

The flow model showed the highest degree of sensitivity to the regional recharge and to the hydraulic conductivities of the transition zone and the upper fractured rock stratigraphic units. The saprolite was largely unsaturated, so most of the groundwater flow is through the transition zone and upper fractured rock. The model was only weakly sensitive to the hydraulic conductivities of the ash and the deeper rock.

### **5.3 Potential Receptor Wells and the Ambient Groundwater Flow System**

The effect of pumping wells on the distribution of hydraulic head is manifested by a curved hydraulic head contour in the vicinity of the Woodland Elementary School wells on Semora Rd. along the west side of the simulated area, and a curved hydraulic head contour in the vicinity of the well at the CertainTeed Building Materials plant on the north side of the simulated area (Figure 15). This affect is minimal at both the Woodland Elementary School wells and CertainTeed Building Materials well and extends out less than a few hundred feet. These wells are assumed to be pumping at rates higher than the domestic supply wells.

Approximately 54 of the wells are located along Dunnaway Rd., McGhees Mill Rd., and Semora Rd., all of which lie along or near groundwater divides. Eight of the remaining wells are on Concord Church Rd., which trends roughly east-west and is upgradient from the WAB.

The water supply wells are located along groundwater divides and upgradient of the groundwater flow systems containing the ash basins. Groundwater flows past the water supply wells toward the ash basins, according to the model results. Water flowing past the Concord Church Rd. wells discharges to Sargents Creek, which discharges to the WAB (Figure 15). Groundwater flowing past the Dunnaway Rd. wells discharges to a stream upgradient from the west lobe of the EAB and groundwater flowing past the McGhees Mill Rd. wells discharges to the impoundment on the east side of the EAB (Figure 15). Wells along Semora Rd., including the wells used by the Woodland Elementary School, are on the divide or outside of the flow system containing the ash basins.

### **5.4 Transport Model Calibration**

The transient flow model used for transport consisted of a sequence of five steady-state flow fields:

- the period when the EAB was in operation (1966-1973);
- the period when both the East and WABs were present and receiving recharge (1974-2004);
- the period (2004-2008) when the recharge in the gypsum storage area was reduced when the geosynthetic clay liner (GCL) placed over the underlying dry fly ash structural fill;
- the period (2008-2014) when the recharge was reduced in areas of the industrial landfill and lined FGD pond areas; and
- the period (2014-present) when recharge was reduced south of eastern lobe of the EAB due to the additional Phase of the industrial landfill (Phase 6).

It is important to point out that the period when the ash basins were open water early in operation history is represented in the model by current conditions where only small parts of the basin is open water and the rest is ash. This is justified because the hydraulic heads in the ash basins are remarkably uniform (they vary by less than 3 feet). This is less than the uncertainty in the stage of the ash basins when they were open water. As a result, the interactions between the groundwater system and the ash basins filled with water would be similar to the interactions when the basins contain ash.

The effective porosity was assumed to decrease with depth to be consistent with the hydrogeological conceptual model. Other distributions of effective porosity were evaluated and it was found that the effect on the predicted concentrations was minor. The transport analysis for boron appears to be insensitive to effective porosity within a reasonable range of values.

Evaluation of the flow system during the calibration process indicated that several of the observed occurrences of boron could not be explained using sources solely from the ash basins. It was inferred that ash in the unlined portions of the industrial landfill and the gypsum storage area underlying structural fill must be acting as sources. The locations of these sources were added during calibration (Figure 9).

## **5.5 Transport Model Sensitivity**

A parameter sensitivity analysis was performed on the calibrated transport model by systematically increasing and decreasing boron  $K_d$  values from their calibrated values (Table 7).

The normalized root mean square error was calculated as the square root of the mean of the residuals between predicted and observed concentrations normalized to the maximum concentration. The calibrated model has a NRMSE of 0.063 (6.3%). Increasing or decreasing the  $K_d$  values by a factor of 5 increased NRMSE by factors of 0.007 to 0.04 (0.7% to 4.0%). This indicates that the value of  $K_d$  used in the model is near an optimal value.

## 5.6 Result of the Transport Simulation

The transport simulation was compared to chemical analysis for boron on samples from 124 wells. The simulated concentrations reasonably match most of the observed concentrations (Table 5). Many of the observation wells where boron was detected are in areas where the predicted concentration gradients are steep (beneath or adjacent to the ash basin, for example), therefore, small changes in location similar to the dimension of a grid block result in significant changes in concentration. This is one factor that explains the differences between predicted and observed concentrations.

Boron concentrations greater than 2L (700  $\mu\text{g/L}$ ) are widespread at shallow depths below and adjacent to the ash basins, according to the simulations (Figure 17). The basic pattern of boron concentration above 2L in the transition zone (Layer 13) of the EAB forms a U-shape that wraps around eastern end, and is open (boron less than 2L) on the western end of the EAB (Figure 17). There are three zones of boron concentration greater than 2L to the north of the EAB associated with the gypsum storage area. A zone of boron concentration greater than 2L occurs along the western and northern sides of the WAB. The pattern in the underlying shallow fractured rock (Layer 15) is similar to the transition zone, except the 2L boron contour is more irregular and covers a broader area. For example, there are zones of concentrations greater than 2L along the axes of the eastern and western lobes of the EAB, and along the eastern, upgradient side of the WAB in Layer 15, but boron concentrations are less than 2L in the overlying transition zone, according to the simulations (Figure 17). Boron concentrations are also above 2L in the results of simulations below the upper fractured rock.

Boron concentrations greater than 2L at the 500-ft. compliance boundary are predicted in five locations in the EAB, but it does not exceed 2L at any locations along the 500-ft. current compliance boundary in the WAB, according to the simulations (Figure 17). However, boron

concentrations are greater than 2L at two locations along the potential future 250-ft. compliance boundary used to evaluate the Excavation scenario in the WAB.

The seven zones where boron is greater than 2L at or near a compliance boundary will be used as reference locations for analyzing changes in boron distribution in simulations of transport following closure. Locations of these exceedance zones are shown in Figure 17 and in subsequent figures. The seven zones are the following;

- a.) Northeast zone, EAB
- b.) North zone, EAB
- c.) Gypsum storage area, EAB
- d.) Northwest zone, EAB
- e.) Southeast zone, EAB
- f.) Northwest zone, WAB
- g.) West zone, WAB;

Most of the zones where exceedances occur at the compliance boundary are in the vicinity of additional sources around the periphery of the EAB. Boron greater than 2L crosses and extends several hundred feet across the compliance boundary in a zone on the northeast side of the EAB. An additional source of relatively high concentration is inferred to occur in this vicinity based on calibration analyses using observed concentrations in monitoring wells (Figure 9) and it is the source of the elevated boron concentration in the northeast EAB zone (location a., Figure 17). The boron plume extends approximately 500 ft. from the source at this location and discharges to the east ash basin discharge canal.

Boron greater than 2L crosses the compliance boundary along the northern side of the EAB, according to the simulations (location b., Figure 17). This exceedance zone extends approximately 200 ft. from an additional source along the periphery of the EAB (Figure 9).

Exceedance zone c. is also related to an additional source along the northern side of the EAB (Figure 9). The length of the plume associated with this exceedance zone is a few 100 ft. The plume associated with location c. appears to be roughly 1,000 ft. (Figure 17); however, there are multiple factors influencing the observation. The available analytical data indicate that there are several sources of boron associated with the gypsum storage area, and these sources create plumes that are transported to the north toward the intake canal (Figure 17). Assessments within the area were inconclusive as to the source of the boron in the gypsum storage area. Potential

sources of the boron include dry fly ash structural fill beneath the gypsum storage area, the industrial landfill, or the adjacent ash basin. Boron is transported several 100 ft. across the compliance boundary at location c. (Figure 17) in the simulation where it merges with the boron sourced from the gypsum storage area. The long plume associated with location c. (Figure 17) is two plumes along the same flowpath in map view.

The northwest exceedance zone in the EAB (location d. Figure 17) is also a location where the size of the plume has been increased by merging with an additional source. In this case, the additional source is inferred to be associated with the dry fly ash handling facility to the west of the gypsum storage area, and slightly north of the compliance boundary. The source of the boron crossing the compliance boundary is an inferred additional source to the east of the primary EAB dam. The existence of this additional source is inferred from calibration of the model. Boron is also transported from the ash basin beneath the dam and the additional source in this vicinity. Boron is transported under the dam and discharges to Plant NPDES treatment water features at the base of the dam, although this plume is contained within the compliance boundary in the simulation.

The groundwater flow direction is to the south along the northern edge of the waste boundary of the EAB. This occurs because recharge outside of the lined portion of the industrial landfill creates an east-west trending ridge in the hydraulic head distribution along the northern edge of the landfill (Figure 15). Boron apparently occurs in dry fly ash structural fill material placed around the periphery of the landfill during historical operations, and some of this material occurs to the north of the divide created by the groundwater ridge. Northward groundwater flow on the north side of the groundwater ridge creates the plumes that extend across the compliance boundary in zones a.-d. (Figure 17).

Boron concentrations greater than 2L also cross the compliance boundary on the southeastern side of the EAB (location e. Figure 17). This zone occurs because the extent of the additional source is inferred to occur outside of the compliance boundary. The extent of the additional source is inferred by calibrating the model using measurements of boron concentration in the vicinity. The groundwater flow on the eastern side of this zone is inferred to be toward the northwest, or inward toward the ash basin. The flow direction swings to the southwest a few

hundred feet to the west; however, this causes boron to be transported toward the upstream end of the western lobe of the EAB (Figure 15 and Figure 17).

There are no locations where boron concentrations greater than 2L cross the 500-ft. compliance boundary in the WAB. This occurs because the groundwater flows out of the ash basin with discharge to the Heated Water Discharge Canal (part of the Plant's NPDES treatment system) which is within a few 100 feet from the waste boundary and results in a large decrease in boron concentrations. Groundwater also discharges to the discharge canal on the west side of the WAB, with lesser flows beneath the primary dam. There are locations near the potential compliance boundaries for the Excavation and Hybrid scenarios where boron concentrations exceed the 2L (locations f and g).

There is no evidence in the simulation that boron is transported to any of the pumping wells at concentrations above the 2L standard. This includes the domestic wells along with the wells at the Woodlands Elementary School and the CertainTeed plant. This is consistent with the simulation of hydraulic heads, which shows that the effect of the domestic wells and public supply wells on the simulated heads was indiscernible (Figure 15). Wells at the Woodland Elementary School and the CertainTeed plant affect the head contours in their vicinity, which can be seen by head contours that wrap around these wells (Figure 15). The well at the Woodland Elementary School is more than ½ mile from the WAB and there is a groundwater divide between the wells and the ash basin. Boron along the western side of the WAB discharges after a short flowpath to the canal along the western side of the ash basin. There is no evidence from the simulations that boron transport is affected by the Woodland Elementary School wells. The groundwater flow direction and significant distance to the WAB further support this conclusion.

Boron concentrations in proximity to the CertainTeed well to the north of the gypsum storage area are predicted to be less than 2L (Figure 17). The model predicts the occurrence of boron that originates in the vicinity of the gypsum storage area and discharges to the intake canal. The CertainTeed well is approximately 700 feet from the edge of the boron 2L exceedances where it discharges to the intake canal. The pumping rate of the CertainTeed well and the permeability distribution in the vicinity of the CertainTeed well are poorly constrained,

which causes uncertainty in the simulations of boron transport in the vicinity of the CertainTeed well. As a result, while the simulation results indicate that the CertainTeed well is unaffected by boron transport, the uncertainty in this result is greater than at the other wells.

The revised model includes the assumption that boron occurs in sediments in the EAB and WAB areas identified as extension impoundments upstream of the main portions of the EAB and WAB. The simulations show that groundwater flows toward and discharges into the extension impoundment areas. Pumping of supply wells is insufficient to alter this flow direction. As a result, boron assumed to occur in the EAB and WAB extension impoundment areas failed to identify any boron exceedance outside the impoundment areas. The boron in the EAB and WAB extension impoundment areas has no effect on the quality of water pumped from domestic or public supply wells in the general vicinity.

## 6.0 PREDICTIVE SIMULATIONS OF CLOSURE ACTION SCENARIOS

Once calibrated to current conditions, the model was used to predict future constituent distribution. This process involved a sequence of two simulations:

1. Interim conditions
2. Closure action

The simulation of interim conditions involves accounting for transport from the present to the time when the closure action is operational. This occurs over the next several years and involves lowering the water level without disturbing sediment, or decanting the ash basin pond especially the WAB. The second step involves simulating transport processes following closure action for several centuries or longer.

Three different types of closure actions were evaluated:

- Excavation
  - With Landfill - Remove ash while leaving the EAB industrial landfill in place. Dredge the EAB and WAB extension impoundments.
  - Complete - Remove the ash from both EAB and WAB and transport it to new on-site landfills located south of EAB and west of WAB, breach dams and dikes, dredge the EAB and WAB extension impoundments.
- Final cover – Cover the ash in both main basins with a low permeability cap and dredge the EAB and WAB extension impoundments.
- Hybrid design – For the WAB, excavate ash from selected locations and move to the vicinity of the FGD ponds where it is covered with a low permeability cap. For the EAB, excavate ash from the western lobe and move to the northern end of the basin where it is covered with a low permeability cap while leaving the EAB industrial landfill in place. Dredge the EAB and WAB extension impoundments.

Three different potential compliance boundaries were provided by Wood, Plc. for different closure scenarios and are shown in the simulation results.

The distribution of recharge, locations of drains, and distribution of material were modified to represent the different closure actions. For example, the recharge was modified from what is shown in Figure 6. The hydraulic head distribution was recalculated and the transport was simulated for each case. The closure action changed the hydraulic head in the vicinity of the ash basins as the engineered designs interacted with the hydrogeologic conditions. This interaction altered the groundwater flow and the transport of dissolved compounds.

There are three compliance boundaries used in the results.

- Final Cover scenario is evaluated using a compliance boundary that is 500 ft. from the current waste boundary.
- Excavation scenarios are evaluated using a compliance boundary that is 250 ft. from the current waste boundary.
- Hybrid scenario is evaluated using a compliance boundary 250 ft. from the final waste boundary.

The extent of field characterization below the upper fractured rock (below 50-100 ft. depth) is limited in some locations, and this causes uncertainty in the parameters controlling groundwater flow and transport in these locations. The periphery of the EAB is one example. Wells are scheduled to be drilled in late 2018 to depths of 300-400 ft. to evaluate the deeper rock at these locations, and data from these wells will be included in the calibration of the model in the future. It is expected that these data will reduce the uncertainty in the results of simulations. The results shown in the following pages of this preliminary modeling report will be limited to hydrostratigraphic layers equivalent to upper fractured rock, transition zone and saprolite because of the uncertainty in results for greater depths. Most of the groundwater flow occurs through these layers, so we expect that the results shown here will be representative of most of the mass transport occurring at the Site. Results from below the upper fractured rock are not within the scope of this preliminary report and will be presented in a future report.

The analyses included here use an average value for the hydraulic conductivity of ash that is based on measurements from 14 ash basins in North Carolina, as outlined in Section 5.1 (Figure 14). This hydraulic conductivity is expected to be an approximation of the properties of the ash at the Roxboro site. Pumping tests using wells completed in the ash in each basin are

being conducted in late 2018 at the Roxboro site. The results of these tests have not been analyzed as of the date of this report, however, they are expected to yield estimates of the ash properties that are more representative of site conditions than the average value used here. The simulations will be revised when the data from the pumping tests have been evaluated, and results from the revised simulations will be presented in a future report revision.

### **6.1 Interim Period with Ash Basin Pond Decanted**

Interim periods from the present to the completion of closure action construction were simulated to determine the initial conditions for the closure action simulations. The analysis began by simulating the boron distribution in year 2020 using a single steady-state groundwater flow field. Differences between the boron distribution using the sequence of five steady-state flow simulations described in Section 5.4 and the distribution using the single steady-state field are negligible. The boron distribution simulated in year 2020 was used as initial conditions for the Interim scenario. The simulations assume that the ash basin pond in the WAB is decanted in 2020, and is maintained with a head at a level of 446 ft. along the upgradient side of the filter dike. This is 1 ft. above the level of the extension impoundment on the south side of the filter dike. It was assumed that the open water features in the EAB and WAB are allowed to drain. By contrast, long-standing open water features that were maintained by sluicing were represented as specified head features in the model for current conditions. These features were switched to drains. The ambient recharge rate of 0.0018 ft/d was assumed to occur over the basins, and the concentration of boron in the recharge was assumed to be zero.

$K_d$  values were unchanged. The most significant change compared to the simulations of the current conditions is that the concentrations in the ash basin were allowed to vary with time.

It was assumed that construction of the Final Cover requires 10 years and the excavation process requires 20 years to complete. It was also assumed that the Hybrid option would require the same time to construct as for the Final Cover (10 years). This is based on an excavation rate of 1 Mton/yr. and a cover rate of 50 acres/yr. As a result, the interim simulation for the Final Cover and Hybrid scenarios are from 2020 to 2030, whereas it is from 2020 to 2040 for the Excavation scenario.

### Results from the Interim Simulation

Hydraulic head distributions during the interim period in the Transition Zone are similar to head distributions prior to decanting the ash basins (Figure 18 and Figure 15). During the interim period hydraulic heads within the WAB were reduced and the hydraulic gradients between the primary ash basin and the southern extension of the WAB decreased (Figure 18 and Figure 15). During the interim period both the EAB and WAB are hydraulically down-gradient from all domestic and public water supply wells in the region (Figure 18).

The results of the simulation show that the distribution of boron at concentrations greater than 2L varies slightly during the Interim period, and there is negligible change in status of boron exceedances at the compliance boundary. The boron concentration at the seven reference locations identified during the current conditions simulations (Figure 17) are largely unchanged in the transition zone and upper fractured rock during the interim period (Figure 19).

## **6.2 Excavation Scenarios**

Two scenarios involving excavation were simulated and are described below. One scenario involves excavation of the WAB and part of the EAB, while leaving the vicinity of the industrial landfill in the EAB in place. This scenario will be called the Excavation with Landfill scenario. The other scenario involves removal of all ash and placed in on-site lined landfills. The scenario will be called the Complete Excavation scenario.

Simulations of both Excavation scenarios use results from the Interim scenario at year 2040 for initial conditions. The boundary conditions, recharge and geometry were adjusted to represent excavation and the simulations were run to evaluate how the boron concentration changed with time. The design of the Excavation with Landfill scenario was based on the Closure Option 1 for the EAB and Closure Option 2 for the WAB, as outlined in AMEC Foster Wheeler (Wood PLC). The design of the Complete Excavation scenario was based on discussions with Duke engineers.

### Excavation with Landfill: Model Set up

The Excavation with Landfill scenario was simulated by assuming ash is removed and acts neither as a source of contaminants, nor as a component of the hydrogeologic flow system.

This is represented in the model by making layers 1-8 inactive, except for the landfill. It is assumed the ground surface is restored to the original topography, and the dam in the WAB is breached (Figure 20). This implies that streams may form in the newly exposed drainages, and part of the former WAB where the original ground surface is less than the level of Plant NPDES treatment water bodies is inundated. These conditions were simulated by including drain boundary conditions along the newly formed topographic drainages, and by including a region of fixed hydraulic head in the area of inundation (Figure 20). Water from the “drains” may need to be collected and treated and discharged per NPDES permit requirements. The filter dike is left in place, so the WAB extension impoundment area is unchanged and the head in the discharge canal to the west of the WAB is assumed to be equal to the current head. These features are unchanged in the model.

The industrial landfill in the EAB is assumed to be left in place. A zone along the western side of the landfill is graded down to the original ground surface. The “halo” region peripheral to the landfill (the unlined area that extends beyond the portion of the landfill with an engineered liner system) was assumed to be capped, along with a graded region on the western side of the landfill. This results in a capped area (Figure 20) where the recharge rate is assumed  $10^{-7}$  ft/d based on estimates of flow through an engineered cap conducted by AMEC Foster Wheeler (Wood PLC). Ash is assumed to occur under the capped zone at concentrations that start at the concentrations simulated in the Interim scenario.

Ash along the western side of the EAB extending north to the main dam is assumed to be excavated down to the original ground surface. The region behind the dam is assumed to be filled with clean material to create a grade that enables water to drain to the Plant NPDES treatment water bodies. This is represented by setting the initial concentration of this material to zero (stippled pattern in Figure 20). It is assumed that streams may form by groundwater discharge in the natural topographic drainages, or in a swale in the filled area behind the dam. The region will be graded so the primary drainage system in the EAB is developed in the western lobe, flows past the corner of the covered area and discharges to the Plant NPDES treatment water bodies. Drain boundary conditions are included to represent these drainage features. Recharge on the excavated area is assumed to be 0.0018 ft/d, the same as the ambient recharge rate on natural surfaces in the watershed.

Excavated ash is transported and placed in two newly constructed lined industrial landfills, located south of the EAB and west of the WAB. These industrial landfills would be constructed with a base liner system and a cap system. It is assumed that the recharge flux over the landfill would be  $10^{-7}$  ft/d based on estimates of cover performance conducted by AMEC Foster Wheeler (Wood PLC).

#### Excavation with Landfill scenario: Results

The hydraulic head changes markedly when the Excavation with Landfill scenario is implemented compared to the initial or interim periods. The change is particularly significant in the WAB where the base level of the heads is lowered by decanting free water and removal of ash. Heads are also lowered due to removal of ash on the western side of the EAB and due to drainage through a breach in the main dam in the EAB. In general, the hydraulic head contours wrap around the new drainage system (Figure 20). Closed head contours in the southern end of the WAB could be addressed by adjusting the grade of the excavated surface.

Lowering the hydraulic head causes the direction of groundwater flow to change. This is particularly significant along the western side of the WAB where groundwater flow is predicted to be westward toward the discharge canal during current conditions. Flow reverses direction and flows eastward as a result of the change in the drainage pattern during the Excavation scenario. The WAB canal is gaining groundwater along the southeastern side of the WAB (e.g. near the 460 ft. hydraulic head contour in Figure 20b), but there appears to be little interaction between the discharge canal along most of the western and northwestern side of the basin. Instead of interacting with the discharge canal, the groundwater flows past the discharge canal to discharge to the recently exhumed drainages where Sargents Creek was historically located.

#### Excavation with Landfill scenario: Spatial Distribution of Boron

The distribution of boron greater than 2L at the presumed future 250-ft. compliance boundary is similar to the plumes identified during current conditions (Figure 21). The extent of boron recedes with time and by year 2100, the areas greater than 2L at the 250-ft. compliance boundary have diminished in vicinity of the gypsum storage area and along the northwestern side of the WAB. Exceedances of 2L persist elsewhere in the EAB and along the western edge of the WAB. The distribution is largely unchanged by year 2250. By year 2350, the 2L contour has

receded in the WAB and no longer crosses the compliance boundary. However, boron concentrations greater than 2L persist at the compliance boundary along the northeastern and southeastern sides of the EAB (locations a, b, and e) in year 2350 in the transition zone (Figure 21).

Boron concentrations are less, and the extent of the 2L contour in the upper fractured rock (Layer 15) is limited compared to the overlying transition zone (Figure 22). This is particularly apparent along the northern and southeastern sides of the EAB. This occurs because the water table is below the transition zone in these areas. As a result, the concentration of boron in groundwater in the northeast and southeast portions of the EAB is better represented by the distribution in the shallow rock (Layer 15) than in the overlying transition zone (Layer 13) (Figure 22).

The simulations show boron concentrations greater than 2L at the compliance boundary at one location in the northeastern side of the EAB (location a) and one location on the western side of the WAB (location g) in year 2250, and these plumes have receded to within the compliance boundary by year 2350 (Figure 22).

#### *Excavation with Landfill scenario: Time Series Following Excavation*

Six reference locations were identified to summarize transient concentrations in the vicinity of the compliance boundary (Figure 23). Four locations (Point 1, Point 3, Point 4 and Point 6) in the EAB are where boron crosses the 500-ft. compliance boundary in the current condition simulation. Point 1 is in the vicinity of the Northeast exceedance zone, whereas Point 3 characterizes the Gypsum Storage Area zone and Point 4 characterizes the Northwest zone. Point 6 characterizes the Southeast exceedance zone.

Boron concentrations greater than 2L are contained within the 500-ft. compliance boundary in the WAB. Reference points 9 and 10 are located along an alternative compliance boundary 250-ft. from the waste, which will be used to evaluate the Excavation scenario. Point 9 is along the northwest corner, whereas Point 10 is along the western side of the WAB. More than 10 locations were evaluated and six were selected to represent the highest concentrations in their vicinity; however, the original numbering scheme was retained for the purposes of the preliminary report. The concentration time series start at the beginning of the simulations in

1966 and the end in approximately year 2500. The time series were taken from the shallow fractured bedrock represented by grid layer 15. The samples were obtained from approximately 50 ft. depth in the model. Specific depths for each point are given in Figure 24.

The general shapes of the time series are similar. The boron concentrations start at zero, increase with time to a maximum value between year 2020 and 2060, and then decrease and return to near-zero or zero concentrations. The boron value above the 2L is noted during operation of the ash basins at all locations. The maximum concentration occurs at Point 10 in the WAB. The concentration decreases during decanting and then increases at the start of the closure period at Point 10, according to the simulations. This behavior occurs due to high boron concentrations in ash near Point 10 that has resulted in high concentrations in the underlying saprolite, transition zone (Figure 21) and shallow rock (Figure 22). Groundwater flow is to the west during operation of the basin, which resulted in elevated concentrations between the basin and the discharge canal. However, the groundwater flow direction at this location reverses as a result of excavation. The change in flow direction causes the high concentration plume created during basin operation to be transported toward Point 10 where it causes the concentration to increase and eventually reach a maximum of 35,000  $\mu\text{g/L}$  in year 2060. Flow of groundwater from west of the basin causes the concentration to decrease to less than 2L at approximately year 2360 (Figure 24).

The reference location with the highest concentration in the EAB is at Point 1, where concentrations exceed 9,000  $\mu\text{g/L}$  in approximately year 2020. The concentrations decrease sharply at the onset of closure and they decrease to less than 2L in year 2160. The concentrations at the other locations reach maximum values at approximately 2020, but then decrease to less than 2L in a few decades, between years 2060 and 2100 (Figure 24).

#### Complete Excavation scenario: Model Set up

The Complete Excavation scenario was simulated by assuming ash and associated dams are removed and act neither as a source of contaminants, nor as a component of the hydrogeologic flow system. This is represented in the model by making layers 1-8 inactive. It is assumed the ground surface is restored to the topography prior to construction of the ash basins

(Figure 25). This implies that streams may form in the newly exposed drainages. Moreover, regions where the topographic surface is below the level of Hyco Lake will be inundated.

These conditions were simulated by including drain boundary conditions along the newly formed topographic drainages, and by including regions of fixed hydraulic head in areas where the elevation of the original topographic surface is below 410 ft. (Figure 25). Water from the “drains” may need to be collected and treated and discharged per NPDES permit requirements.

Recharge on the excavated area is assumed to be 0.0018 ft/d, the same as the ambient recharge rate on natural surfaces in the watershed.

#### Complete Excavation scenario: Results

The hydraulic head changes markedly when the Complete Excavation scenario is implemented compared to the initial or interim periods. The head change is particularly significant in the WAB where the base level of the heads is lowered by decanting and removal of ash. Heads are also lowered due to removal of ash in the EAB. In general, the hydraulic head contours wrap around the new drainage system (Figure 25).

Lowering the hydraulic head causes the inferred direction of groundwater flow to change. This is particularly significant along the western side of the WAB where groundwater flow is predicted to be westward toward the discharge canal during current conditions. Flow reverses direction and flows eastward as a result of the change in the drainage pattern during the Excavation scenario. The WAB canal is gaining groundwater along the southeastern side of the WAB (e.g. “V” shaped head contours near the 450 ft. contour label in Figure 25), but the water table is below the discharge canal upstream and downstream of this location, as evidenced by the straight hydraulic head contours. Instead of interacting with the discharge canal, the groundwater flows past the discharge canal to discharge to the recently exhumed drainages where Sargents Creek was historically located.

The hydraulic head gradients are considerably steeper in the Complete Excavation scenario near the landfill in the EAB than they are in the Excavation with Landfill scenario. This is because the heads decrease from approximately 460 ft. when the landfill is left in place (Figure 20) to less than 420 ft. when it is removed (Figure 25).

### Complete Excavation: Spatial Distribution of Boron

The distribution of boron in the Complete Excavation scenario in the WAB is similar to that of the Excavation with Landfill scenario, but the distributions are different in the EAB (Figure 26 and Figure 27). The extent of boron recedes with time in both scenarios and by year 2100, the areas greater than 2L at the 250-ft. compliance boundary have diminished in vicinity of the gypsum storage area and along the northwestern side of the WAB. Exceedances of 2L at the compliance boundary at 2100 years persist elsewhere in the EAB and along the western edge of the WAB, for example, at locations a. b. d. e. and g. in Figure 26 and Figure 27. The extent of the zones of boron concentrations greater than 2L crossing the compliance boundaries are generally similar between the two scenarios, but there are notable differences in shallow rock. The zone exceeding 2L in the vicinity of location e. is larger for the Complete Excavation scenario than it is for the Excavation with Landfill scenario in year 2100 (Figure 22 and Figure 27), for example. A similar, but smaller effect occurs near location c. These differences also affect the results of the time series presented below.

A difference between the boron distributions in the two excavation scenarios is evident in year 2250. Concentrations exceeding 2L are within the compliance boundary in year 2250 in the Complete Excavation scenario (Figure 26 and Figure 27), whereas they cross the compliance boundary when the landfill is left in place (Figure 21 and Figure 22). The difference in boron distributions in the two scenarios is greater in the transition zone than in the fractured rock. This is particularly apparent along the northern and southeastern sides of the EAB. This occurs because the water table is below the transition zone and recharge is small in these areas when the landfill is left in place. By comparison, boron concentrations are diminished by recharge and groundwater flow more rapidly when the landfill is removed.

### Complete Excavation: Time Series

The six reference locations used to summarize transient concentrations in the vicinity of the compliance boundary for the Excavation with Landfill scenario (Figure 23) were also used to evaluate the Complete Excavation scenario.

The general shapes of the time series for the two excavation scenarios are similar, and at several locations they are essentially identical. Notable differences occur at points 3 and 6 where

concentrations decrease to below 2L in the Excavation with Landfill scenario several decades sooner than they do in the Complete Excavation scenario (Figure 28). Point 6 is near location e., and it was pointed out above that the extent of boron concentrations greater than 2L is larger in the Complete Excavation than in the Excavation with Landfill scenarios. A similar effect occurs at location c. in Figure 22 and Figure 27.

These findings show that even though the overall boron distribution in the Complete Excavation scenario decreases more rapidly than it does in the Excavation with Landfill scenario, the times when concentrations decrease to 2L at the compliance boundary can be longer for the Complete Excavation scenario. This occurs because the transport rate of boron in the subsurface during current conditions increases toward the compliance boundaries when the landfill is excavated compared to when it is left in place. The increased transport rate causes local increases in boron concentration near the compliance boundary, such as in the vicinity of locations c. and e.

The results indicate that the time for concentrations to decrease to 2L at Point 10 for the Complete Excavation scenario is several decades less than the time for the Excavation with Landfill scenario (Figure 28). Point 10 is in the WAB and the two excavation scenarios are similar in the WAB. The different responses at Point 10 occur because the location of the drainage in the vicinity of Point 10 for the Complete Excavation model was slightly different from the location used in the Excavation with Landfill model. The Complete Excavation model was completed several months after the Excavation with Landfill model and the drainage was adjusted slightly to improve the accuracy of the model. Future versions of the Excavation with Landfill model will use this revised drainage and this will cause the boron time series at Point 10 to be essentially identical. As a result, the differences in the responses at Point 10 in Figure 28 do not reflect differences in the performance of the two Excavation scenarios.

### **6.3 Final Cover Scenario**

Simulations of the Final Cover scenario use results from the Interim scenario at year 2030 for initial conditions. The boundary conditions, recharge and geometry were adjusted to represent the Final Cover scenario and the simulations were run to evaluate how the boron concentration decrease to less than the 2L. The design of the model was based on the closure

options outlined in AMEC Foster Wheeler (Wood PLC) Option 1 for the EAB, and for the WAB the design is modified from Option 5/6 in AMEC Foster Wheeler as outlined in AMEC Foster Wheeler (Wood PLC).

### Model Set Up

The Final Cover scenario was simulated by assuming ash is graded to drain along a path similar to the underlying topography, and then the graded surface is capped with a low permeability cover that limits infiltration. The capped area includes the current extent of ash (Figure 29). It was assumed that the cap will be extended to cover the structural fill area that extends beyond the industrial landfill footprint around the periphery of the EAB. The industrial landfill in the EAB will be left in place. It is assumed that the recharge flux over the covered area would be  $10^{-7}$  ft/d based on estimates of cover performance conducted by AMEC Foster Wheeler (Wood PLC).

Drains will be used to lower the hydraulic head beneath the cover (Figure 29). The drains are 5 ft. below the graded surface of the ash. Drains are included in the WAB and in the western side of the EAB. Drains are not included in the central and eastern side of the EAB beneath the existing landfill (Figure 29). It is assumed that water from the drains would be collected, treated and discharged as required by the NPDES permit. The actual drains in the ash were represented by boundary conditions called “drains” in MODFLOW. The use of “drain” boundary conditions assumed the actual drains had idealized behavior. For example, a “drain” boundary condition allows water to flow from ash into the drain, but it prevents water from flowing from a drain into ash. The analysis also ignores head losses that might occur due to localized pore clogging in the drain. It also ignores head losses due to flow along the drain. These assumptions are consistent with a goal of evaluating transport characteristics during the Final Cover scenario, but additional calculations beyond those shown here will be needed to fully evaluate the hydraulic performance of drains in the ash. The transport model was set up using flows from the groundwater model. The distribution of boron concentrations in 2030 from the interim simulation was used as the initial concentration conditions.

The simulation was started in 2030 and run for 1,000 years. Results were saved every few years early in the simulation and the interval between the saved results increased with time.

This causes the temporal resolution to be finer at early time than it is later in the simulation when changes are expected to be slow.

### Results

The hydraulic head distribution from the Final Cover scenario simulation is controlled by the drains beneath the cap. The heads are equal to, or below the level of the drains at the drains and they are generally slightly above this level between the drains. The hydraulic head in the covered area (Figure 29) was compared to the level of the cap in the current design and the results indicate that the head is below the cap. The hydraulic heads are lower than during the current conditions, although the general pattern of the head distribution and the directions of groundwater flow are similar to current conditions (Figure 29). The flow direction is predicted to change in a few directions, but the effect of these changes on the boron transport is minor.

### Spatial Distribution Following Final Cover

Boron concentrations greater than 2L cross the compliance boundary in year 2040 in five locations in the EAB, and concentrations of this magnitude are contained within the compliance boundary in the WAB. The plumes in the EAB recede with time, but the simulations indicate values above 2L occur in the transition zone (Layer 13) in the southeast exceedance zone in year 3030 (location e., Figure 30).

The long persistence of high boron concentrations in Layer 13 (Figure 30) occurs in areas where these cells are in the vadose zone above the water table. Transport through the vadose zone is slow beneath the cover, which accounts for the persistent concentrations in Layer 13.

Boron concentrations in fractured rock (Layer 15) provide a better representation of the concentrations that would be expected in groundwater (Figure 31). In Layer 15, boron concentrations cross the compliance boundary in several locations in year 2040, but they recede over the next few decades. Boron concentrations in greater than 2L cross the compliance boundary at the northeast and southeast zones (locations a. and e.), and the 2L boron contour abuts the compliance boundary in the northwest zone (location d. Figure 31) in year 2100. By year 2230, boron concentrations have receded to within the compliance boundary everywhere

except at the northwest zone where the 2L contour abuts the compliance boundary (location d. Figure 31).

#### Time Series Following Final Cover

The highest concentration at the reference locations occur at Points 10 and 1, the same points as during the Excavation scenario. The concentration at Point 10 decreases with time and falls below 2L at approximately year 2360. Concentration at Point 1 decreases below 2L at approximately year 2160, and similar times to reach 2L occur at points 4 and 9. The concentrations reduce to 2L earlier than year 2160 at Points 3 and 6 (Figure 32).

The time series for the Final Cover scenario (Figure 32) differ compared to the concentrations predicted for the Excavation scenario at some locations (Figure 24 and Figure 28), but there are some important similarities. The time for the concentrations to reach 2L for the two points with the highest concentrations is similar between the two scenarios. It occurs in approximately year 2160 at Point 1 in both scenarios. The time series at Point 10 have different shapes, but they both reach 2L in approximately 220 years (between years 2320 to 2360). The time to reach 2L at the Points 3 and 6 is approximately 2100 for Excavation with Landfill and Final Cover scenarios, and approximately 2120-2140 for Complete Excavation scenario. The most significant difference occurs at Points 4 and 9 where the 2L concentration is reached in year 2060 during the Excavation scenario (Figure 24 and Figure 28), but it takes 70 to 130 years longer to reach 2L for the Final Cover scenario (Figure 32).

#### **6.4 Hybrid Design Scenario**

Simulations of the Hybrid scenario use results from the Interim scenario from year 2030 for initial conditions. The boundary conditions, recharge and geometry were adjusted to represent excavation and the simulations were run to evaluate how the boron concentration changed with time. The design of the model was based on the closure options outlined as Option 3 for the EAB and Option 4 for the WAB in AMEC Foster Wheeler (Wood PLC).

#### Model set up

The Hybrid scenario involves excavating ash from the south and east sides of the WAB and transporting it to the northwestern side of the WAB, where it is capped with a low

permeability cover. Clean fill is used to adjust the grade so water accumulating in the footprint of the WAB would flow to the north at a grade of 0.5% and discharge to the heated water discharge canal.

The Hybrid design assumes ash in the western lobe of the EAB is removed and this area is filled with clean material. The periphery of the industrial landfill in the EAB is covered with a low permeability cap to limit infiltration into the unlined area of the landfill and structural fill around the periphery. The western end of the EAB is graded to slope to the west.

The Hybrid design is represented by using a recharge rate associated with a low permeability cap ( $10^{-7}$  ft/d) over the covered areas (based on estimates of cover performance), and a rate equal to the recharge under natural conditions (0.0018 ft/d) in the areas where ash is removed or in areas where ash was removed and replaced with clean fill. The hydraulic conductivity of the fill was assumed to be equal to the hydraulic conductivity of ash.

Drains were included in the model along swales in the surface grading. The elevation of the drains in the WAB was selected to maintain a 0.5% slope, according the specifications in the closure design. Elevations of the drains in the EAB were selected so the drains would slope toward the discharge point on the western side of the EAB. It is assumed that water from the drains be handled as required by the NPDES permit. Drains used in the model and shown in Figure 33 are assumed to be at the ground surface in areas that are not covered, and they are assumed to be below grade in covered areas. The actual drainage paths shown in Figure 33 are represented in the model using “drain” boundary conditions in MODFLOW. These “drains” act as sinks for groundwater, but the model does not include effects of surface water flow. The drains are also idealized in that the head losses due to flow along the drain, and head losses that might occur due to clogging in the vicinity of the drain. These assumptions are consistent with a goal of evaluating transport characteristics during the Hybrid scenario, but additional calculations beyond those shown here will be needed to fully evaluate the hydraulic performance of drains.

The transport model was set up using flows from the groundwater model. The distribution of boron concentrations in 2030 from the interim simulation was used as the initial concentration conditions.

The simulation was started in 2030 and run for 1,000 years. Results were saved every few years early in the simulation and the interval between the saved results increased with time. This causes the temporal resolution to be finer at early time than it is later in the simulation when changes are expected to be slow.

### Results

The hydraulic head slopes to the northwest in the WAB following the grade of the axial drain (Figure 33). The axial drain causes the heads along the axis of the basin to be lower than in the Final Cover scenario (Figure 29). This causes the flow direction to change from west to east in the western side of the WAB. The change in flow direction is similar to the change that occurs in the simulation of the Excavation scenario. However, the covered area in the Hybrid design affects the details of the flow direction. As a result, the flow direction in the vicinity of location g. in Figure 33 and Point 10 (Figure 23) during the Hybrid simulation is more to the north compared to the results of the simulation for the Excavation scenario. This causes the concentration time series for the Excavation scenario (Figure 33) to be quite different from the time series for the Hybrid scenario, even though the groundwater flow direction reverses in the vicinity of Point 10 in both scenarios.

Closed, head contours at the upstream end of the western lobe of the EAB are low points in the hydraulic head surface that results from changes in the grades of the natural material and the clean fill. Refinements in the detail of the grade would avoid the formation of these local depressions.

### Spatial Distribution Following Hybrid Scenario

The distribution of boron is similar to the other scenarios. Some significant differences emerge, however, when the boron distribution is evaluated relative to the presumed future compliance boundary. The compliance boundary for evaluation of the Hybrid scenario is 250-ft. from the limit of waste in the hybrid design. This results in a compliance boundary that is co-located with the compliance boundary used for the Excavation scenario in some locations, and within that boundary in other locations (Figure 34 and Figure 35). The result is that there are more zones where the 2L boron concentration contour crosses the compliance boundary in the Hybrid scenario as compared to the other two closure scenarios. For example, in Layer 15 and at

year 2230, there are two locations where the 2L contour crosses the compliance boundary in the EAB and one location where it crosses the compliance boundary in the WAB. There is another location at the main dam in the WAB where the 2L boron concentration contour abuts the compliance boundary (Figure 35).

#### *Time Series Following Hybrid Scenario*

The time series data are all taken at the same locations for the other closure scenarios, so they are located independently of the closure-specific compliance boundary. Points 9 and 10 are on the Hybrid compliance boundary, whereas the other points are outside of the boundary (Figure 23). The maximum concentration in the Hybrid scenario occurs at Point 10 (Figure 36), as in the other scenarios. The concentration decreases to 2L in the Hybrid scenario, but it takes longer for this to occur than in the other cases. The boron concentration decreases to 2L in approximately year 2460 at Point 10, for example, but in the Excavation and Final Cover scenarios, it reaches 2L roughly 100 years earlier in year 2360. The results elsewhere indicate that 2L is reached at approximately year 2160 at Points 1, and 4, and year 2100 at Points 3 and 6 (Figure 36). Those results are similar to the findings for the Final Cover. The most significant improvement in performance occurs at Point 9 in the EAB where concentrations decrease to 2L in year 2060 (Figure 36), but another 100 years is required to reach 2L in the Final Cover scenario (Figure 32).

## **6.5 Conclusions**

A groundwater flow and transport model was developed based on a hydrogeologic conceptual model typical of the Piedmont physiographic province, and this model was calibrated using hydraulic heads and chemical analyses from more than 100 sampling wells in the vicinity of the Roxboro site. Pumping wells used for water supply to homes, a school, and a business in the vicinity of the Roxboro site were also included in the model.

The NRMSE between predicted and observed heads is less than 4 percent, which is small. The residuals between predicted and observed boron concentrations are small enough to give confidence that the model provides a reasonable representation of conditions at the Roxboro site.

The calibrated model was adjusted to represent conditions that would occur during four closure scenarios, termed Excavation with Landfill, Complete Excavation, Final Cover, and Hybrid, which are outlined in the closure options analysis (AMEC Foster Wheeler). The simulations were conducted to simulate 1,000 years into the future, and the results describing the distribution of boron concentration were used to evaluate the performance of the three closure scenarios.

Three closure-specific compliance boundaries were used to evaluate the results based on regulatory permit requirements. The 500-ft. compliance boundary was delineated 500-ft. from the current waste boundary and used to evaluate the Final Cover scenario. The 500-ft. compliance boundary was also used to evaluate current conditions. A compliance boundary 250-ft. from the current waste boundary was used to evaluate the two Excavation scenarios. Another boundary 250-ft. from the waste boundary in the hybrid design was used to evaluate the Hybrid scenario.

#### *Boron exceedances at the 500-ft. compliance boundary*

Under current conditions, boron is predicted to exceed the 2L standard of 700  $\mu\text{g/L}$  at the 500-ft. compliance boundary at five locations in the EAB, and at no locations in the WAB (Figure 17). The existence of the boron source material outside the waste boundary is inferred based on calibrating the model to observed concentrations (Table 5), and it is consistent with the known occurrence of structural fill around the periphery of the EAB, in an area called the “halo zone.” The boron source material is within a few 100 ft. of the compliance boundary. Boron sources occur in the southeastern corner of the EAB outside of the compliance boundary, according to the model.

The distance that boron is transported is less than 1,000 ft., and in many locations it is less than a few 100 ft. from a boron source. The most prominent plumes with concentrations greater than the 2L standard occur along the northeastern and northwestern sides of the EAB. Two zones of boron that appear to be particularly long plumes in the vicinity of the gypsum storage area (Figure 17) are actually multiple shorter plumes that have merged together. In both cases, a plume with a source in the peripheral halo zone of the EAB merges with a plume sourced in the vicinity of the gypsum storage area.

### Boron in the WAB

Under current conditions there are no locations where boron concentrations greater than the 2L standard cross the 500-ft. compliance boundary in the WAB (Figure 17). This occurs because the groundwater flows out of the ash discharge to the Heated Water Discharge Canal within a few 100 ft. from the waste boundary. Most groundwater discharges to the canal on the west side of the basin, and some flow beneath the main dam on the north side of the WAB.

### Comparison of boron concentration distributions in the future

The distribution of boron in the saprolite and rock adjacent to the ash basins resulted from hydrologic and mass loading conditions during operation of the ash basin. These conditions will change during the interim period when free water in the ash basins is decanted and during closure as ash is regraded, removed and/or covered. When implemented in the model, these changes cause the head to drop and the direction of groundwater flow to change in some locations (Figure 20, Figure 25, Figure 29, and Figure 33). Changes are larger in the WAB than the EAB, where the landfill is left in place for all the closure scenarios.

Groundwater flow directions reverse on the western side of the WAB relative to the initial conditions for the Excavation and Hybrid scenarios (Figure 20, Figure 25, and Figure 33). The flow directions change locally and the head gradients flatten as the groundwater flow through the ash decreases in the Final Cover scenario (Figure 15 and Figure 29).

Changes in the groundwater flow through the EAB are modest in the Excavation with Landfill, Final Cover, and Hybrid scenarios. The flow direction changes locally in response to drains in the Excavation with Landfill scenario, but only limited changes occur in the groundwater flow system around the periphery of the EAB where the contaminants cross the compliance boundary. This explains why the response at the compliance boundary around the periphery is similar for the three scenarios. Changes in the groundwater flow through the EAB are more significant in the Complete Excavation scenario due to the increase in recharge rate over the excavated landfill footprint.

The simulations indicate (Figure 21 and Figure 37) that in year 2240 boron concentrations greater than 2L in the transition zone (Layer 13) will cross the closure-specific compliance boundaries at several locations along the northern EAB for the two Excavation

scenarios and the Hybrid scenario, and reach the northern closure-specific compliance boundary for the Final Cover scenario. Simulations indicate that in year 2240 boron concentrations greater than 2L in the transition zone (Layer 13) will cross the closure specific compliance boundaries at the southeastern corner (location e.) of the EAB for all scenarios except for the Complete Excavation scenario. Simulations indicate that in year 2240 boron concentrations greater than 2L extend to the western side of the closure-specific compliance boundaries for the Excavation and Hybrid scenarios in the WAB (location g.). Boron is persistent in Layer 13 in the simulations with landfill left in place because much of the periphery of the EAB is above the water table, and transport through the vadose zone is slow in the model. A source of boron is inferred to occur outside the compliance boundary in location e. In comparison, boron concentrations are diminished by recharge and groundwater flow more rapidly when the landfill is removed, as shown in the Complete Excavation simulation (Figure 37 and Figure 38).

The extent of boron contamination in 2240 is smaller in the shallow rock (Layer 15) than in the overlying transition zone (Figure 37, Figure 21, and Figure 22). This occurs because the shallow rock is largely below the water table and the boron is more mobile than in the overlying vadose zone. As a result, the distribution of boron in the top of bedrock (Layer 15) in Figure 37 and Figure 22 is likely more representative of the concentrations in groundwater than the distribution in the transition zone (Layer 13).

The results for the shallow rock (Layer 15) indicate that boron in excess of 2L crosses the closure-specific compliance boundary in year 2240 in the EAB at one location for the Excavation with Landfill, Complete Excavation, and Final Cover scenarios and at two locations for the Hybrid scenario (Figure 37 and Figure 22). Boron in excess of 2L crosses the compliance boundary in year 2100 but it is within the compliance boundary by year 2250 for the Complete Excavation scenario (Figure 37). In the WAB, boron concentrations greater than 2L cross the closure-specific compliance boundary at location g. in the two Excavation scenarios and the Hybrid scenario, but not the Final Cover scenario (Figure 38 and Figure 22).

Simulations indicate that in the transition zone (Layer 13) in year 3040 there are exceedances of the 2L standard for boron beyond the northern closure-specific compliance boundaries in the EAB for the Excavation with Landfill and Hybrid scenarios (Figure 38 and

Figure 21). Exceedances extend to the northern closure-specific compliance boundary for the Final Cover scenario in the transition zone (Layer 13) in year 3040 (Figure 38). Simulations indicate that boron concentrations greater than 2L occur in the above three scenarios at the closure-specific compliance boundaries along the southeastern portion of the EAB (location e.) in year 3040. In year 3040 boron concentrations greater than 2L only occur at the western WAB compliance boundary for the Hybrid scenario (Figure 38). There is no exceedance in the Complete Excavation scenario anywhere in the transition zone in year 3040 (Figure 38).

The distribution of boron in the top of bedrock (Layer 15) in year 3040 (Figure 38 and Figure 22) shows that there are no exceedances at compliance boundaries in groundwater for the four closure scenarios. However, boron concentrations do exceed the 2L standard within the compliance boundary for all closure options.

Boron concentrations greater than 2L occur in the simulations at depths below the shallow fractured rock represented by grid layer 15. Details of the distribution of boron in the deeper rock are uncertain because only a few wells in the deeper rock are available at Roxboro. Additional deeper wells are being drilled and data from those wells will be used to sharpen the constraints on the distribution of boron. These results will be included in a later report.

#### Comparison of boron time series

Time series results from the four closure scenarios at reference locations are virtually identical (Figure 39). The relative performance at the other locations is variable. At location 3 the boron concentration drops below 2L in approximately year 2080 in the Excavation with Landfill, Final Cover, and Hybrid scenarios, but takes approximately another 30 years to reach the 2L limit in the Complete Excavation scenario. At location 4 the boron concentration in both Excavation scenarios drops below 2L in approximately year 2060, but it takes approximately another 100 years to reach the 2L limit in the Final Cover and Hybrid scenarios. At location 6 the boron concentration drops below 2L in approximately year 2100 in the Excavation with Landfill, Final Cover, and Hybrid scenarios, but takes approximately another 50 years to reach the 2L limit in the Complete Excavation scenario. At Point 10 there are two concentration peaks for the two Excavation scenarios and only one peak for the other closure scenarios. The second peak occurs because flow directions change due to construction of the closure scenarios resulting in

high concentrations being transported towards Point 10 during the Excavation scenarios, but away from it for the other closure scenarios. After the second peak for the two Excavation scenarios the boron concentration rapidly falls off (Figure 39). Boron concentrations at Point 10 reach the 2L standard for the Excavation scenarios between year 2280 and year 2350. They reach 2L at Point 10 for the Final Cover scenarios around year 2380, and for the Hybrid scenario around year 2480 (Figure 39). The difference between the times to reach 2L for the two Excavation scenarios at Point 10 is a result of minor alterations to the model and it does not reflect differences in the performance of the designs. Changes in the groundwater flow system caused by closure also affect the boron concentration at Point 9, which is on the northwestern corner of the WAB. The groundwater flow directions change significantly at this location during the Excavation and Hybrid scenarios, whereas they are similar to the current conditions for the Final Cover scenario. As a result, the boron concentrations decay in several decades for the two Excavation scenarios and the Hybrid scenario, but another 100 years is required for boron concentrations to decrease to 2L for the Final Cover scenario, according to the simulations (Figure 39).

Boron groundwater concentration distributions for the Excavation with Landfill, Final Cover, and Hybrid conceptual closure design simulations are similar as shown on Figure 21, Figure 22, and Figure 40 through Figure 43. In the Complete Excavation scenario (Figure 40 through Figure 43), the time to reach the 2L standard is similar to the other three scenarios in the upper bedrock layer, but it occurs sooner in the transition zone due to higher recharge over the landfill footprint. However, boron distribution in the upper bedrock is likely more representative of the concentrations in groundwater than the distribution in the transition zone, because the transition zone is partially above the water table. The relative times to reach the 2L standard at selected representative time-series locations are variable—some closure options generate the fastest times to reach 2L at some locations, but they are slower to reach 2L at other locations (Figure 39). In conclusion, in terms of the time required to meet 2L standard at the respective compliance boundary, the performance of the four closure scenarios is generally similar with variations depending on location within the WAB and EAB.

Effects on water supply wells

The simulations indicate that there are no exposure pathways between the groundwater flow through the ash basins and the pumping wells used for water supply in the vicinity of the Roxboro site. Domestic and public water supply wells are outside, or upgradient of the groundwater flow system containing the ash basins. Domestic and public water supply wells are not affected by constituents released from the ash basins or by the different closure options, according to the simulations.

## 7.0 REFERENCES

- AMEC Foster Wheeler, 2016a. West Ash Basin Narrative of Options Considered. Draft 01/08/2016.
- AMEC Foster Wheeler, 2016b. Drawing of Final Ash Grades, West Ash Basin. Drawing Rox\_C901.008.038.
- AMEC Foster Wheeler, 2017. East Ash Basin Narrative of Options Considered. Draft 01/11/2017.
- Daniel, C.C., Douglas G. Smith, and Jo Leslie Eimers, 1997, Hydrogeology and Simulation of Ground-Water Flow in the Thick Regolith-Fractured Crystalline Rock Aquifer System of Indian Creek Basin, North Carolina, USGS Water-Supply 2341.
- HDR and SynTerra, 2017. Statistical Methods for Developing Reference Background Concentrations for Groundwater and Soil at Coal Ash Facilities. HDR Engineering, Inc. and SynTerra Corporation.
- Haven, W. T. 2003. Introduction to the North Carolina Groundwater Recharge Map. Groundwater Circular Number 19. North Carolina Department of Environment and Natural Resources. Division of Water Quality, 8 p.
- Langley, W.G., S. Oza, 2015, Sorption Evaluation of the. Roxboro Steam Electric Plant. Charlotte Department of Civil and Environmental Engineering, report prepared for SynTerra.
- Legrand, H. 1988. Piedmont and Blue Ridge. Back, W., J. Rosenshein, and P. Seaber, eds. 1988. Hydrogeology: The Geology of North America O-2: The Decade of North American Geology. Boulder, Colorado: Geological Society of America. Geological Society of America. P. 201-208.
- Maupin, M., Joan F. Kenny, Susan S. Hutson, John K. Lovelace, Nancy L. Barber, and Kristin S. Linsey. 2014. Estimated Use of Water in the United States in 2010, USGS Circular 1405.
- McDonald, M.G. and A.W. Harbaugh, 1988, A Modular Three-Dimensional Finite-Difference Ground-Water Flow Model, U.S. Geological Survey Techniques of Water Resources Investigations, book 6, 586 p.
- Niswonger, R.G., S. Panday, and I. Motomu, 2011, MODFLOW-NWT, A Newton formulation for MODFLOW-2005, U.S. Geological Survey Techniques and Methods 6-A37, 44-.
- North Carolina Water Supply and Use, in "National Water Summary 1987 - Hydrologic Events and Water Supply and Use". USGS Water-Supply Paper 2350, p. 393-400.
- North Carolina; Estimated Water Use in North Carolina, 1995, USGS Fact Sheet FS-087-97
- Radcliffe, D.E., L.T. West, L.A. Morris, and T. C. Rasmussen. 2006. Onsite Wastewater and Land Application Systems: Consumptive Use and Water Quality, University of Georgia.
- SynTerra, 2014, L.V. Roxboro Steam Electric Plant, Semora, NC, Water Supply Well Survey Report of Findings, September 30, 2014.

- SynTerra, 2015, Comprehensive Site Assessment Report, Roxboro Steam Electric Plant, Semora, NC. September 2, 2015.
- SynTerra, 2016, Corrective Action Plan, Part 2. Roxboro Steam Electric Plant, Semora, NC, February 29, 2016.
- Tiedeman, C.R. and P.A. Hsieh. 2001. Assessing and open hole aquifer test in fractured crystalline rock. *Ground Water*, v. 39, n.1, p 68-78.
- Trapp, H. and M.A. Horn. 1997. *Ground Water Atlas of the U.S. North Carolina and vicinity (HA 730-L)*. USGS. [http://pubs.usgs.gov/ha/ha730/ch\\_1/L-text4.html](http://pubs.usgs.gov/ha/ha730/ch_1/L-text4.html).
- Treece, M.W, Jr., Bales, J.D., and Moreau, D.H., 1990, North Carolina water supply and use, in *National water summary 1987 Hydrologic events and water supply and use: U.S. Geological Survey Water-Supply Paper 2350*, p. 393-400.
- US EPA, 2015, <http://www.epa.gov/watersense/pubs/indoor.html> accessed 8/26/15.
- Watermark Numerical Computing, 2004, *PEST Model-Independent Parameter Estimation User Manual: 5<sup>th</sup> Edition*.
- Zheng, C. and P.P. Wang, 1999, *MT3DMS: A Modular Three-Dimensional Multi-Species Model for Simulation of Advection, Dispersion and Chemical Reactions of Contaminants in Groundwater Systems: Documentation and User's Guide*, SERDP-99-1, U.S. Army Engineer Research and Development Center, Vicksburg, MS.

**TABLES**

PRELIMINARY UPDATED GROUNDWATER FLOW AND TRANSPORT MODELING REPORT FOR  
 ROXBORO STEAM ELECTRIC PLANT, SEMORA, NORTH CAROLINA  
 NOVEMBER 2018, REVISED JANUARY 2019

Table 1. Comparison of observed and computed heads (in ft.) for the calibrated flow model.

Well	Observed Head	Computed Head	Residual Head
ABMW-01	463.64	461.09	2.55
ABMW-01BR	462.73	460.94	1.79
ABMW-02	462.67	467.65	-4.98
ABMW-02BR	462.69	467.65	-4.96
ABMW-03	463.96	453.96	10.00
ABMW-03BR	447.70	452.42	-4.72
ABMW-03BRL	427.42	428.59	-1.17
ABMW-04	468.58	471.16	-2.58
ABMW-04BR	468.38	470.88	-2.50
ABMW-05	467.20	462.50	4.70
ABMW-05D	434.46	442.01	-7.55
ABMW-06	468.26	469.08	-0.82
ABMW-06BR	468.59	468.99	-0.40
ABMW-07	466.66	469.79	-3.13
ABMW-07BR	463.82	469.58	-5.76
ABMW-07BRL	456.97	468.73	-11.76
BG-01	495.51	496.53	-1.02
BG-01BR	495.31	496.50	-1.19
BG-01BRLR	483.80	487.02	-3.22
BG-01D	496.82	496.75	0.07
BG-02BR	483.34	494.43	-11.09
CCR-100BR	470.89	470.24	0.65
CCR-100D	471.73	470.39	1.34
CCR-101BR	442.88	444.61	-1.73
CCR-101D	445.61	444.31	1.30
CCR-102BR	412.43	424.20	-11.77

**PRELIMINARY UPDATED GROUNDWATER FLOW AND TRANSPORT MODELING REPORT FOR  
ROXBORO STEAM ELECTRIC PLANT, SEMORA, NORTH CAROLINA  
NOVEMBER 2018, REVISED JANUARY 2019**

CCR-103BR	418.53	416.82	1.71
CCR-104BR	458.00	456.79	1.21
CCR-105BR	480.49	476.34	4.15
CCR-106BR	486.28	488.89	-2.61
CCR-107BR	486.17	489.39	-3.22
CCR-108BR	489.16	488.53	0.63
CCR-109BR	474.58	470.42	4.16
CCR-110BR	470.29	473.17	-2.88
CCR-111BR	498.45	496.95	1.50
CCR-112BR-BG	530.88	540.82	-9.94
CCR-200BR	458.92	466.98	-8.06
CCR-201BR	458.65	462.12	-3.47
CCR-202BR	425.50	432.94	-7.44
CCR-202D	431.77	433.69	-1.92
CCR-203BR	412.35	413.13	-0.78
CCR-203D	411.47	413.15	-1.68
CCR-203S	409.96	413.45	-3.49
CCR-204BR	413.38	414.93	-1.55
CCR-205BR	435.88	436.92	-1.04
CCR-206BR	455.73	447.84	7.89
CCR-206S	453.94	448.01	5.93
CCR-207BR	447.92	446.61	1.31
CCR-207S	449.94	446.25	3.69
CCR-208BR	450.22	447.69	2.53
CCR-208S	450.27	447.57	2.70
CCR-209BR	457.52	454.49	3.03
CCR-209S	456.63	454.73	1.90
CCR-210BR	451.98	449.97	2.01
CCR-210S	457.92	449.95	7.97
CCR-211BR	454.82	454.27	0.55

**PRELIMINARY UPDATED GROUNDWATER FLOW AND TRANSPORT MODELING REPORT FOR  
ROXBORO STEAM ELECTRIC PLANT, SEMORA, NORTH CAROLINA  
NOVEMBER 2018, REVISED JANUARY 2019**

CCR-211S	458.34	454.52	3.82
CCR-212BR	463.04	467.73	-4.69
CCR-213BR	467.08	473.38	-6.30
CCR-214BR	461.21	468.18	-6.97
CCR-215BR	466.18	471.51	-5.33
CCR-216BR	468.93	470.71	-1.78
CCR-217BR	462.25	465.41	-3.16
CCR-218BR	454.86	451.73	3.13
CW-01	485.39	483.43	1.96
CW-02	410.94	409.51	1.43
CW-02D	410.93	409.62	1.31
CW-03	446.73	446.07	0.66
CW-03D	448.96	446.63	2.33
CW-04	450.71	447.93	2.78
CW-05	449.15	448.00	1.15
GMW-01A	412.22	423.68	-11.46
GMW-06	455.07	455.62	-0.55
GMW-07	469.81	473.19	-3.38
GMW-08	481.50	485.35	-3.85
GMW-09	512.77	504.88	7.89
GMW-10	462.76	468.09	-5.33
GMW-11	474.50	474.30	0.20
GPMW-01BR	414.30	413.99	0.31
GPMW-01D	417.35	414.07	3.28
GPMW-01S	418.20	414.17	4.03
GPMW-02BR	411.63	414.03	-2.40
GPMW-02D	412.56	414.13	-1.57
GPMW-03BR	413.68	415.05	-1.37
GPMW-03D	420.06	414.30	5.76
MW-01	410.50	411.58	-1.08

**PRELIMINARY UPDATED GROUNDWATER FLOW AND TRANSPORT MODELING REPORT FOR  
ROXBORO STEAM ELECTRIC PLANT, SEMORA, NORTH CAROLINA  
NOVEMBER 2018, REVISED JANUARY 2019**

MW-01BR	478.06	482.22	-4.16
MW-02	410.07	413.12	-3.05
MW-02BR	478.04	479.64	-1.60
MW-03BR	427.20	422.69	4.51
MW-04BR	455.91	452.83	3.08
MW-04BRL	458.90	454.97	3.93
MW-05BR	430.83	435.41	-4.58
MW-05D	448.43	447.17	1.26
MW-06BR	408.05	414.38	-6.33
MW-06D	411.23	414.60	-3.37
MW-07BR	463.10	459.61	3.49
MW-08BR	442.23	448.00	-5.77
MW-09BR	416.56	421.26	-4.70
MW-10BR	513.09	509.92	3.17
MW-11BR	462.13	460.44	1.69
MW-11D	460.90	460.13	0.77
MW-12BR	451.95	448.50	3.45
MW-13BR	513.37	510.98	2.39
MW-14BR	465.20	469.71	-4.51
MW-14D	466.24	470.03	-3.79
MW-15BR	499.06	496.63	2.43
MW-15D	500.22	496.76	3.46
MW-16BR	489.97	488.58	1.39
MW-17BR	496.99	500.00	-3.01
MW-18BR	486.76	489.17	-2.41
MW-18D	487.15	490.80	-3.65
MW-19BRL	525.90	527.75	-1.85
MW-20BRL	487.11	487.60	-0.49
MW-21BRL	481.40	484.34	-2.94
MW-22BR	455.21	443.86	11.35

PRELIMINARY UPDATED GROUNDWATER FLOW AND TRANSPORT MODELING REPORT FOR  
ROXBORO STEAM ELECTRIC PLANT, SEMORA, NORTH CAROLINA  
NOVEMBER 2018, REVISED JANUARY 2019

MW-22D	455.39	445.25	10.14
MW-23BR	470.00	478.30	-8.30
MW-24BR	486.58	486.82	-0.24
MW-25BR	492.99	498.24	-5.25
MW-26BR	483.17	483.89	-0.72
MW-27BR	450.61	461.06	-10.45
MW-28BR	433.92	427.05	6.87
MW-30BR	459.64	462.48	-2.84
MW-31BR	455.17	467.97	-12.80
MW-32BR	470.41	469.42	0.99
MW-33BR	456.31	464.16	-7.85

\* Wells BG-01BRL, MW-23BRR, PZ-12, PZ-14 were excluded from the calibration.

Table 2. Calibrated hydraulic parameters.

Unit	Grid layer	$K_h$ (ft/d)	$K_h/K_v$
Ash	1-8	2	10
Saprolite	9-11	1	1
Transition zone	12-13	1	1
Upper rock	14-16	0.3	1
Middle rock	17-20	0.005	1
Lower Rock	21-23	0.002	1

Table 3. Recharge in different zones in the model.

Recharge zone	Recharge flux (ft/d)				
	1966	1974	2004	2008	2014
east lake	0				
north halo	0.0018				
stormwater nw of lined landfill	0.004				
south halo	0.0018				
new capped landfill	0.0018				0.00001
Plant	0				
northeast halo	0.0018				
lined gypsum storage area	0.0018			0.00001	
west side gyp storage area	0.0018				
NW side of gypsum storage	0.0018				
east lake filter dam	0.00001				
west of gyp storage area	0.0018			0.001	
lined landfill (EAB)	0.0018	0.00001			
east ash basin	0.004				
gravel parking lot	0.004				
SW lake	0				
sw ash basin lake	0				
drainage north of lined EAB	0.0018		0.004		
east gypsum storage area	0.0018				
central gyp storage area	0.0018				
sluice line ditch	0.0018				
west ash basin	0.0018	0.004			
west ash basin dam	0				
west ash basin capped	0.0018	0.004		0.00001	
lake and Plant	0.0001				
Hyco lake	0				
Regional	0.0018				

PRELIMINARY UPDATED GROUNDWATER FLOW AND TRANSPORT MODELING REPORT FOR  
 ROXBORO STEAM ELECTRIC PLANT, SEMORA, NORTH CAROLINA  
 NOVEMBER 2018, REVISED JANUARY 2019

Table 4. Flow parameter sensitivity analysis. Results are expressed as model normalized root mean square error (NRMSE) of the simulated and observed heads.

<b>Unit</b>	<b>Layer #</b>	<b>K<sub>h</sub> or R (ft/d)</b>	<b>0.5 x calibrated</b>	<b>Calibrated</b>	<b>2x calibrated</b>
Ash K <sub>h</sub>	1-8	2	0.0399	0.0385	0.0377
Saprolite K <sub>h</sub>	9-11	1	0.0407	0.0385	0.0376
Transition zone K <sub>h</sub>	12-13	1	0.0419	0.0385	0.0374
Shallow rock K <sub>h</sub>	14-16	0.3	0.0546	0.0385	0.0452
Mid rock K <sub>h</sub>	17-20	0.005	0.0390	0.0385	0.0378
Lower rock K <sub>h</sub>	21-23	0.002	0.0389	0.0385	0.0380
Regional recharge	1-23	0.0018	0.0554	0.0385	0.0918

PRELIMINARY UPDATED GROUNDWATER FLOW AND TRANSPORT MODELING REPORT FOR  
 ROXBORO STEAM ELECTRIC PLANT, SEMORA, NORTH CAROLINA  
 NOVEMBER 2018, REVISED JANUARY 2019

Table 5. Comparison of observed and simulated boron concentrations in monitoring wells.

<b>Well ID</b>	<b>observed (ppb)</b>	<b>simulated (ppb)</b>
ABMW-01	10900	10900
ABMW-01BR	446	2753
ABMW-02	2320	1466
ABMW-02BR	0	245
ABMW-03	284	284
ABMW-03BR	3080	3080
ABMW-03BRL	77	560
ABMW-04	41200	41200
ABMW-04BR	0	24758
ABMW-05	26100	26100
ABMW-05D	2260	23252
ABMW-06	2790	2790
ABMW-06BR	0	921
ABMW-07	5670	5670
ABMW-07BR	1080	1080
ABMW-07BRL	109	13
BG-01	0	0
BG-01BR	0	0
BG-01BRLR	0	0
BG-02BR	0	0
CCR-100BR	0	0
CCR-100D	0	0
CCR-101BR	0	8
CCR-101D	0	14
CCR-102BR	0	3
CCR-103BR	3300	5529
CCR-104BR	6560	5917
CCR-105BR	663	415
CCR-106BR	1140	8685
CCR-107BR	2060	9748
CCR-108BR	11700	11445

**PRELIMINARY UPDATED GROUNDWATER FLOW AND TRANSPORT MODELING REPORT FOR  
ROXBORO STEAM ELECTRIC PLANT, SEMORA, NORTH CAROLINA  
NOVEMBER 2018, REVISED JANUARY 2019**

CCR-109BR	779	199
CCR-110BR	22900	14231
CCR-111BR	2710	2710
CCR-112BR-BG	0	0
CCR-200BR	0	0
CCR-201BR	0	2659
CCR-202BR	2700	2619
CCR-202D	2640	2700
CCR-203BR	651	711
CCR-203D	385	723
CCR-203S	0	732
CCR-204BR	4750	2731
CCR-205BR	3160	11432
CCR-206BR	9420	22025
CCR-206S	30400	25000
CCR-207BR	18600	17985
CCR-207S	16300	23868
CCR-208BR	53800	36049
CCR-208S	34200	47829
CCR-209BR	4090	3104
CCR-209S	3200	2239
CCR-210BR	2410	2085
CCR-210S	960	2740
CCR-211BR	2110	1069
CCR-211S	3330	1479
CCR-212BR	0	59
CCR-213BR	0	0
CCR-214BR	0	0
CCR-215BR	0	0
CCR-216BR	0	0
CCR-217BR	0	197
CCR-218BR	0	111
CW-01	0	5541

**PRELIMINARY UPDATED GROUNDWATER FLOW AND TRANSPORT MODELING REPORT FOR  
ROXBORO STEAM ELECTRIC PLANT, SEMORA, NORTH CAROLINA  
NOVEMBER 2018, REVISED JANUARY 2019**

CW-02	0	1
CW-02D	0	10
CW-03	0	0
CW-03D	0	0
CW-04	0	48
CW-05	372	0
GMW-01A	162	10
GMW-02 CCR	4940	1
GMW-06	2180	5981
GMW-07	1555	8533
GMW-08	4175	5000
GMW-09	0	22
GMW-10	119	81
GMW-11	4890	4890
GPMW-01BR	1700	7
GPMW-01D	970	30
GPMW-01S	1500	11
GPMW-02BR	2600	19
GPMW-02D	0	10
GPMW-03BR	280	1590
GPMW-03D	1800	1800
MW-01BR	1310	6891
MW-02	2140	4020
MW-02BR	0	0
MW-03BR	2440	5388
MW-04BR	0	7
MW-05BR	0	0
MW-05D	746	0
MW-06BR	0	0
MW-06D	0	0
MW-07BR	0	0
MW-08BR	0	0
MW-09BR	0	0

**PRELIMINARY UPDATED GROUNDWATER FLOW AND TRANSPORT MODELING REPORT FOR  
ROXBORO STEAM ELECTRIC PLANT, SEMORA, NORTH CAROLINA  
NOVEMBER 2018, REVISED JANUARY 2019**

MW-10BR	0	0
MW-11BR	0	73
MW-11D	0	98
MW-12BR	0	13
MW-13BR	0	0
MW-14BR	0	0
MW-15BR	0	0
MW-15D	0	0
MW-16BR	0	0
MW-17BR	0	0
MW-18BR	0	0
MW-18D	0	0
MW-19BRL	0	0
MW-20BRL	0	1
MW-22BR	604	600
MW-22D	348	400
MW-23BRR	0	0
MW-24BR	0	0
MW-25BR	0	0
MW-26BR	0	0
MW-27BR	0	1183
MW-28BR	0	0
MW-29BR	0	0
MW-30BR	0	0
MW-31BR	0	0
MW-32BR	0	0
MW-33BR	0	0

Table 6. Distribution coefficients for boron.

<b>Layer</b>	<b>K<sub>d</sub> (mL/g)</b>
1-8	0.4
9-13	1
14-23	0.02

**PRELIMINARY UPDATED GROUNDWATER FLOW AND TRANSPORT MODELING REPORT FOR  
ROXBORO STEAM ELECTRIC PLANT, SEMORA, NORTH CAROLINA  
NOVEMBER 2018, REVISED JANUARY 2019**

Table 7. Sensitivity of the simulated boron concentration to different values of  $K_d$ . Calculated values that are the same as observed are concentrations in the ash that were used as boundary conditions. Normalized Root Mean Squared Error (NRMSE) is used to compare observed and calculated.

Sample ID	Observed Boron (ppb)	Modeled boron		
		calibrated $K_d$	1/5x $K_d$	5x $K_d$
	NRMSE	6.7%	7.0%	10.3%
ABMW-01	10900	10900.0	10900.0	10900.0
ABMW-01BR	446	1869.0	5662.0	38.7
ABMW-02	2320	2102.0	2278.0	1273.0
ABMW-02BR	0	15.6	86.4	0.1
ABMW-03	284	284.0	284.0	284.0
ABMW-03BR	3080	1766.0	1930.0	1240.0
ABMW-03BRL	77	97.6	348.2	2.6
ABMW-04	41200	41200.0	41200.0	41200.0
ABMW-04BR	0	52.8	1466.0	0.1
ABMW-05	26100	26100.0	26100.0	26100.0
ABMW-05D	2260	23555.0	24054.0	18886.0
ABMW-06	2790	2790.0	2790.0	2790.0
ABMW-06BR	0	136.9	1027.0	0.7
ABMW-07	5670	5670.0	5670.0	5670.0
ABMW-07BR	1080	2696.0	5775.0	154.4
ABMW-07BRL	109	76.0	2488.0	0.0
BG-01	0	0.0	0.0	0.0
BG-01BR	0	0.0	0.0	0.0
BG-01BRLR	0	0.0	0.0	0.0
BG-02BR	0	0.0	0.0	0.0
CW-01	0	201.9	323.8	15.9
CW-02	0	25.5	106.7	0.2
CW-02D	0	71.4	143.7	6.8
CW-03	0	0.0	0.0	0.0
CW-03D	0	0.0	0.0	0.0
CW-04	0	29.5	44.9	8.0
CW-05	372	73.2	81.1	28.0
GMW-06	2180	2292.0	2514.0	1295.0
GMW-07	1555	2629.0	2855.0	1239.0
GMW-08	4175	4732.0	4848.0	2507.0
GMW-09	0	1200.0	1202.0	791.0
GMW-10	119	543.6	800.0	35.0

**PRELIMINARY UPDATED GROUNDWATER FLOW AND TRANSPORT MODELING REPORT FOR  
ROXBORO STEAM ELECTRIC PLANT, SEMORA, NORTH CAROLINA  
NOVEMBER 2018, REVISED JANUARY 2019**

GMW-11	4890	3463.0	3443.0	2919.0
GPMW-01BR	1700	445.3	734.8	52.5
GPMW-01D	970	1198.0	1292.0	968.6
GPMW-01S	1500	1500.0	1500.0	1500.0
GPMW-02BR	2600	1076.0	1407.0	238.0
GPMW-02D	0	969.9	1545.0	316.8
GPMW-03BR	280	355.6	851.7	20.4
GPMW-03D	1800	1827.0	2362.0	1055.0
MW-01BR	1310	893.0	1144.0	114.2
MW-02	2140	2062.0	2812.0	464.0
MW-02BR	0	0.0	0.4	0.0
MW-03BR	2440	4048.0	4209.0	3366.0
MW-04BR	0	4.4	12.7	0.4
MW-05BR	0	36.1	39.4	16.9
MW-05D	746	129.8	135.9	81.9
MW-06BR	0	0.0	0.3	0.0
MW-06D	0	0.0	0.5	0.0
MW-07BR	0	0.0	0.0	0.0
MW-08BR	0	0.0	0.0	0.0
MW-09BR	0	0.0	0.0	0.0
MW-10BR	0	0.0	0.0	0.0
MW-11BR	0	73.8	193.7	0.0
MW-11D	0	140.7	318.0	0.1
MW-12BR	0	10.8	18.2	1.0
MW-13BR	0	0.0	0.0	0.0
MW-14BR	0	0.0	0.0	0.0
MW-15BR	0	0.0	0.0	0.0
MW-15D	0	0.0	0.0	0.0
MW-16BR	0	0.0	0.0	0.0
MW-17BR	0	0.0	0.0	0.0
MW-18BR	0	0.0	0.0	0.0
MW-18D	0	0.0	0.0	0.0
MW-19BRL	0	0.0	0.0	0.0
MW-20BRL	0	0.0	0.1	0.0
MW-22BR	604	176.3	463.6	20.0
MW-22D	348	228.0	466.4	61.5
MW-23BRR	0	0.0	0.0	0.0
MW-24BR	0	0.0	0.0	0.0
MW-25BR	0	0.0	0.0	0.0
MW-26BR	0	0.0	0.0	0.0

**PRELIMINARY UPDATED GROUNDWATER FLOW AND TRANSPORT MODELING REPORT FOR  
ROXBORO STEAM ELECTRIC PLANT, SEMORA, NORTH CAROLINA  
NOVEMBER 2018, REVISED JANUARY 2019**

MW-27BR	0	38.1	110.0	0.1
MW-28BR	0	0.0	0.0	0.0
MW-29BR	0	0.0	0.0	0.0
MW-30BR	0	0.0	0.0	0.0
MW-31BR	0	0.0	0.0	0.0
MW-32BR	0	0.0	0.0	0.0
MW-33BR	0	0.0	0.0	0.0
CCR-100BR	0	0.0	0.1	0.0
CCR-100D	0	0.0	0.3	0.0
CCR-101BR	0	943.2	1175.0	204.0
CCR-101D	0	363.8	576.9	33.6
CCR-102BR	0	569.6	735.9	101.0
CCR-103BR	3300	3943.0	4663.0	1141.0
CCR-104BR	6560	2472.0	2884.0	1035.0
CCR-105BR	663	194.4	274.4	46.5
CCR-106BR	1140	1801.0	2178.0	283.7
CCR-107BR	2060	1956.0	2216.0	475.7
CCR-108BR	11700	7145.0	7564.0	3127.0
CCR-109BR	779	2368.0	2660.0	656.4
CCR-110BR	22900	13762.0	13740.0	13338.0
CCR-111BR	2710	2382.0	2388.0	1326.0
CCR-112BR-BG	0	0.0	0.0	0.0
CCR-200BR	0	0.1	2.6	0.0
CCR-201BR	0	18.8	23.2	3.3
CCR-202BR	2700	1428.0	1555.0	626.0
CCR-202D	2640	1230.0	1388.0	292.2
CCR-203BR	651	695.7	783.7	440.1
CCR-203D	385	723.4	782.4	461.4
CCR-203S	0	729.4	741.6	642.0
CCR-204BR	4750	2001.0	2521.0	756.7
CCR-205BR	3160	3420.0	6353.0	390.0
CCR-206BR	9420	14130.0	17830.0	7678.0
CCR-206S	30400	18038.0	19080.0	14635.0
CCR-207BR	18600	13209.0	23130.0	2719.0
CCR-207S	16300	14619.0	20762.0	7939.0
CCR-208BR	53800	26188.0	26046.0	7570.0
CCR-208S	34200	38926.0	40923.0	11602.0
CCR-209BR	4090	3446.0	3718.0	1127.0
CCR-209S	3200	2901.0	3325.0	477.7
CCR-210BR	2410	2460.0	2623.0	1400.0

**PRELIMINARY UPDATED GROUNDWATER FLOW AND TRANSPORT MODELING REPORT FOR  
ROXBORO STEAM ELECTRIC PLANT, SEMORA, NORTH CAROLINA  
NOVEMBER 2018, REVISED JANUARY 2019**

CCR-210S	960	2810.0	2837.0	2584.0
CCR-211BR	2110	1350.0	1389.0	635.7
CCR-211S	3330	1775.0	1814.0	941.1
CCR-212BR	0	58.1	86.0	14.5
CCR-213BR	0	0.1	0.5	0.0
CCR-214BR	0	1.4	10.8	0.0
CCR-215BR	0	0.0	0.0	0.0
CCR-216BR	0	0.0	0.1	0.0
CCR-217BR	0	136.4	374.3	1.8
CCR-218BR	0	77.3	153.7	17.2
GMW-01A CCR	162	333.8	506.6	21.6
GMW-02 CCR	4940	2869.0	3530.0	393.3

## FIGURES

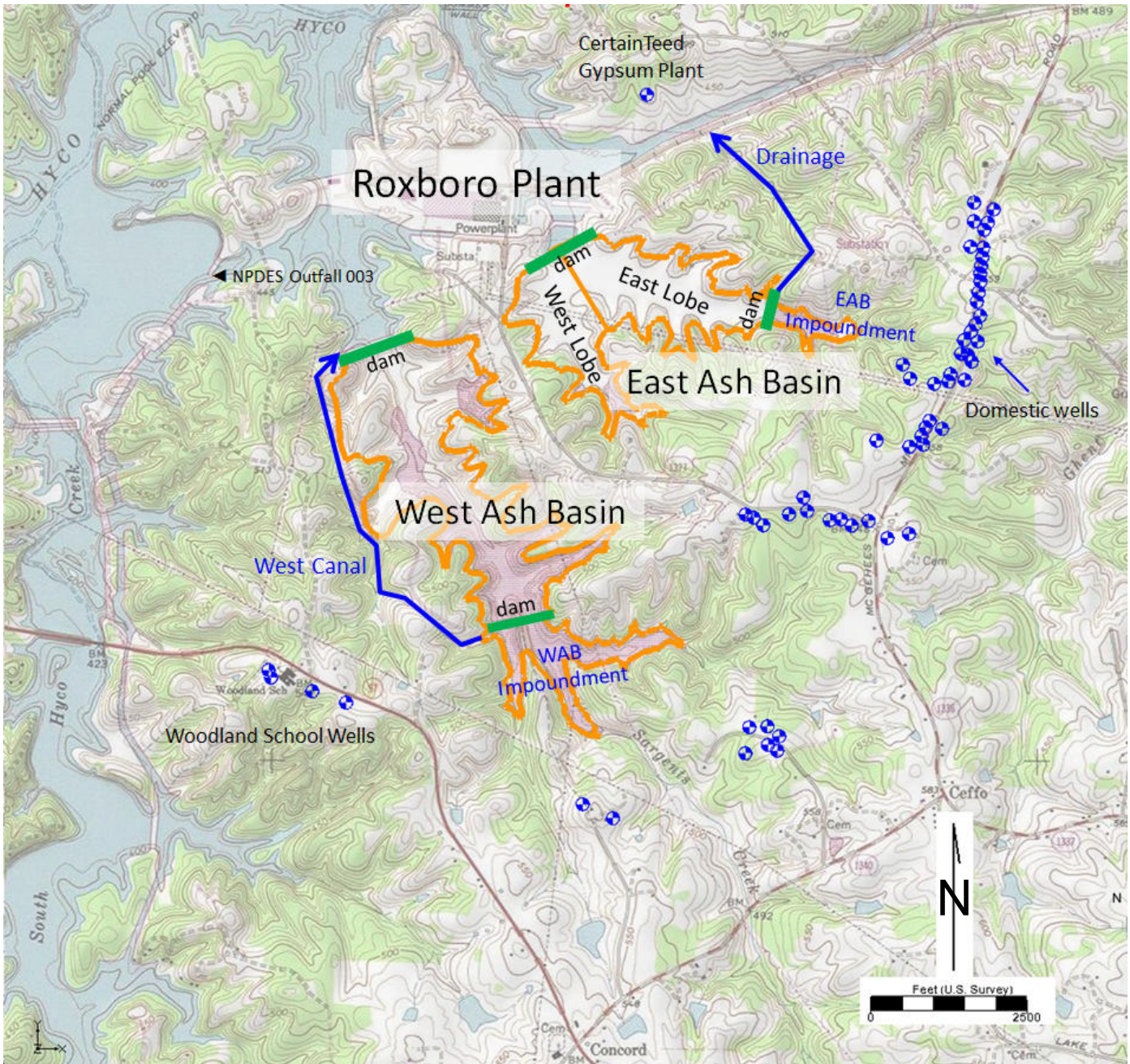


Figure 1. Site location map of the Roxboro Steam Electric Plant, Person County, NC. Figure shows the ash basins (orange) and hydrologic features

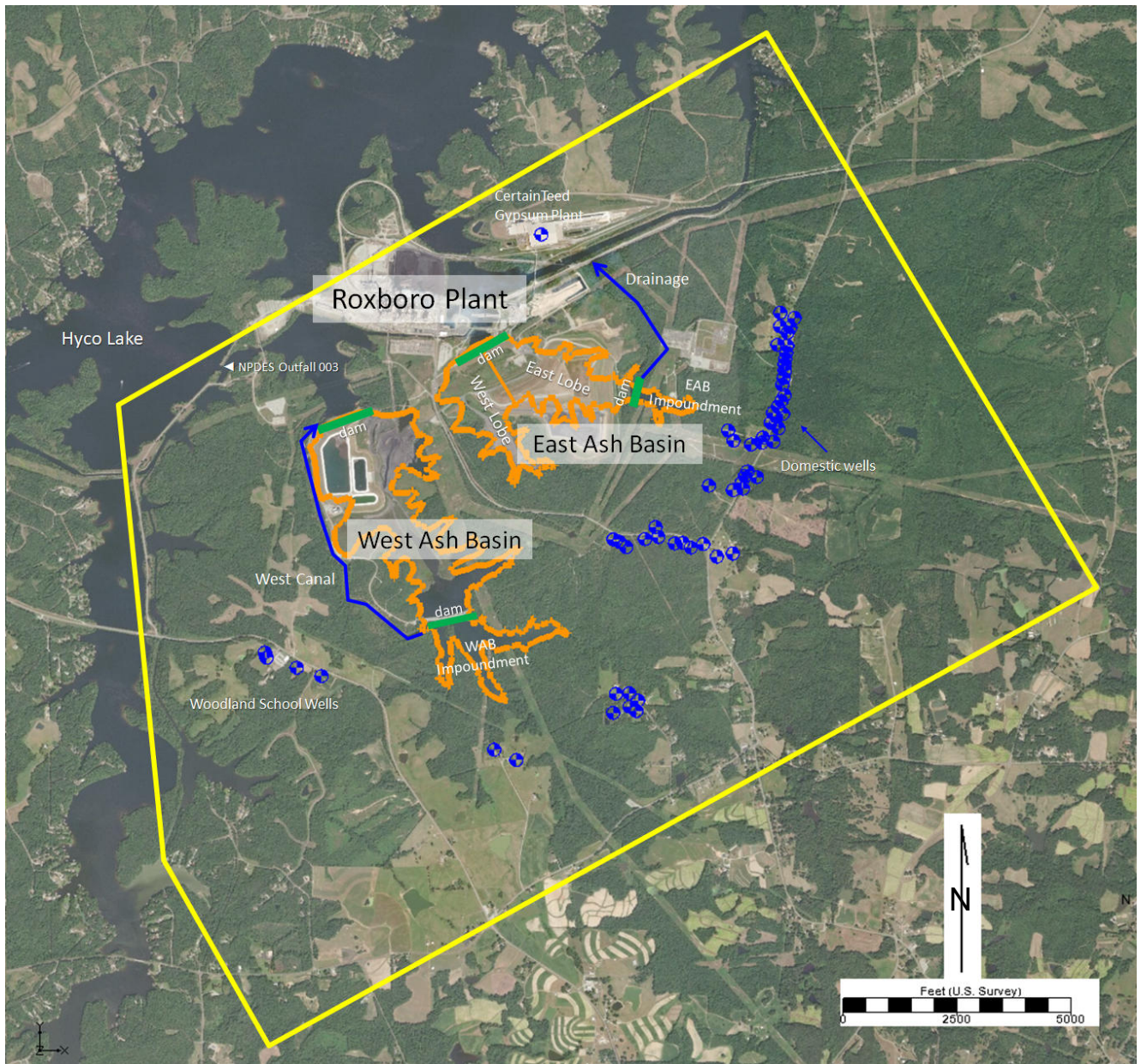


Figure 2. Air photo of the Roxboro Steam Electric Plant showing ash basins (orange) and hydrologic features and boundary of model region (yellow).

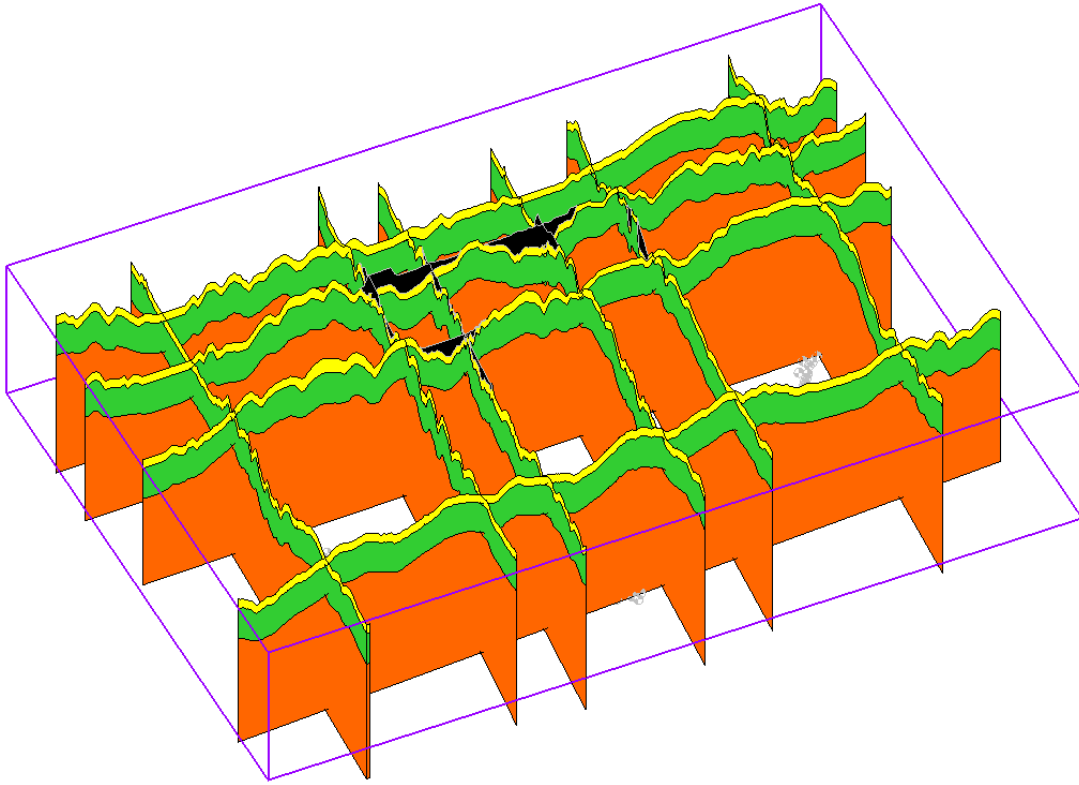


Figure 3. Fence diagram of the 3D hydrostratigraphic model (Solids) used to generate hydrostratigraphy. Black represents ash, yellow is weathered rock, green is fractured rock, and orange is rock. Perspective is looking northeast with 10x vertical exaggeration.

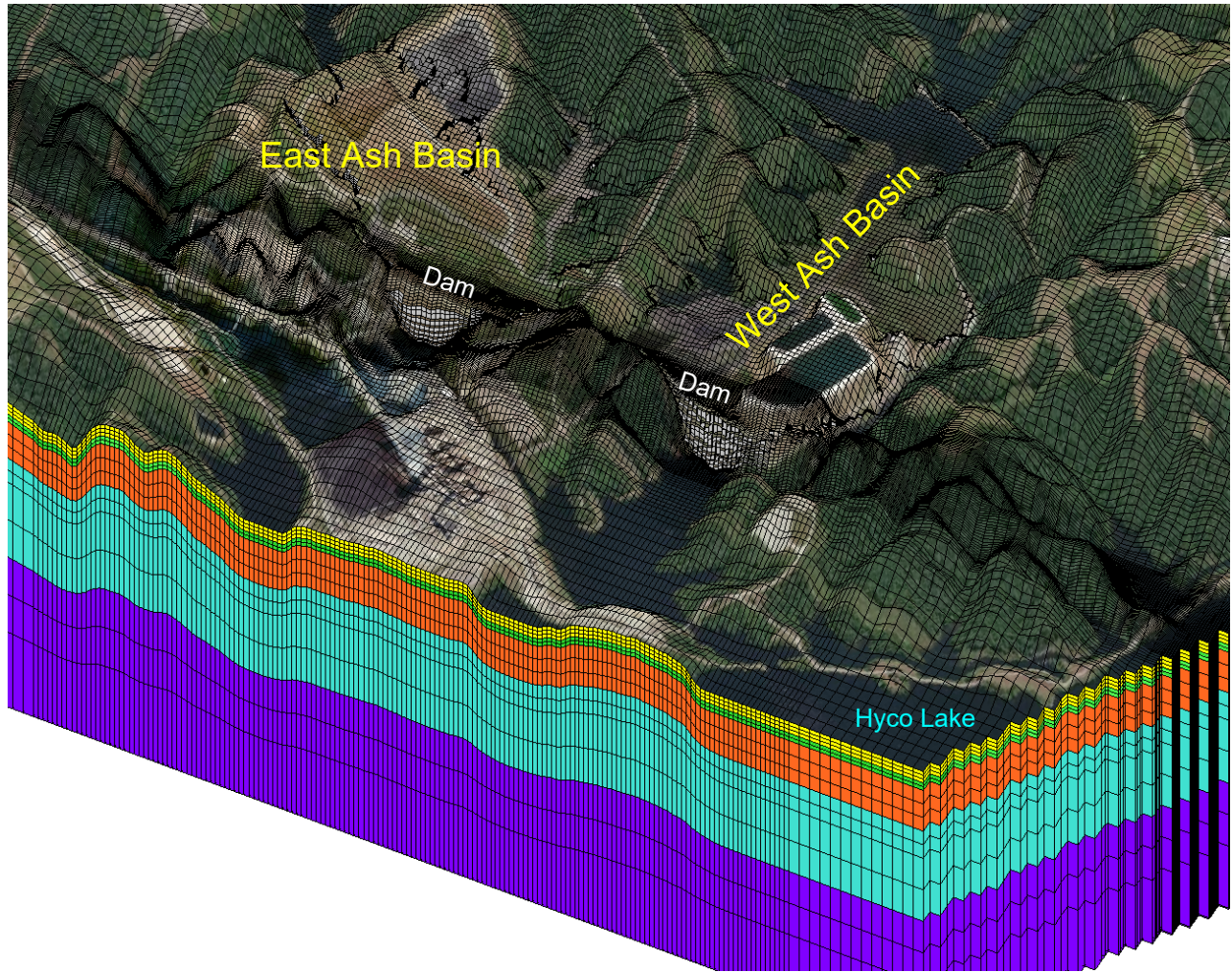


Figure 4. Computational grid used in the model, showing the ash basin. Perspective is looking southeast with 10x vertical exaggeration. Yellow represents sapolite, green is the transition zone, orange is upper rock, cyan is middle rock, and purple is lower rock.

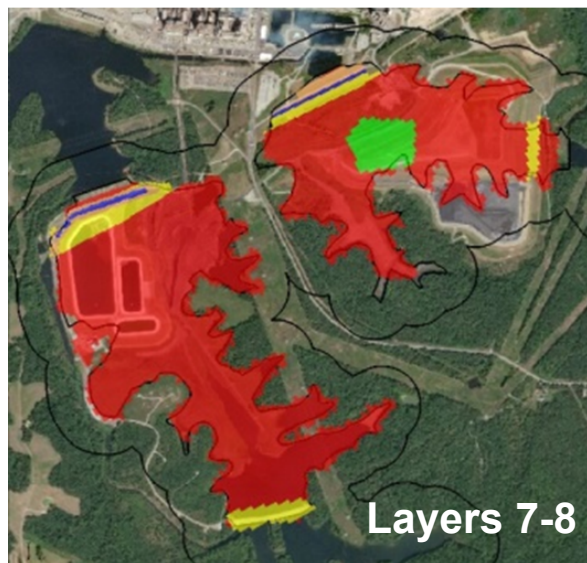
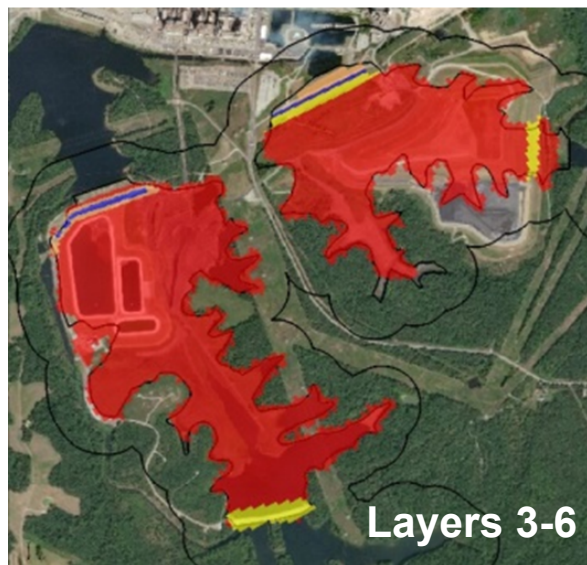
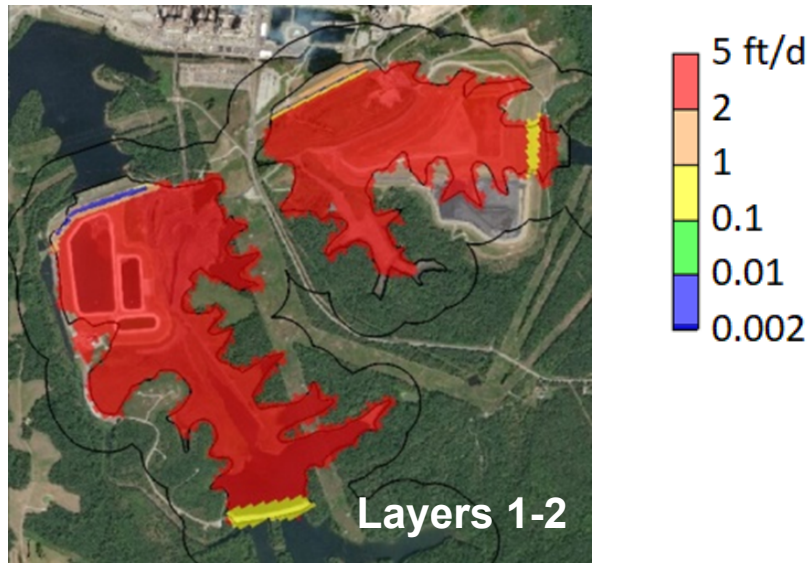


Figure 5a. Hydraulic conductivity (ft/d) distribution. Grid layers 1-8 in the model.

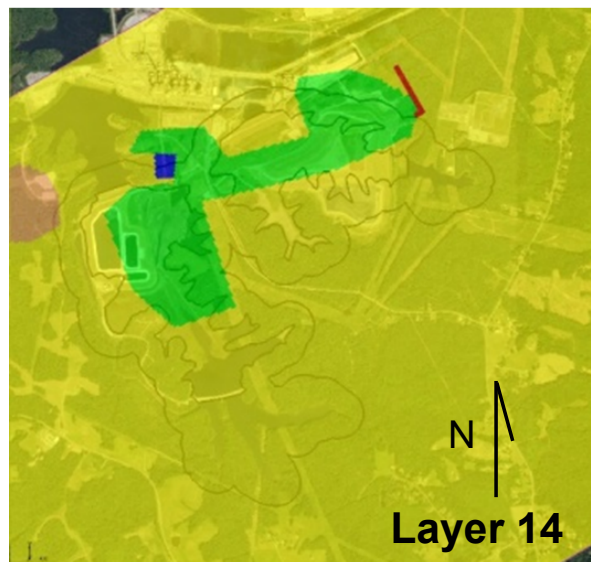
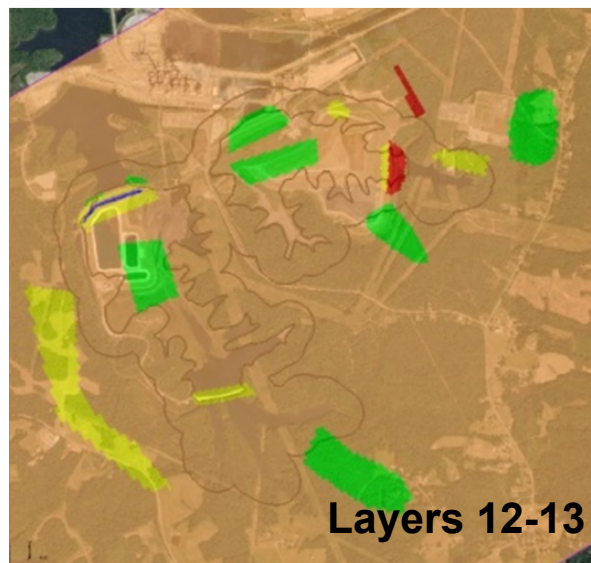
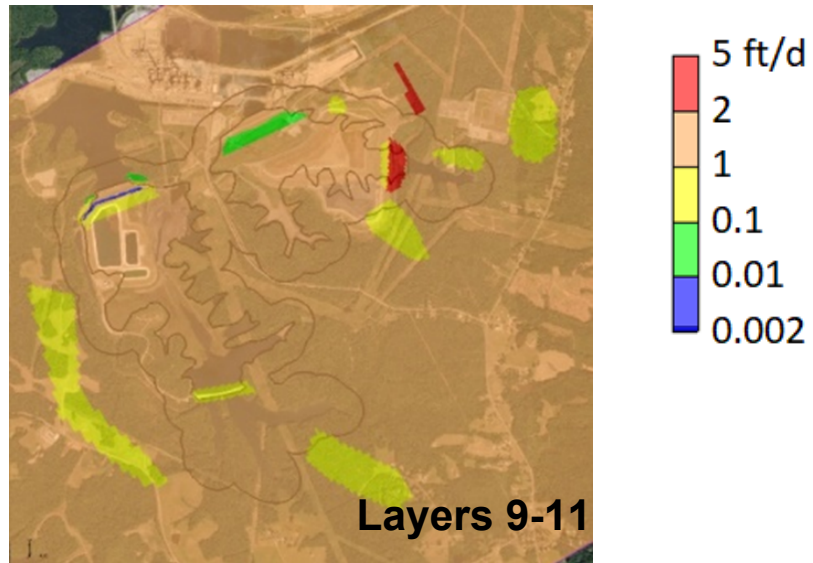


Figure 5b. Hydraulic conductivity (ft/d) distribution. Grid layers 9-14 in the model.

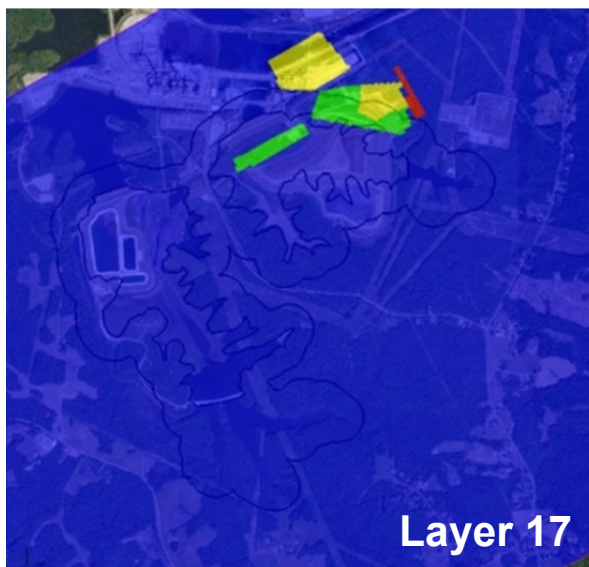
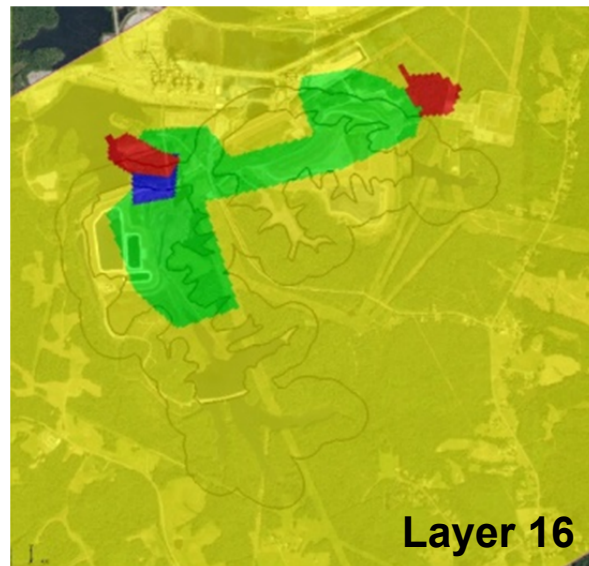
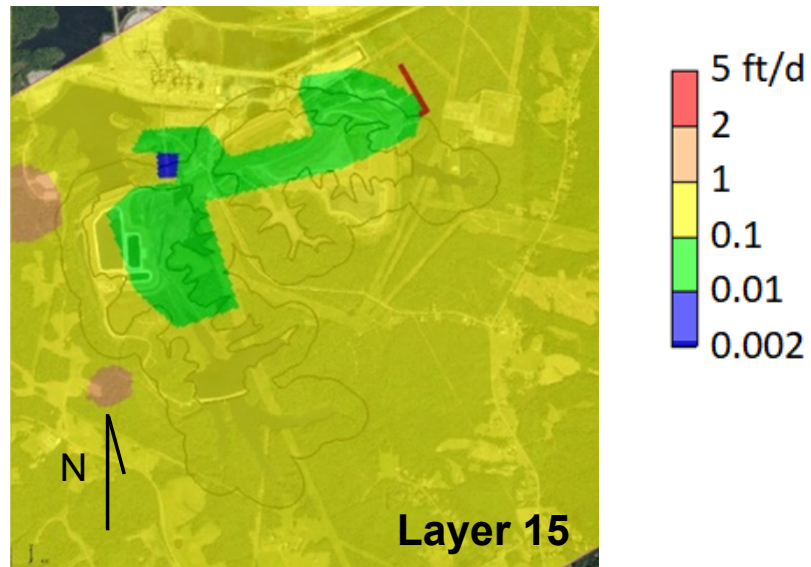


Figure 5c. Hydraulic conductivity (ft/d) distribution. Grid layers 15-17 in the model.

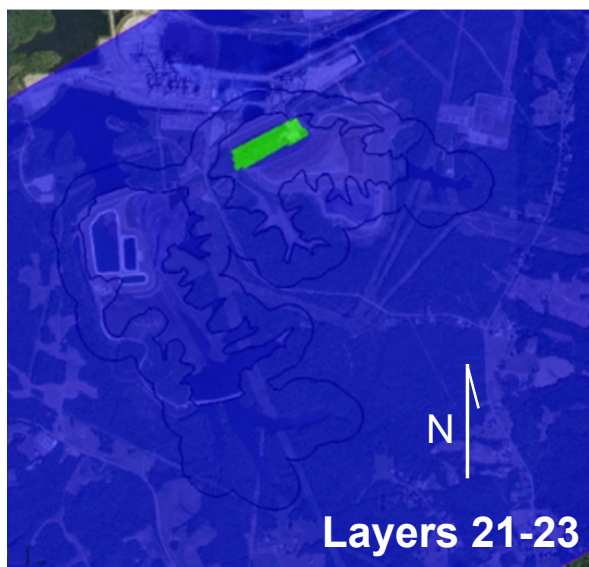
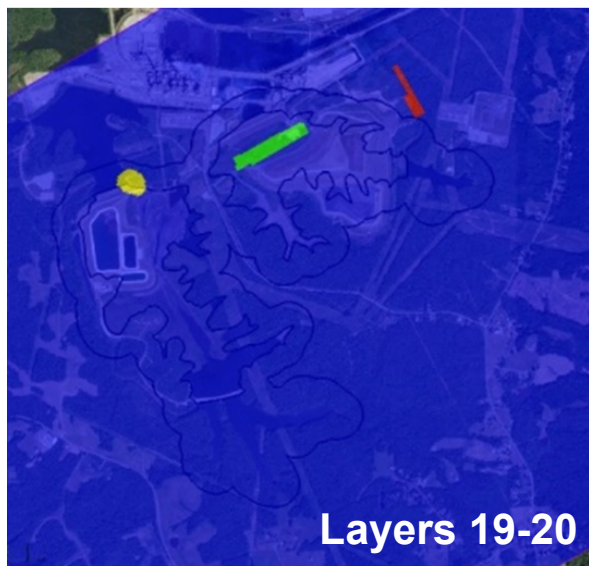
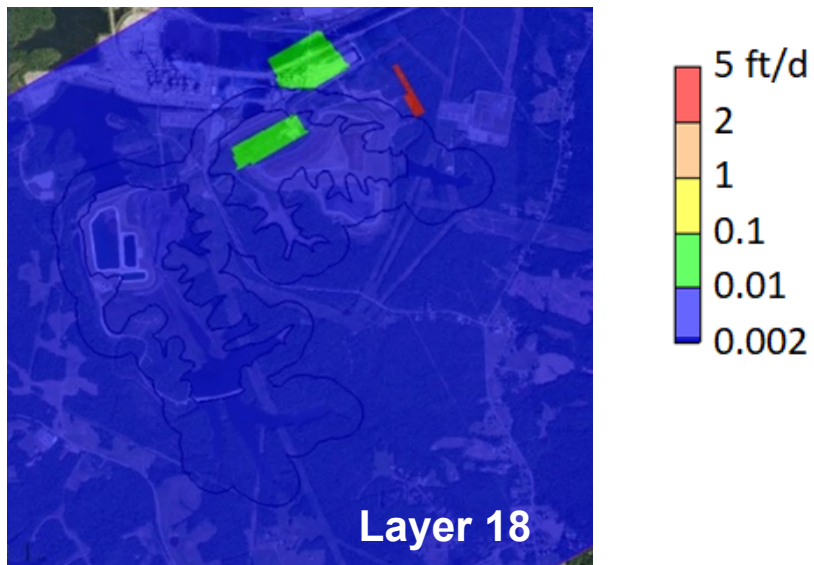


Figure 5d. Hydraulic conductivity (ft/d) distribution. Grid layers 18-23 in the model.

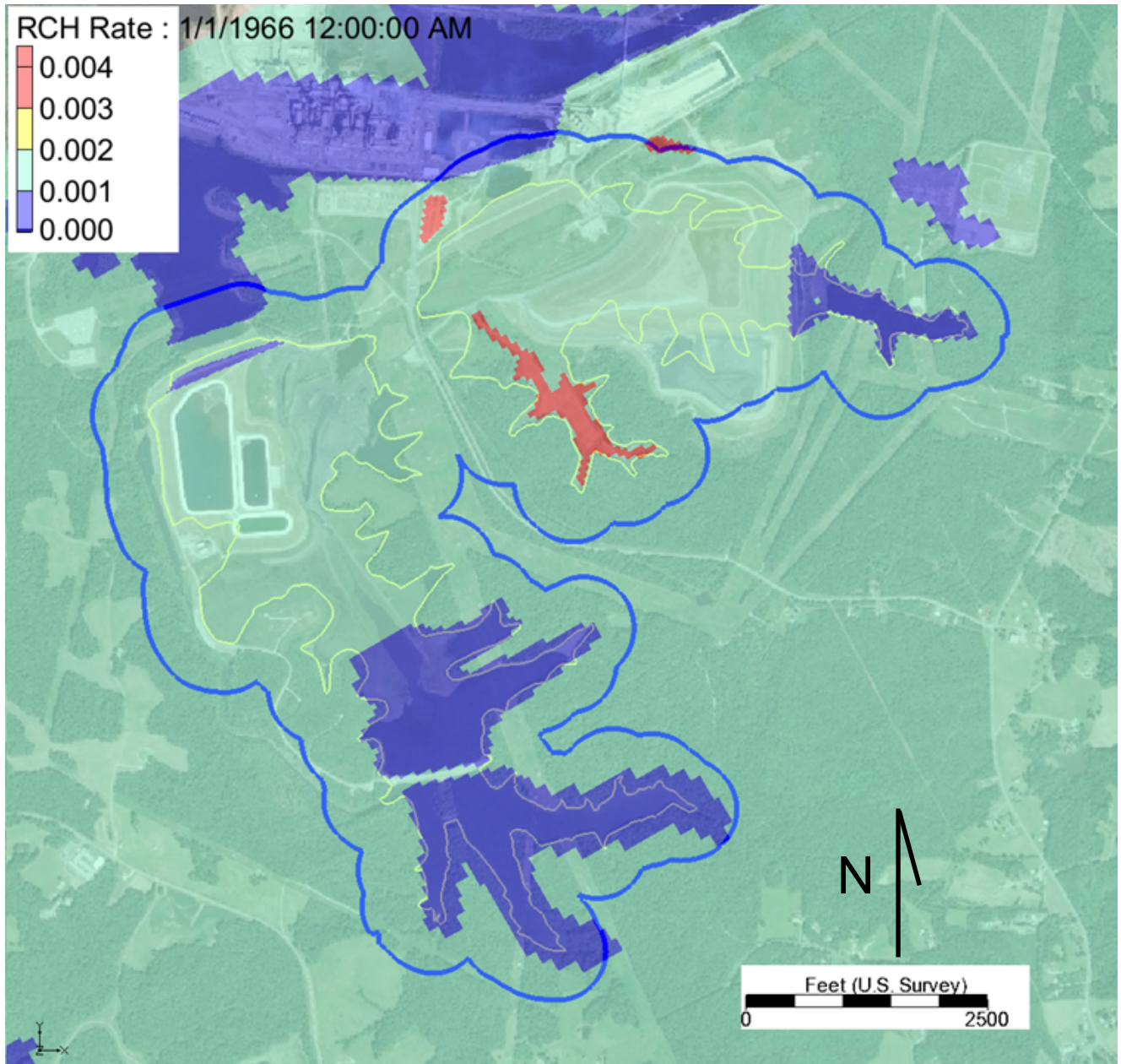


Figure 6a. Distribution of recharge flux used in the model during 1966-1974. Legend is in ft/d.

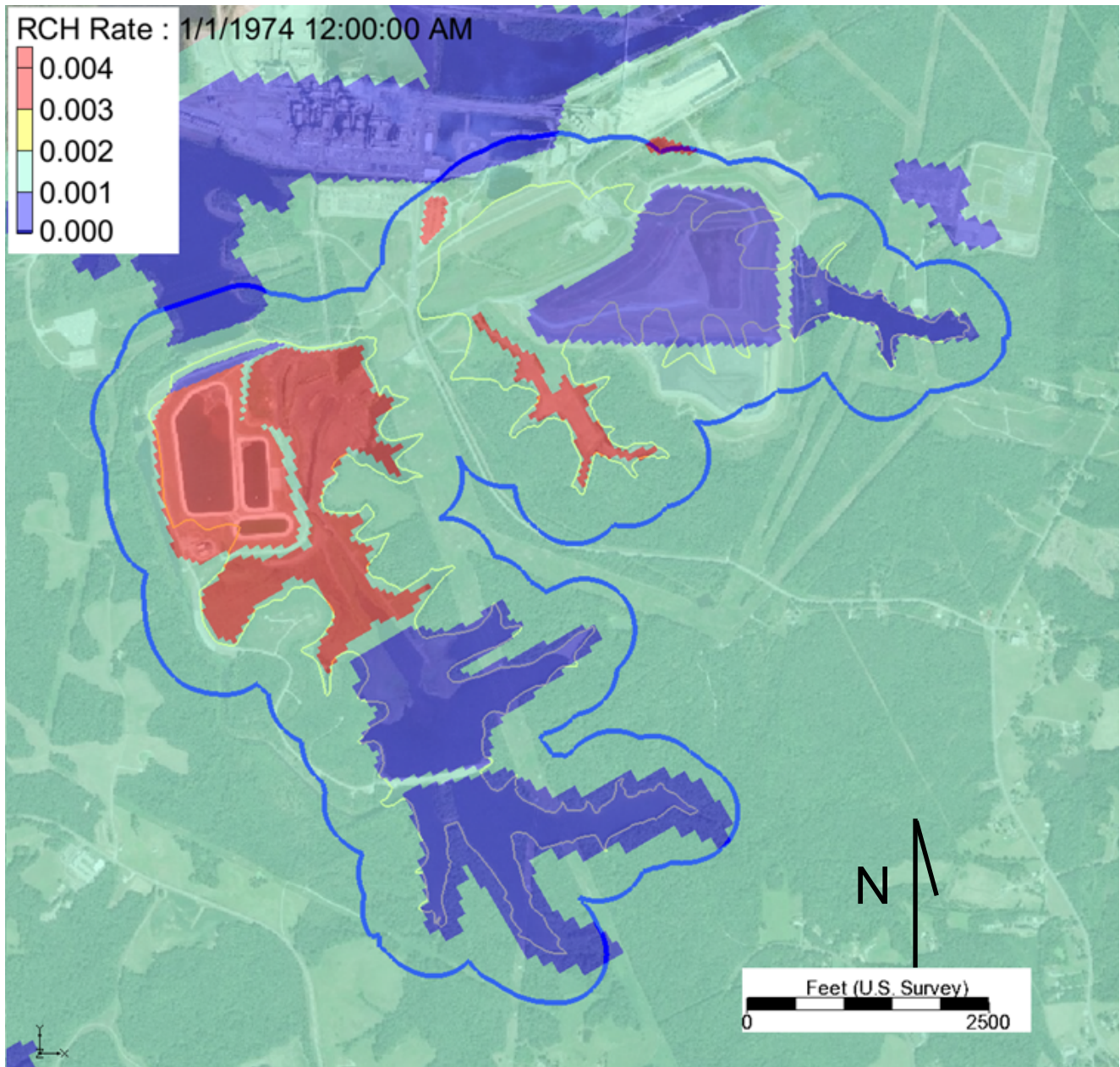


Figure 6b. Distribution of recharge flux used in the model during 1974-2004. Legend is in ft/d.

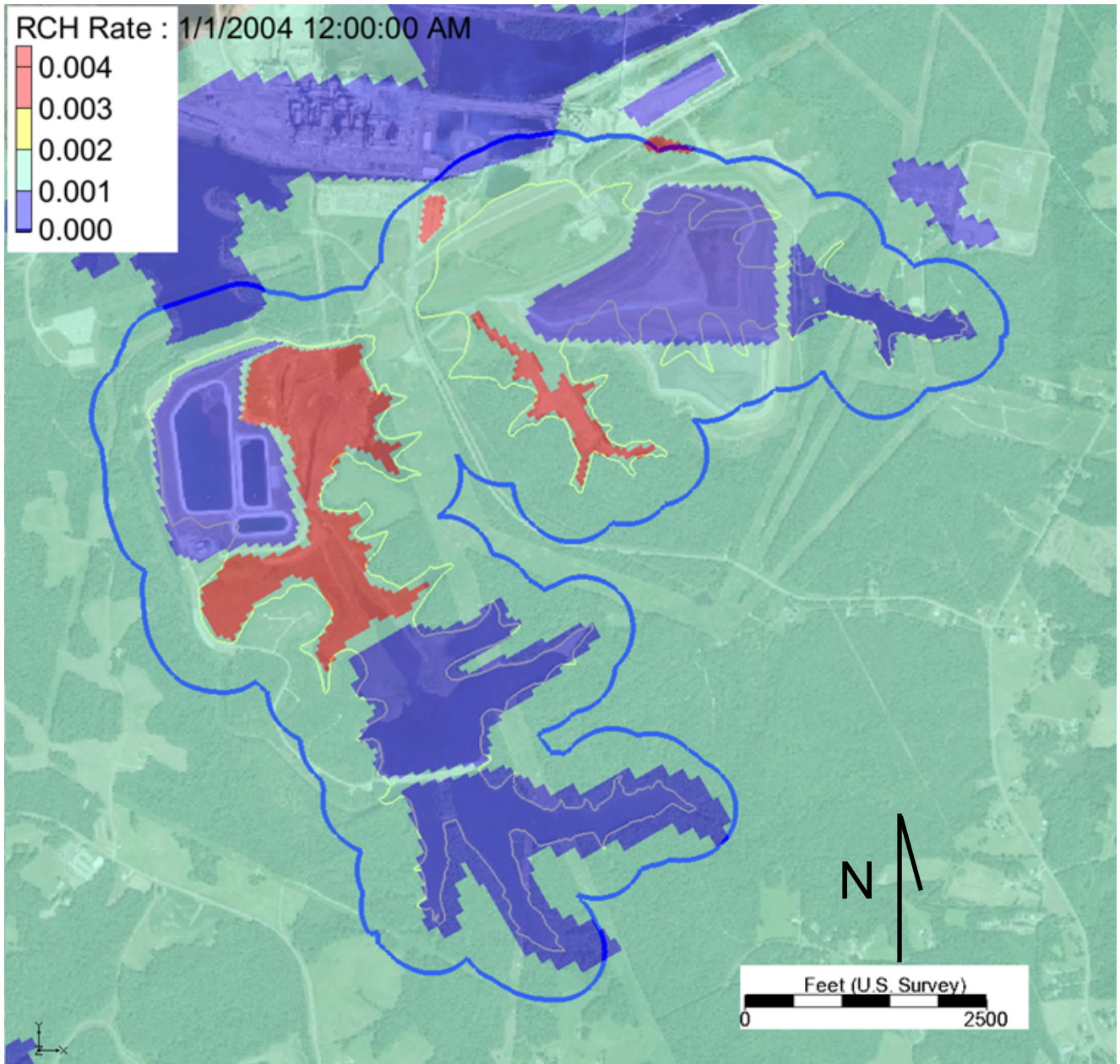


Figure 6c. Distribution of recharge flux used in the model during 2004-2014. Legend is in ft/d.

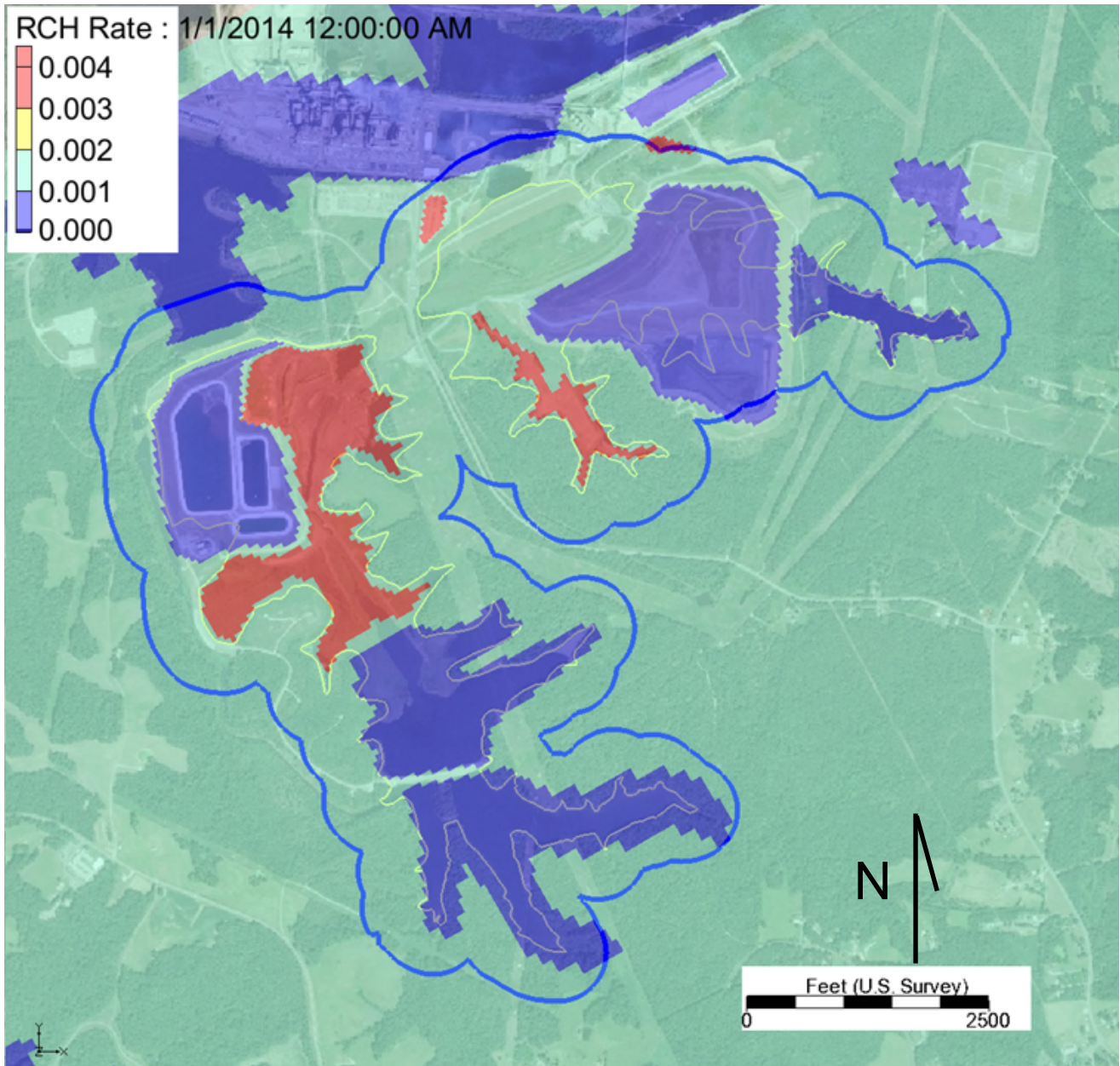


Figure 6d. Distribution of recharge flux used in the model during 2014-2020. Legend is in ft/d.

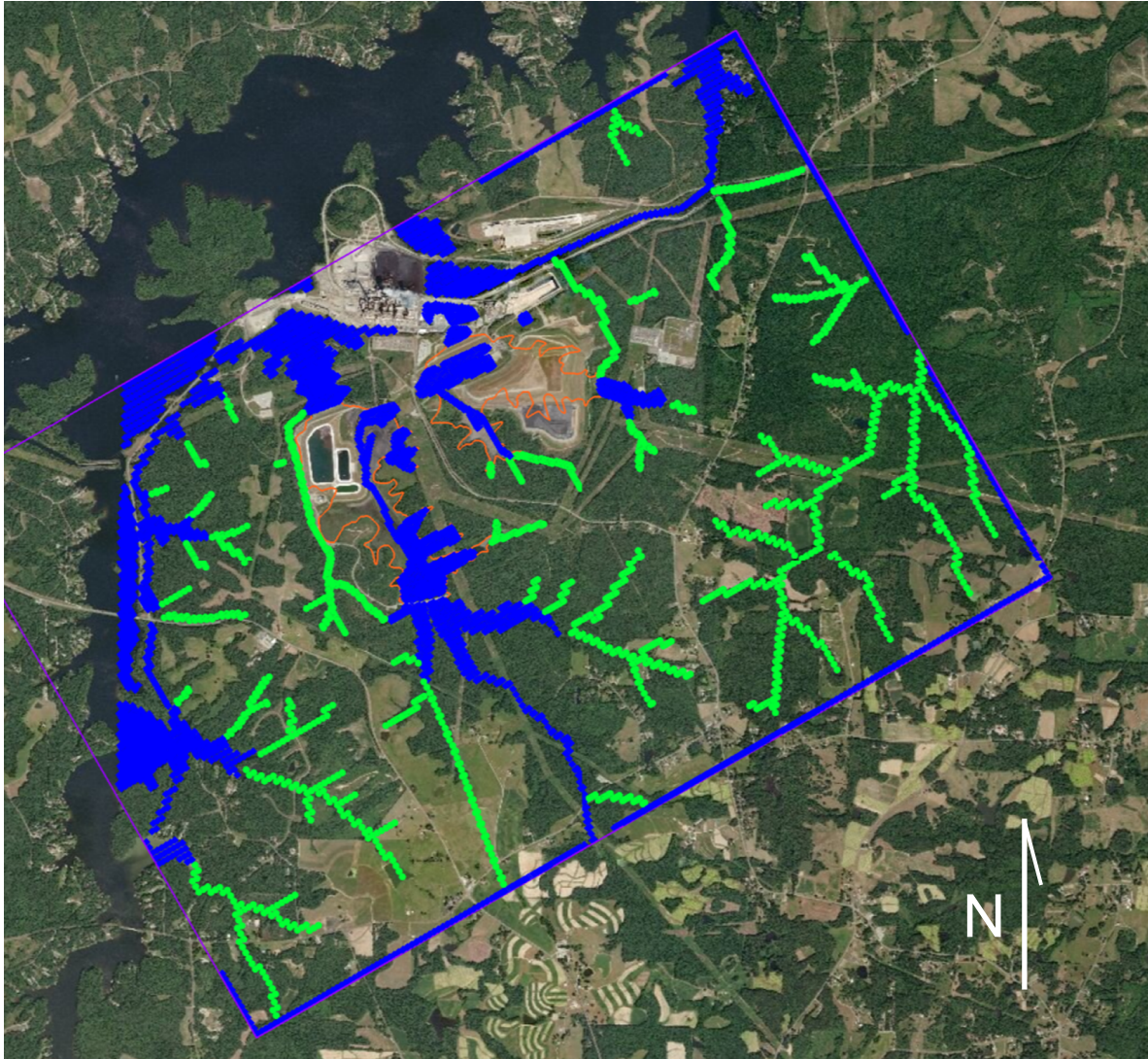


Figure 7. Surface water features in the vicinity of the Roxboro Plant. Lakes, channels, ash basin ponds and impoundments are represented as constant head cells (blue). Streams and discharge canals are represented as drains (green) in the model.

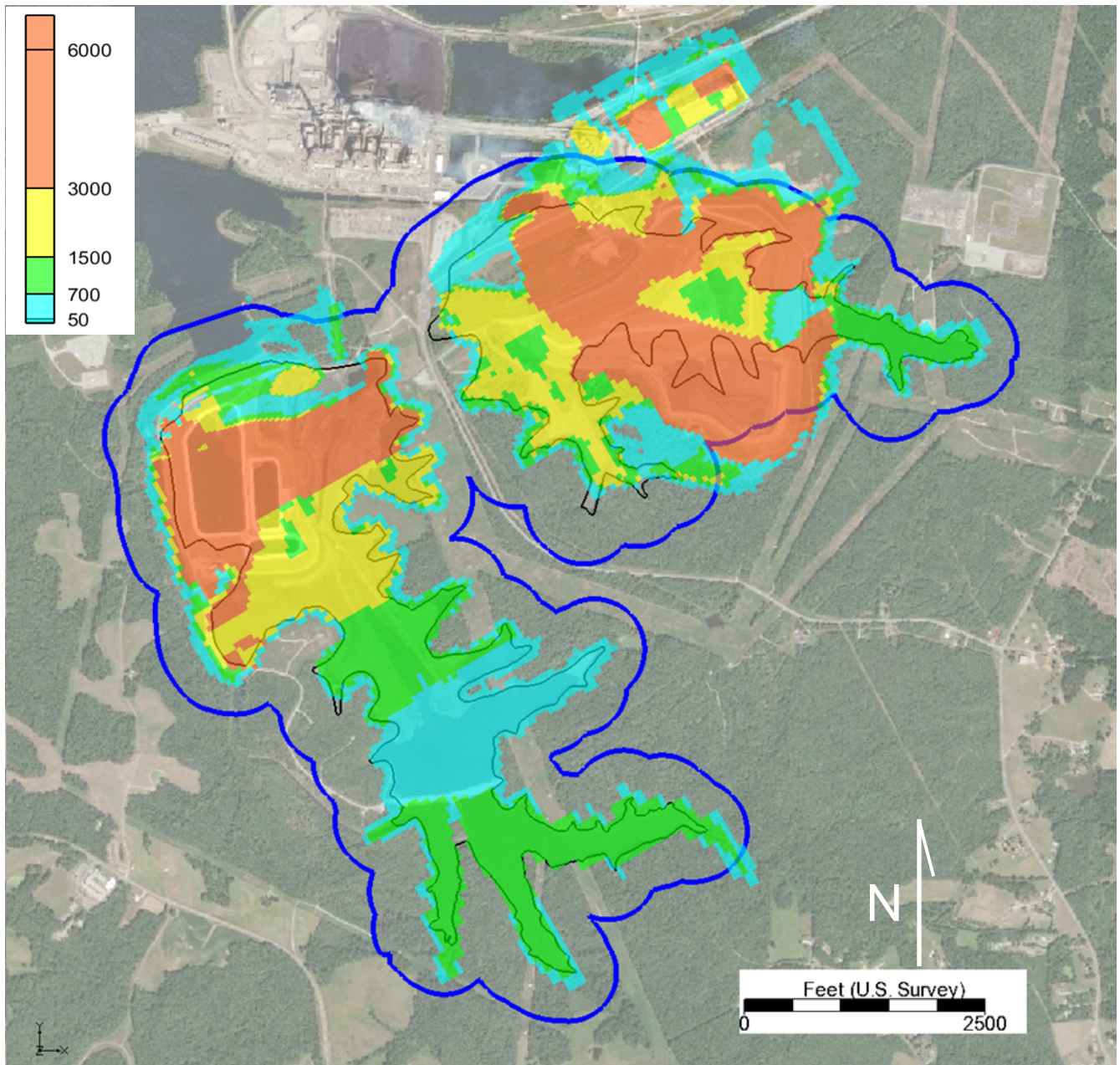


Figure 8. Assumed distribution of concentration of boron ( $\mu\text{g/L}$ ) in 2017.

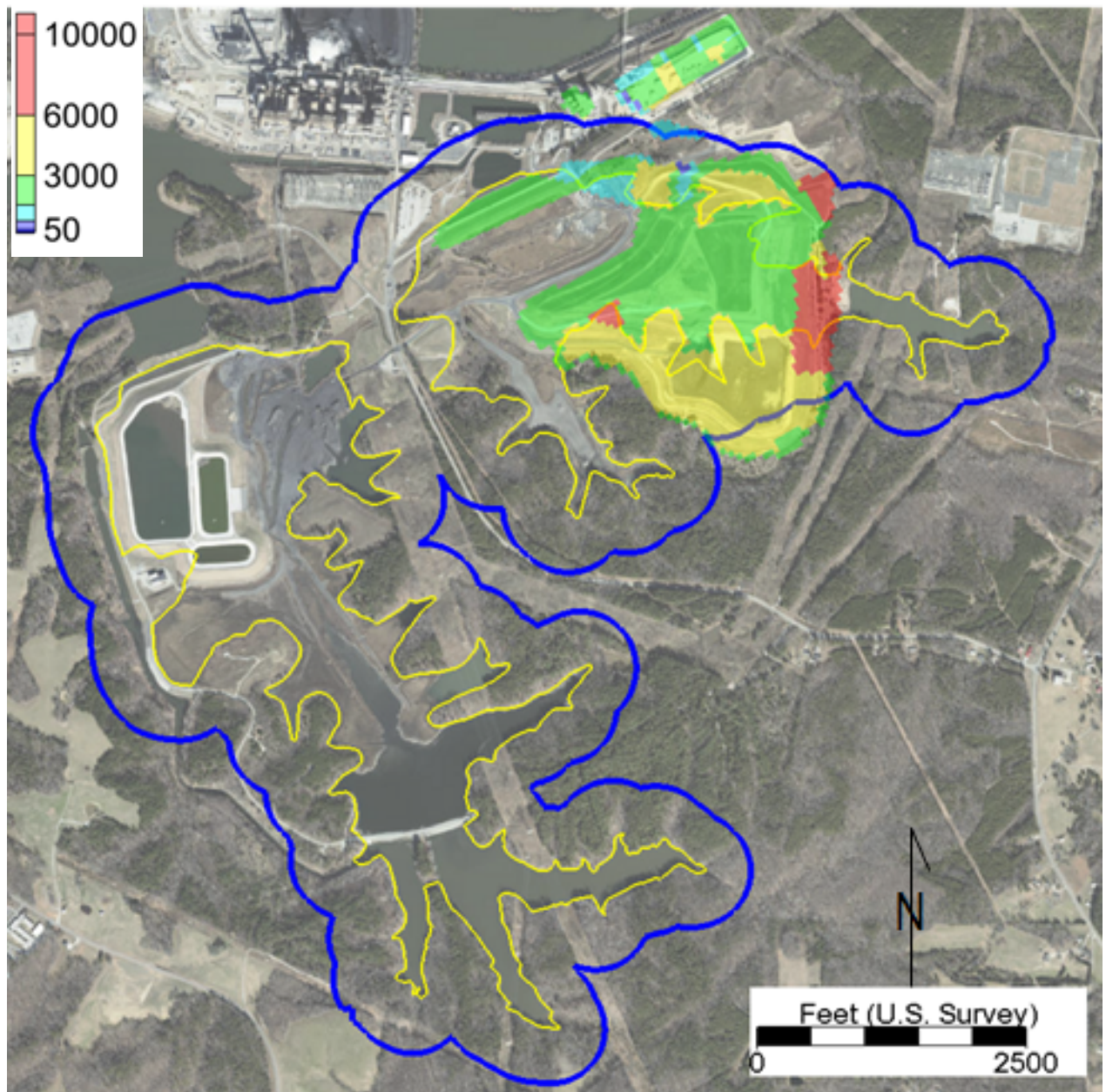


Figure 9. Secondary boron sources created by concentrations ( $\mu\text{g/L}$ ) in recharge.

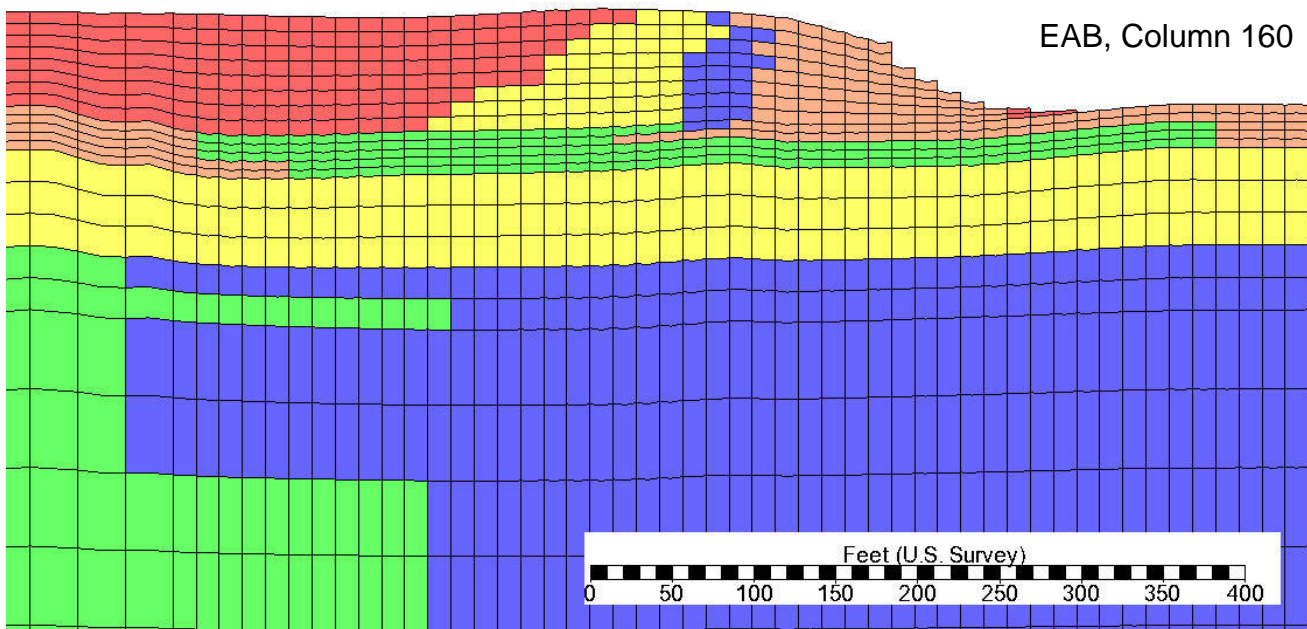
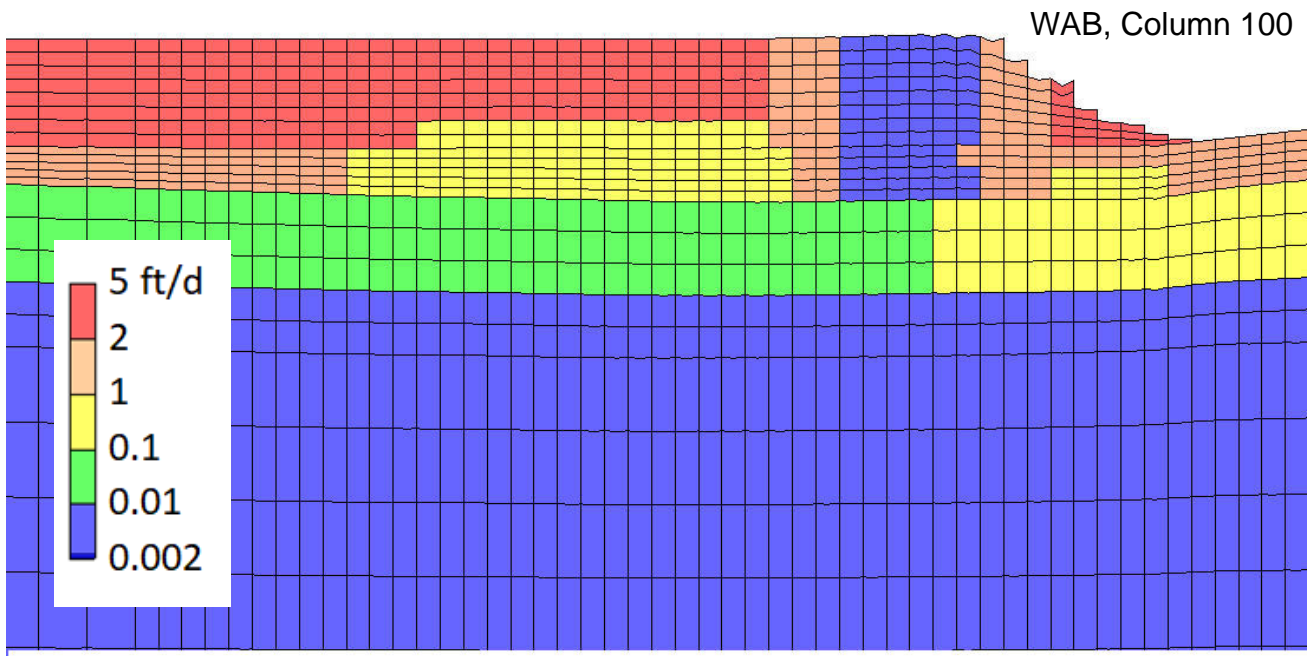


Figure 10. Hydraulic conductivity of the dam in the West Ash Basin and East Ash Basin.

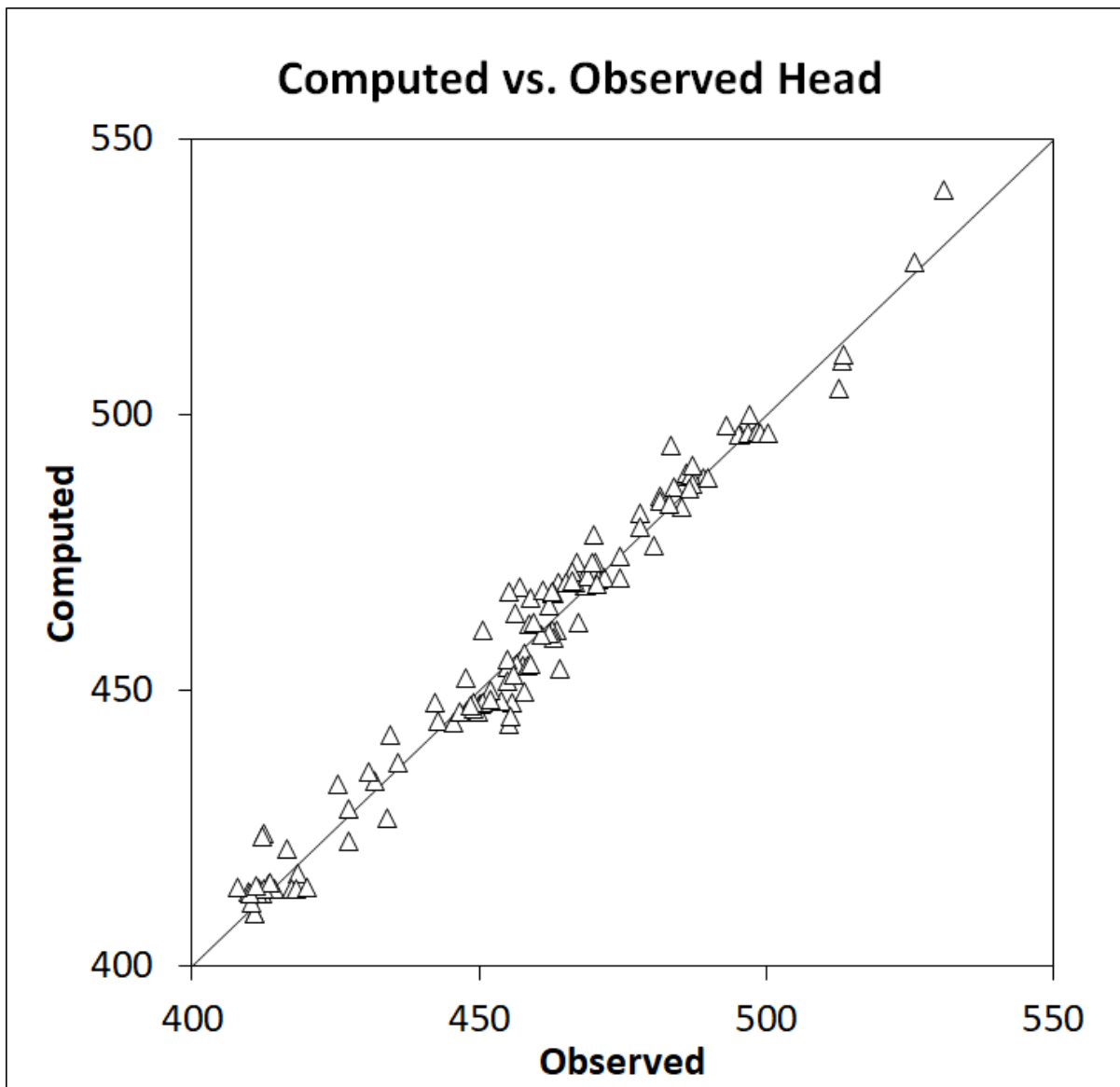


Figure 11. Comparison of observed and computed heads from the calibrated steady state flow model.

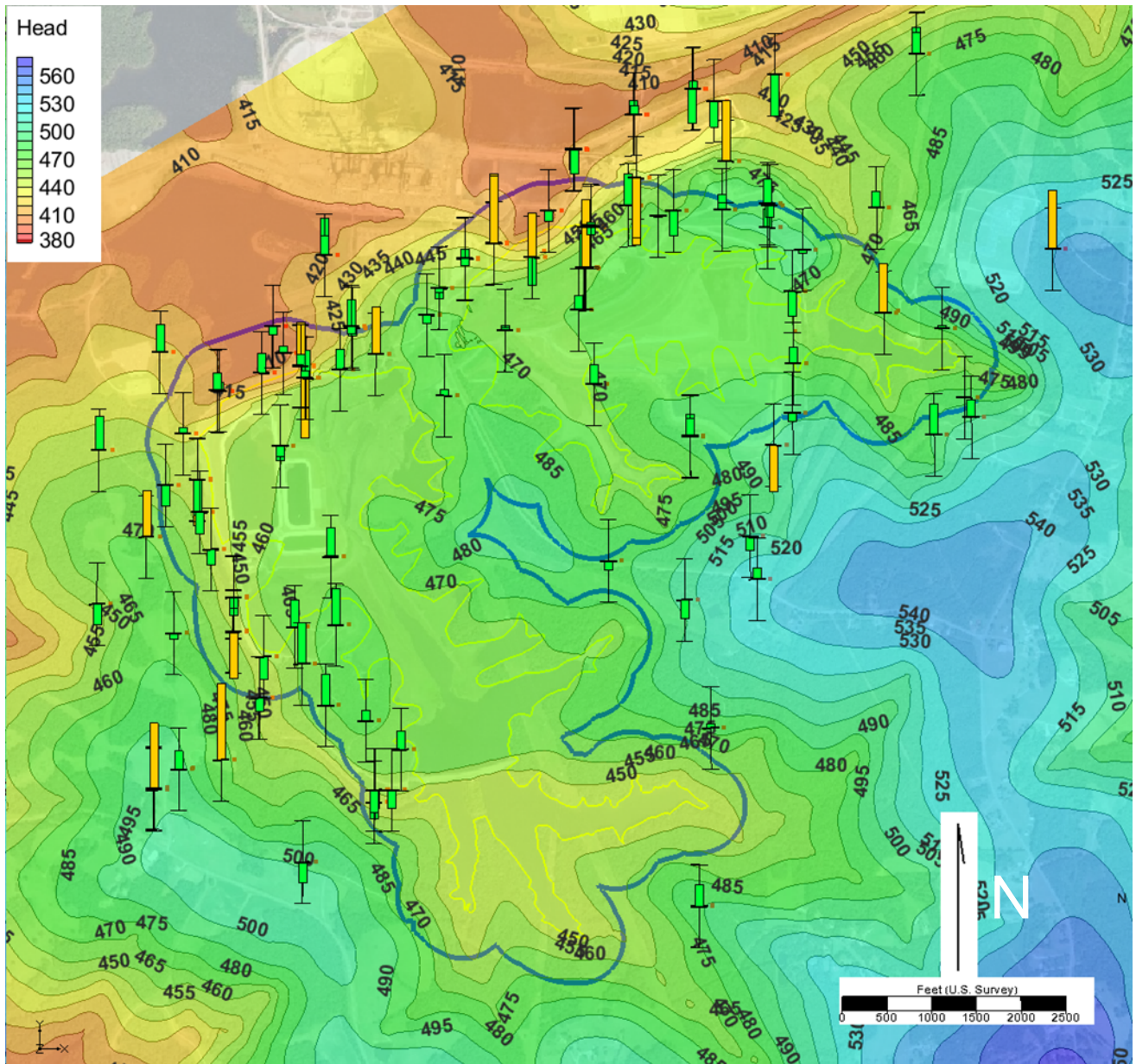


Figure 12. Simulated steady state hydraulic head distribution in the vicinity of the ash basins in the Transition Zone (layer 13). Green bar indicates that simulated heads are within 7 ft of observed heads, yellow bar indicates simulated heads are between 7 and 14 ft of the observed heads.

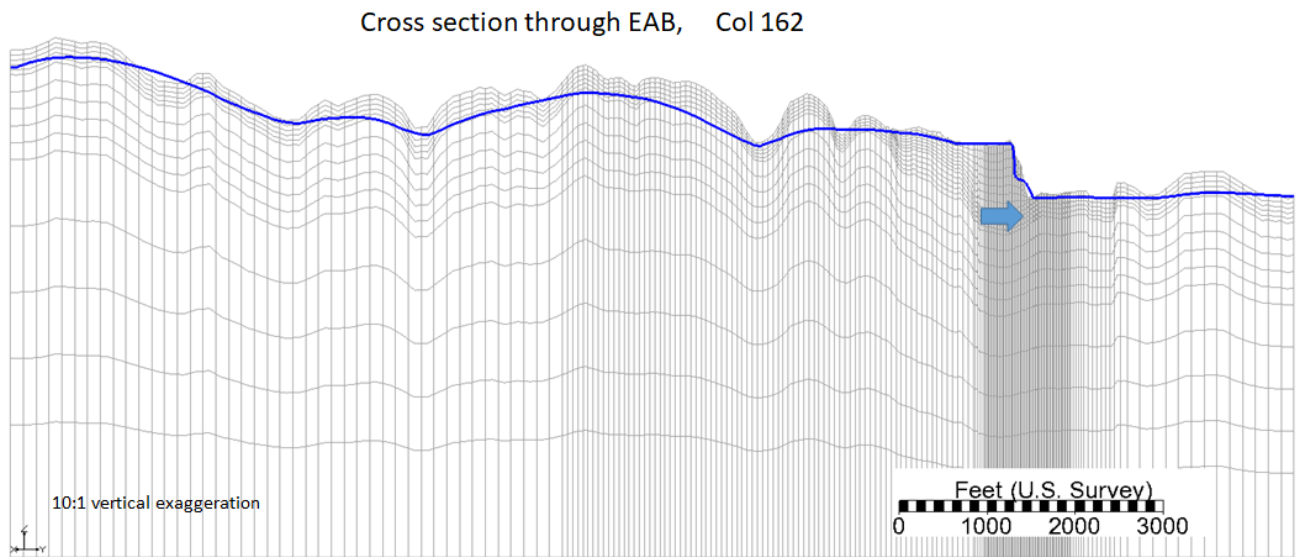
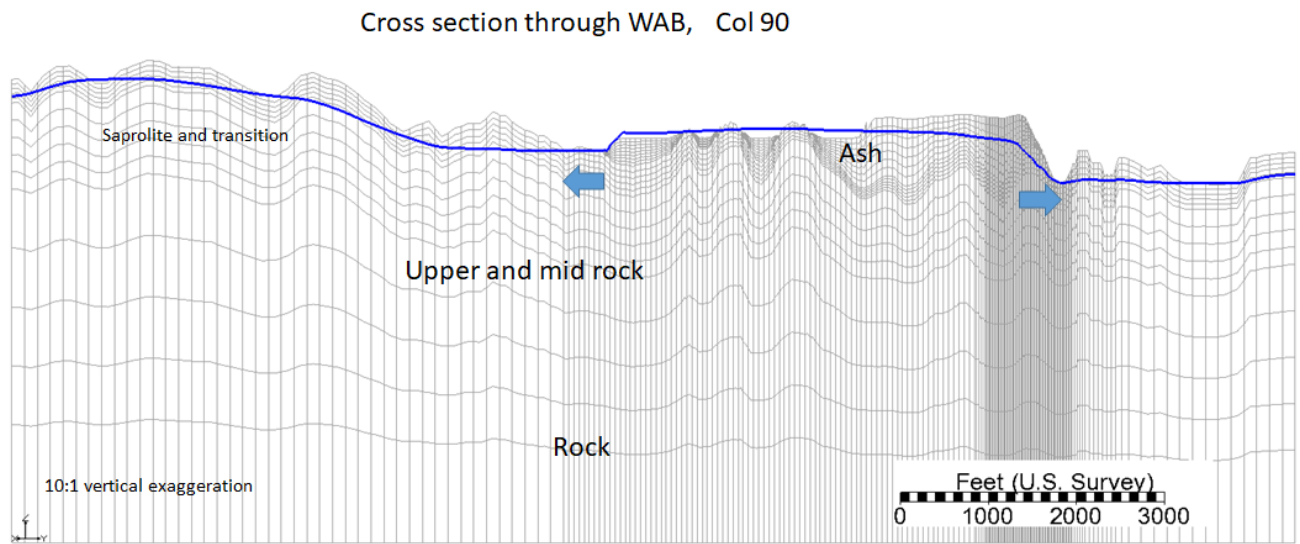


Figure 13. Simulated local groundwater flow systems showing hydraulic heads in the vicinity of the East Ash Basin and West Ash Basin. Blue arrows are inferred groundwater flow directions and indicate the inferred groundwater divide.

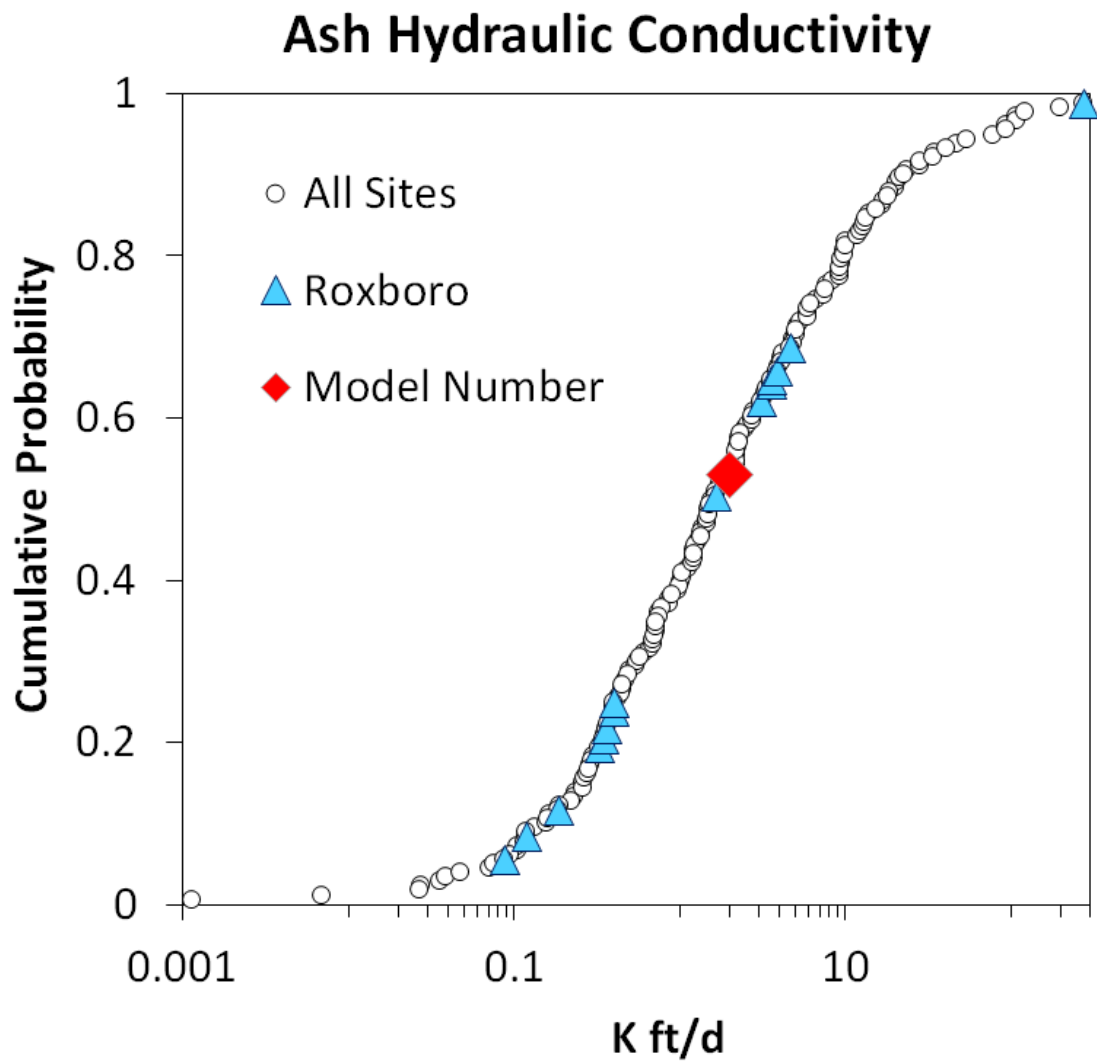


Figure 14. Hydraulic conductivity measurements from slug tests in ash from ash basins in North Carolina, and from the Roxboro site.

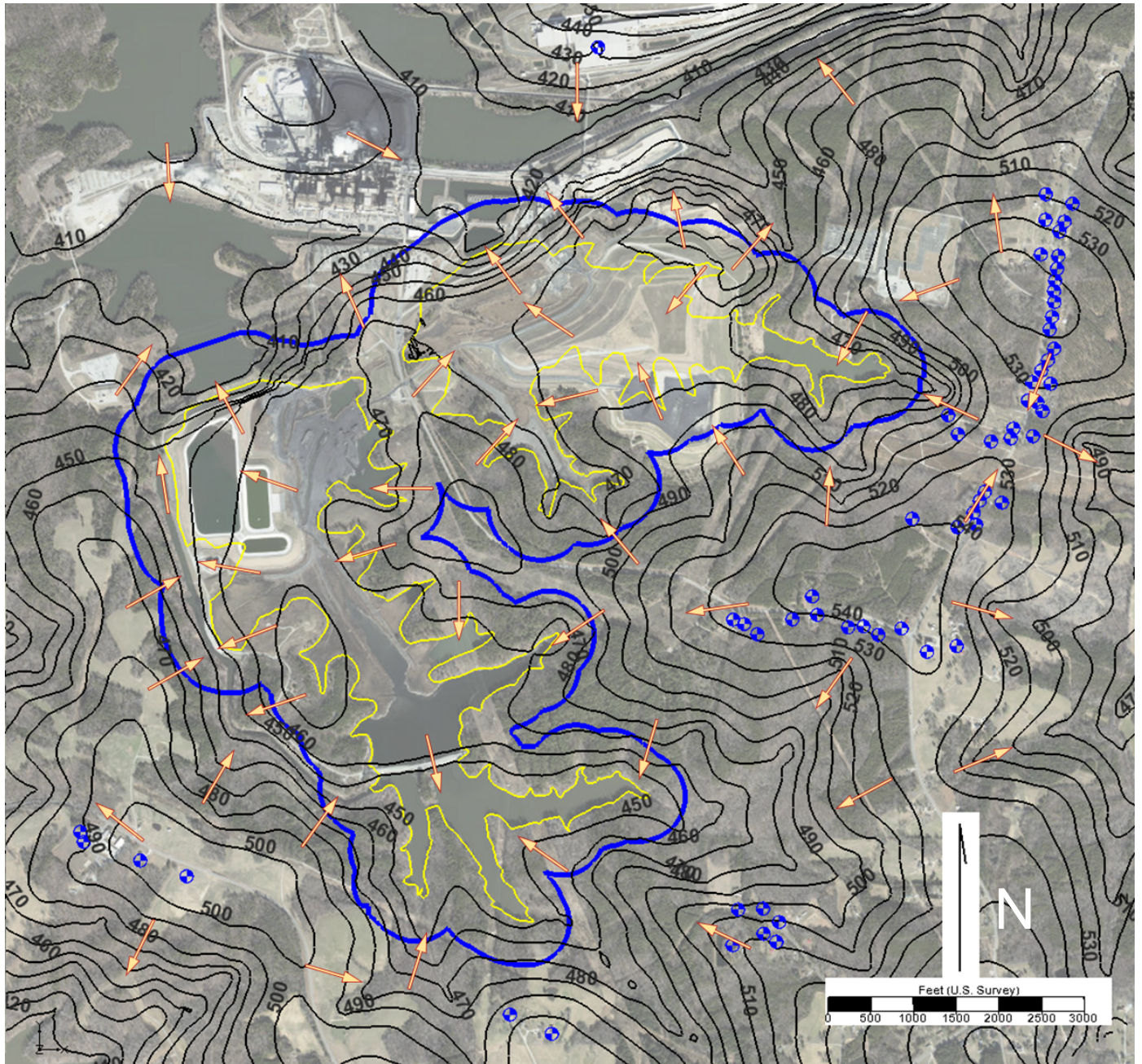


Figure 15. Simulated steady state hydraulic head distribution (feet above NAVD88) in the Transition Zone (layer 13) with inferred groundwater flow directions (orange arrows). Domestic wells shown as blue symbols. Existing 500-ft compliance boundary shown as blue line, ash basin waste boundary shown as yellow line.



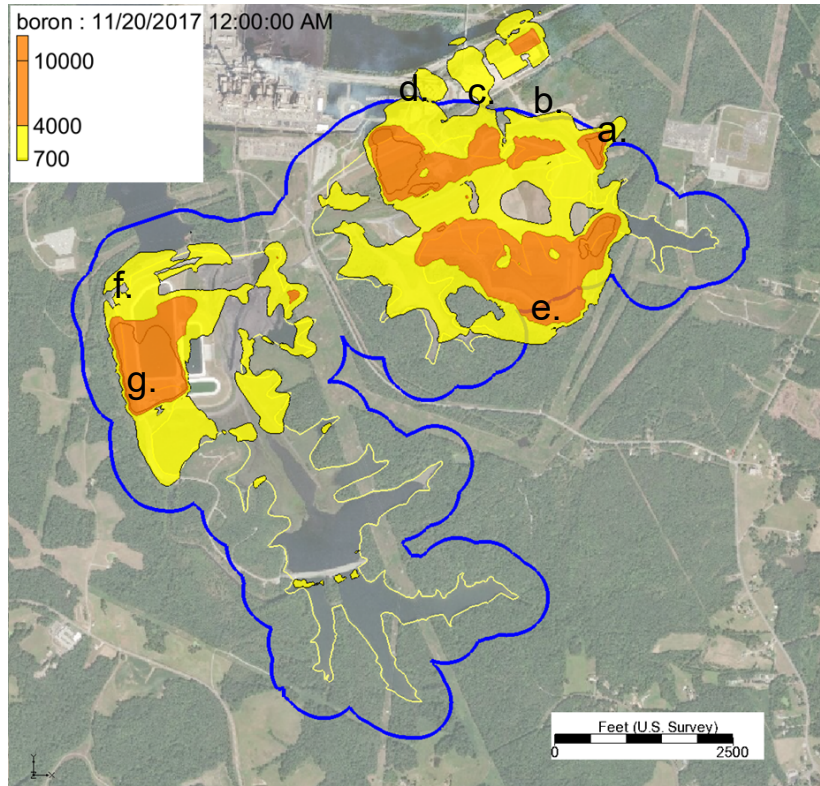
<b>WAB Ash</b>	IN gpm	OUT gpm
Surface water	133	117
Direct Recharge	63	0
Groundwater	74	108
Dam	0	10
Filter dam	0	34
	269	269

<b>EAB Ash</b>	IN gpm	OUT gpm
Surface water	4	41
Direct Recharge	35	0
Groundwater	27	15
Dam	0	5
Filter dam	0	5
	66	66

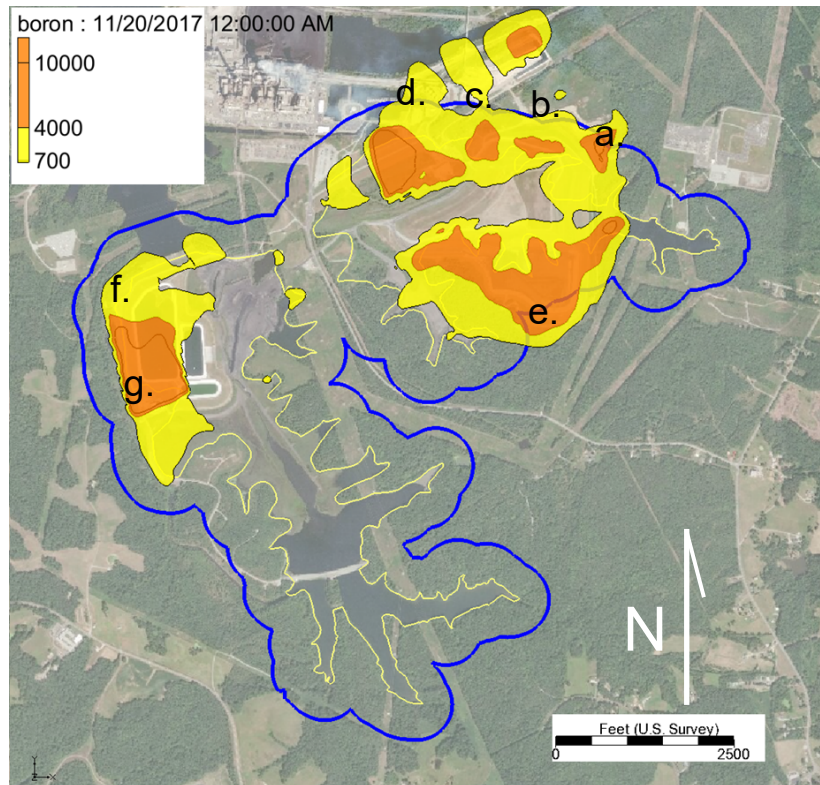
<b>Upgradient Recharge Area</b>	IN	OUT
Recharge	73	
Streams/Seeps		10
Groundwater		63
	73	73

<b>Upgradient Recharge Area</b>	IN	OUT
Recharge	60	
Streams/Seeps		33
Groundwater		27
	60	60

Figure 16. Water balance for East Ash Basin (EAB) and West Ash Basin (WAB). Upper figure shows groundwater divides (black dashed lines) and groundwater drainage areas associated with EAB and WAB, along with inferred flow directions (blue arrows). Sizes of different regions shown in acres. Hydraulic head contours as colored lines. Region outside the areas draining into the ash basins covered with transparent mask. Ash basin waste boundary as orange line. Tables show the components of the water balance in gal/min.



**Layer 13**



**Layer 15**

Figure 17. Simulated boron distribution (700 and 4000  $\mu\text{g/L}$ ) in the Transition Zone (layer 13) and shallow rock (layer 15) in 2017. Letters are reference locations. a.) northeast EAB; b.) north EAB; c.) gypsum storage area, EAB; d.) northwest EAB; e.) southeast EAB; f.) northwest WAB; g.) west WAB.

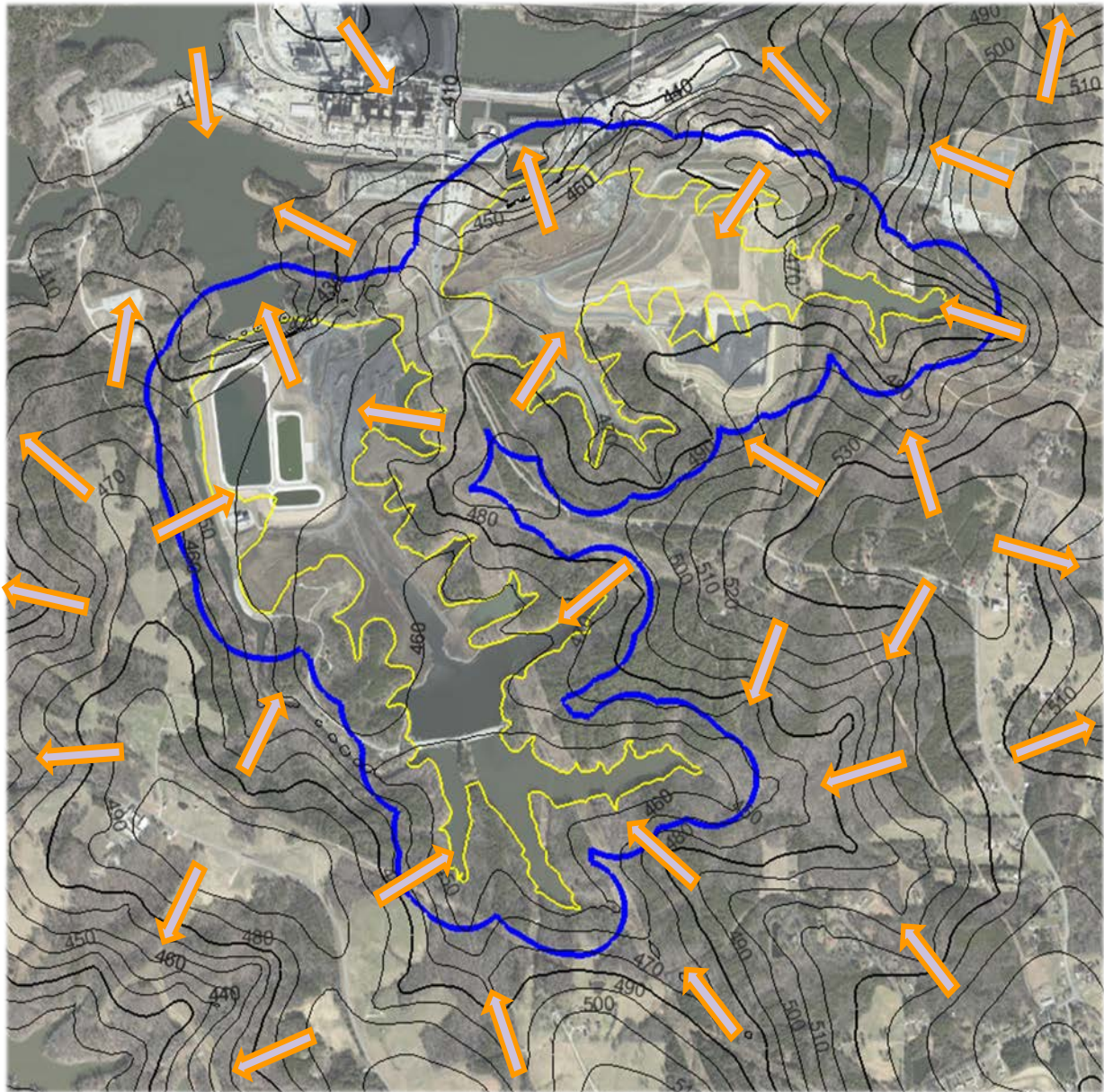


Figure 18. Simulated hydraulic head distribution (feet above NAVD88) in the transition zone (layer 13) during the interim period. Existing 500-ft compliance boundary shown as blue line, ash basin waste boundary shown as yellow line, and approximate groundwater flow direction shown as orange arrows.

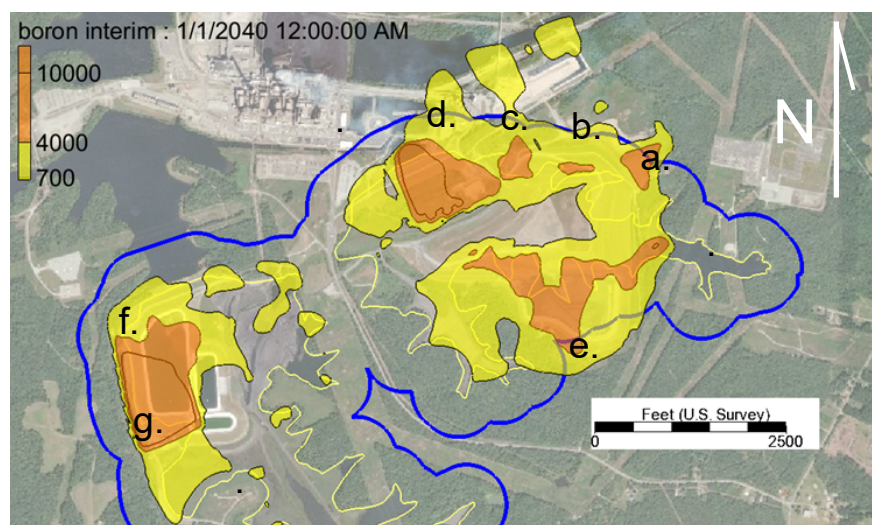
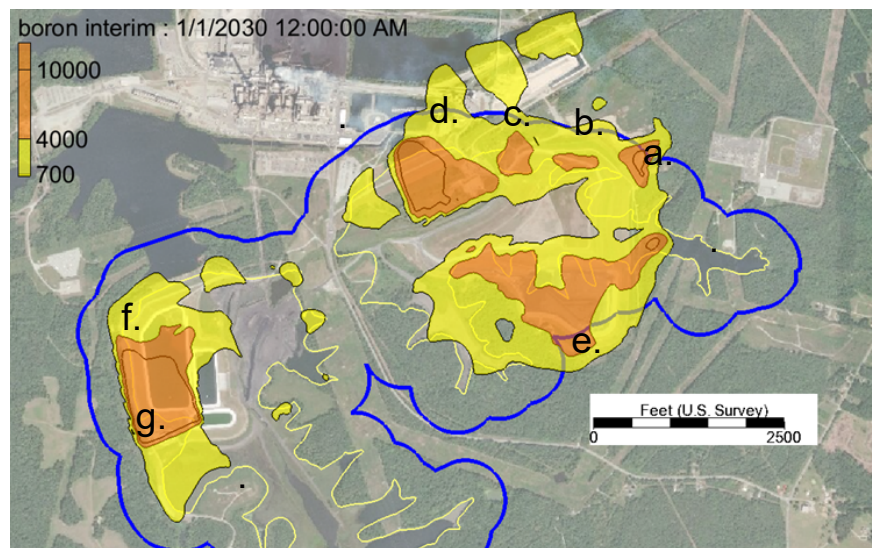
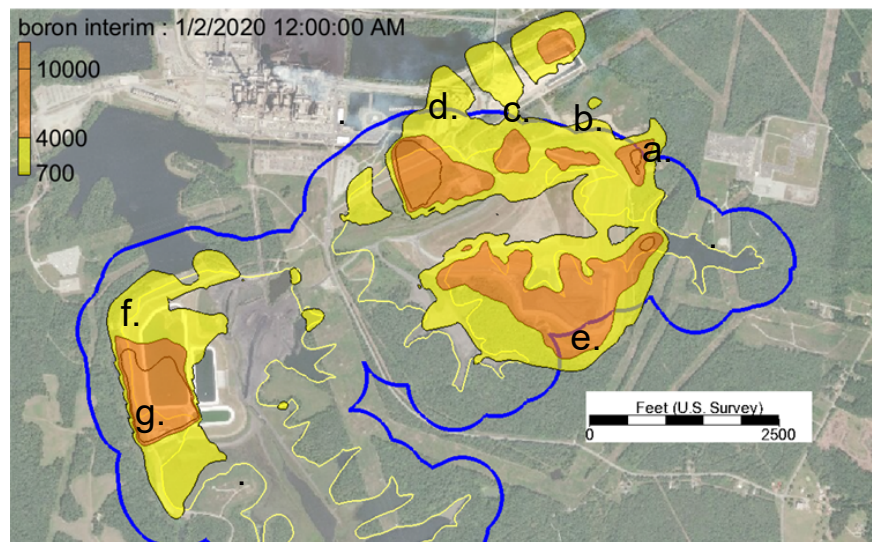


Figure 19. Simulated boron concentrations ( $\mu\text{g/L}$ ) during the interim period 2020-2027 in shallow fractured rock (layer 15). Letters are reference locations. a.) northeast EAB; b.) north EAB; c.) gypsum storage area, EAB; d.) northwest EAB; e.) southeast EAB; f.) northwest WAB; g.) west WAB.

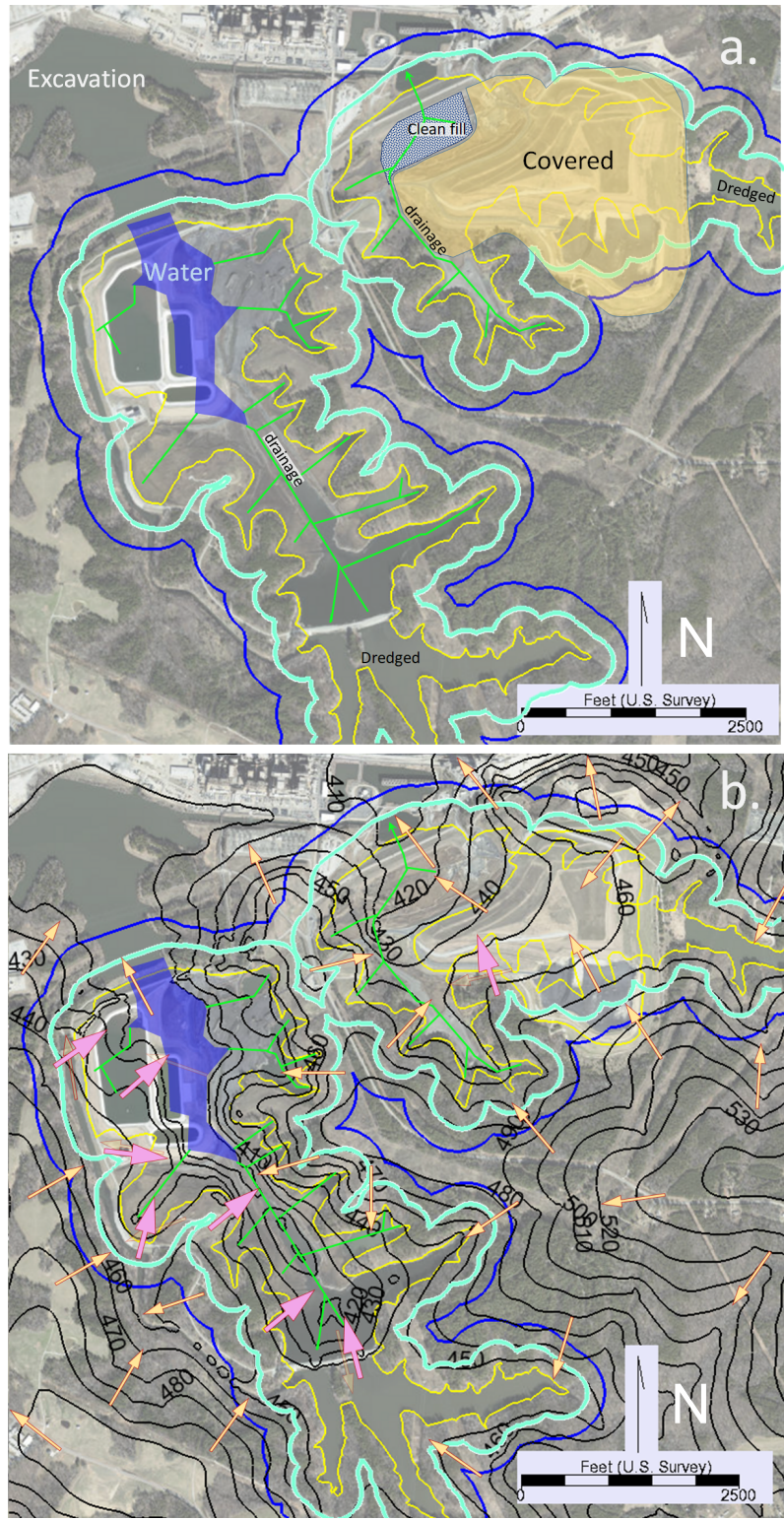


Figure 20. Configuration of features used to represent the Excavation with Landfill scenario in the model (a) and simulated hydraulic heads (b). a.) Green lines are drains and blue area is region that will be covered with surface water. Stippled area will be excavated and graded with clean fill to create surface drainage. b.) Hydraulic head contours (feet above NAVD88) and flow directions for the Excavation scenario. Pink arrows are flow directions that differ from current conditions, orange arrows are flow directions similar to current directions. Existing 500-ft compliance boundary shown as blue line, future 250-ft compliance boundary for the Excavation scenario shown as light blue line, and waste boundary shown as yellow line.

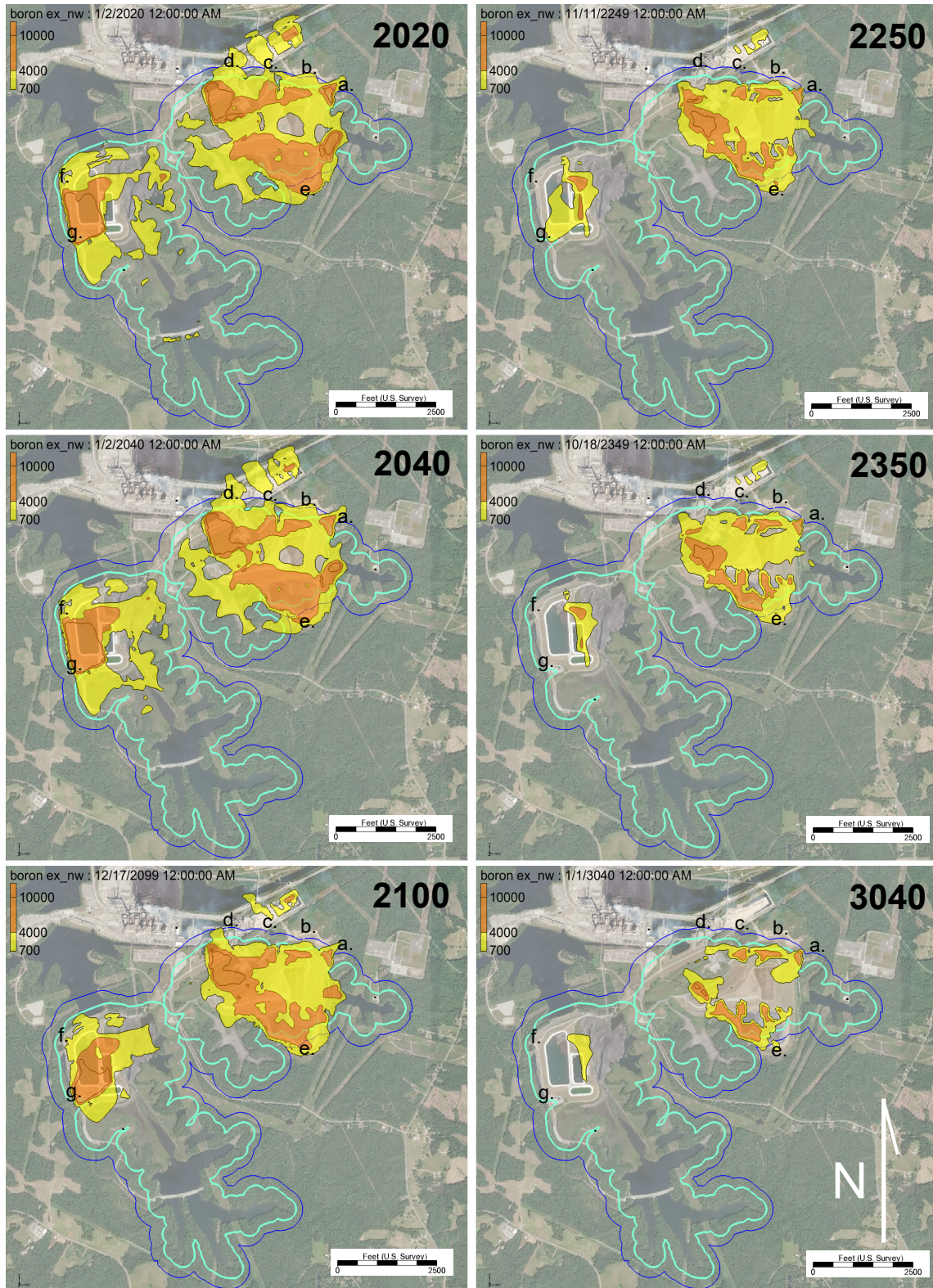


Figure 21. Distribution of boron concentrations ( $\mu\text{g/L}$ ) during the Excavation with Landfill scenario at representative times in the Transition Zone (layer 13). Persistent boron concentrations in the EAB are above the water table. Existing 500-ft compliance boundary shown as blue. Future 250-ft compliance boundary for the Excavation scenario shown as light blue line. Letters are reference locations. a.) northeast EAB; b.) north EAB; c.) gypsum storage area, EAB; d.) northwest EAB; e.) southeast EAB; f.) northwest WAB; g.) west WAB.

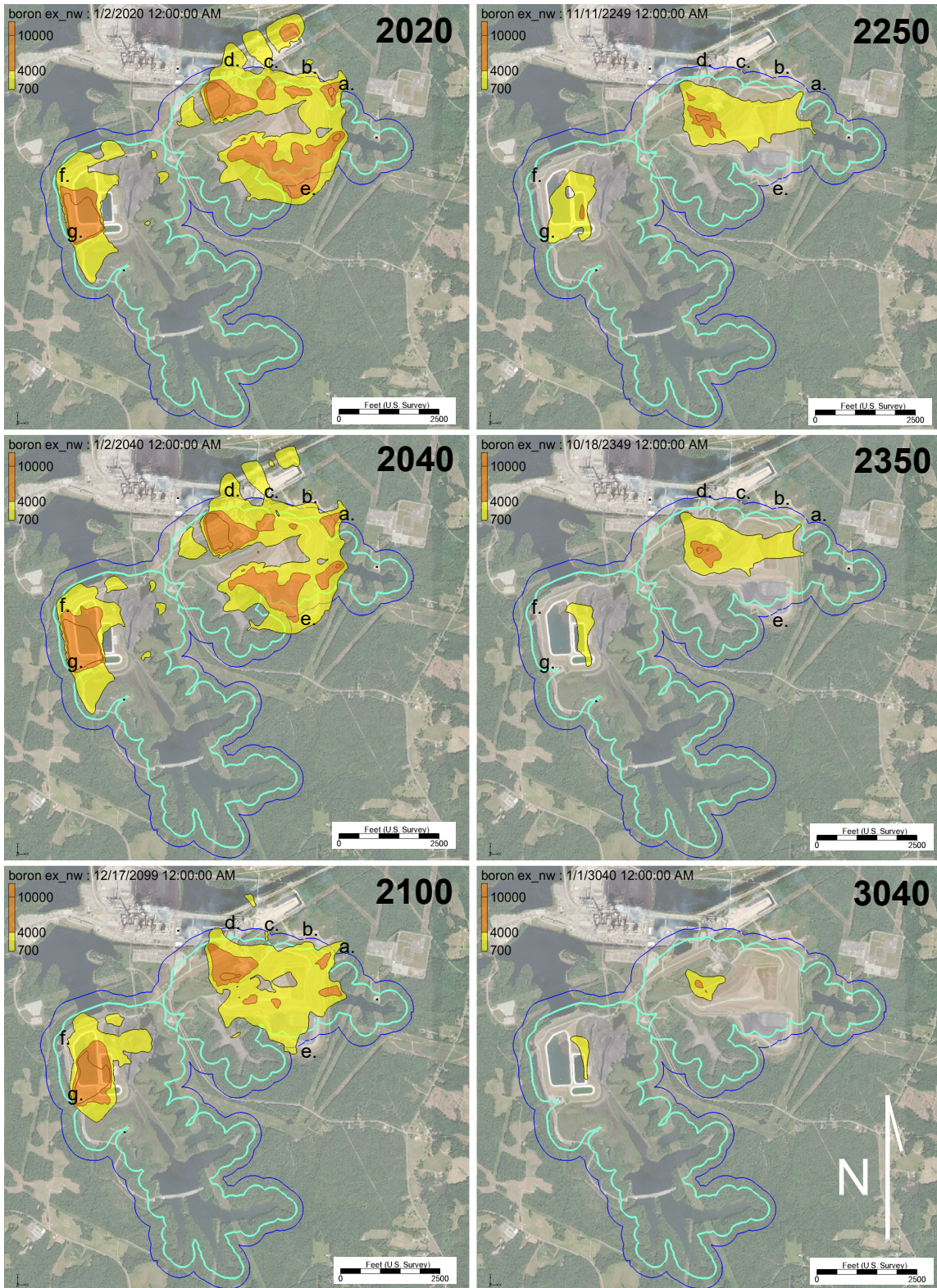


Figure 22. Distribution of boron concentrations ( $\mu\text{g/L}$ ) during the Excavation with Landfill scenario at representative times in the Shallow Rock Zone (layer 15). Existing 500-ft compliance boundary shown as blue line, future 250-ft compliance boundary for the Excavation scenario shown as light blue line. Letters are reference locations. a.) northeast EAB; b.) north EAB; c.) gypsum storage area, EAB; d.) northwest EAB; e.) southeast EAB; f.) northwest WAB; g.) west WAB.

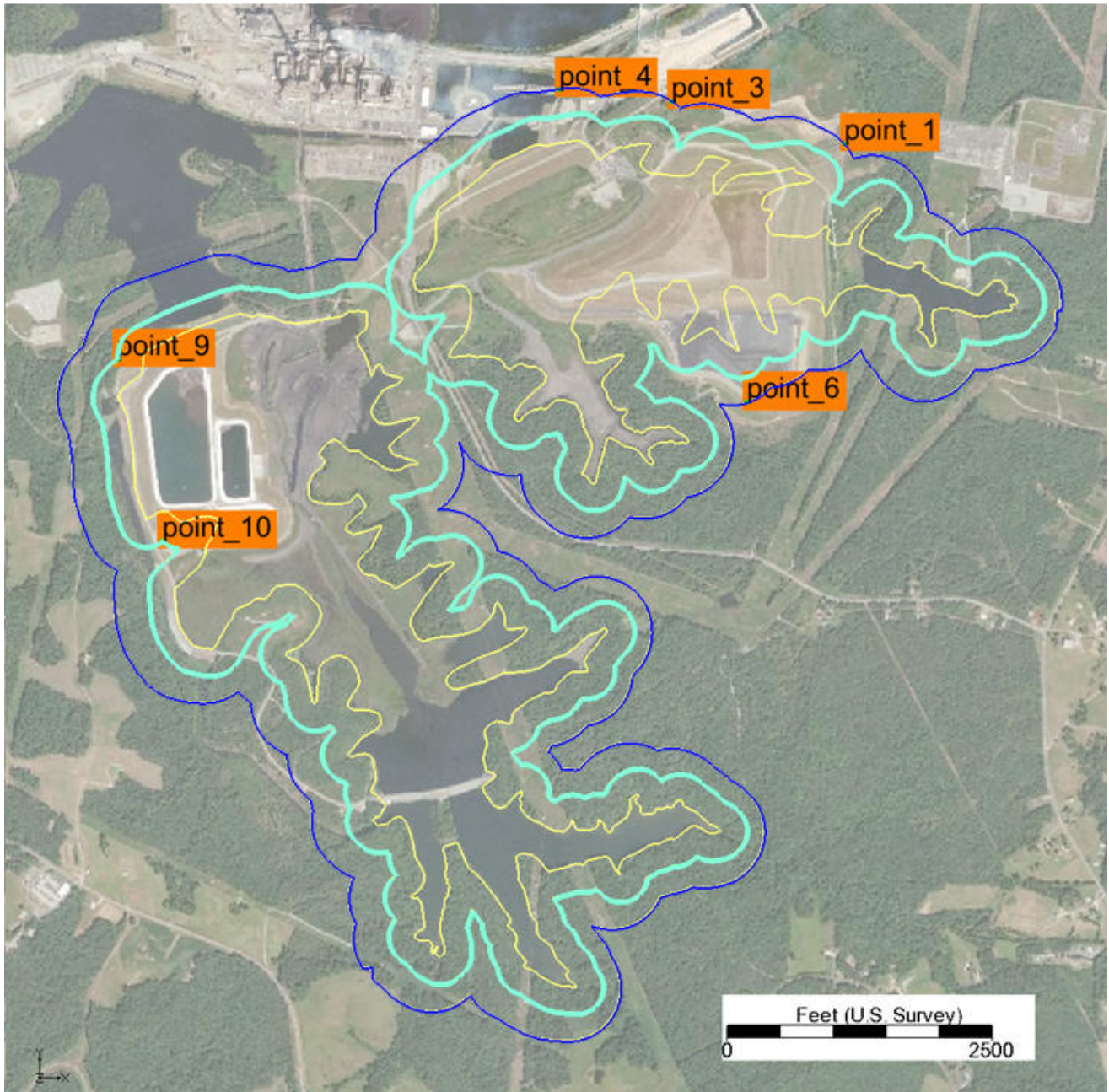


Figure 23. Observation points for time series plots. Existing 500-ft compliance boundary shown as blue line, future 250-ft compliance boundary for the Excavation with Landfill scenario shown as light blue line, waste boundary shown as yellow line.

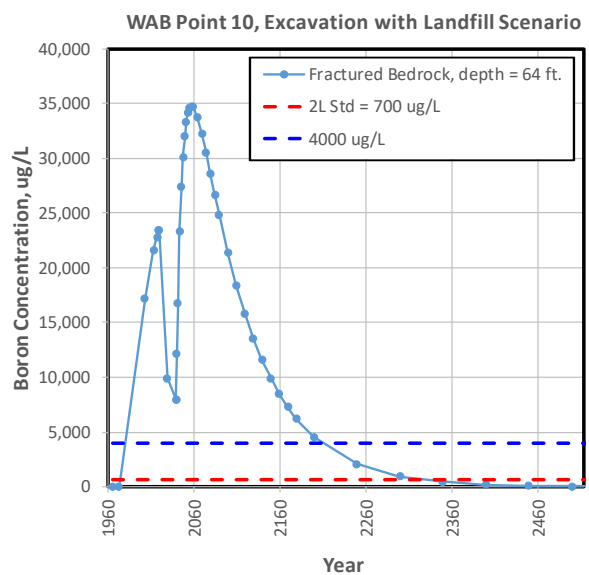
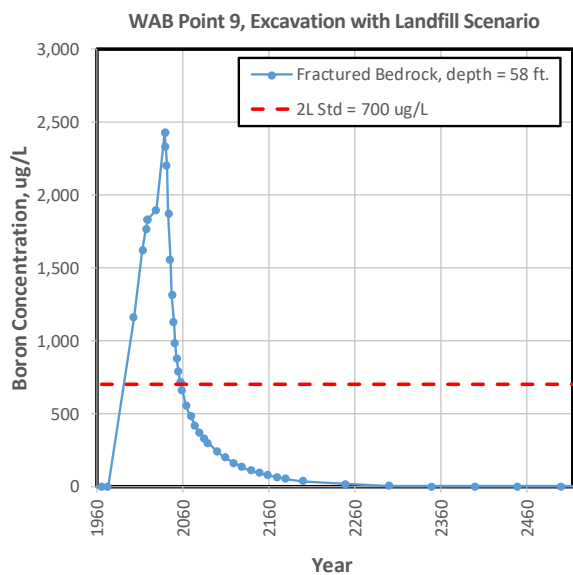
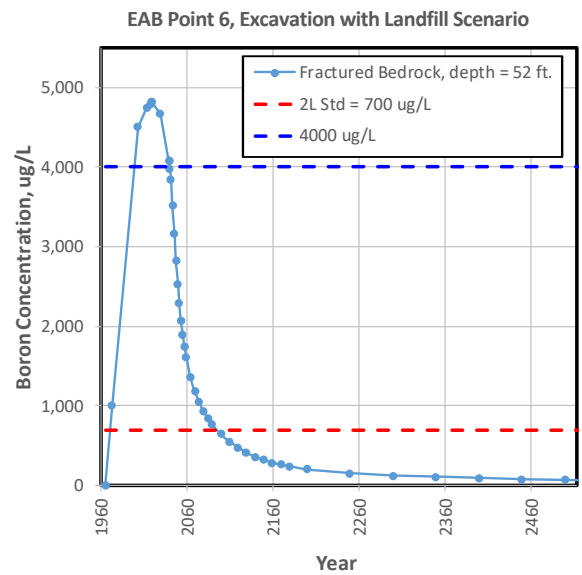
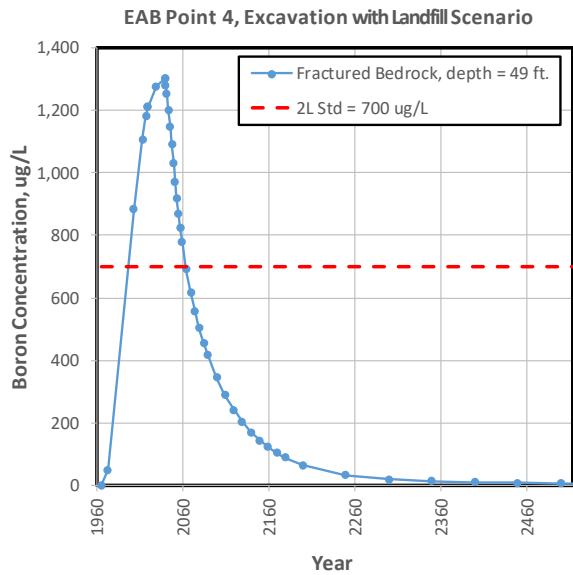
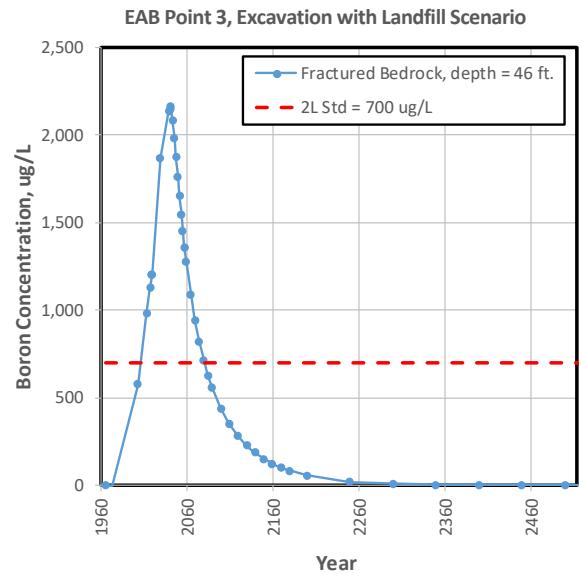
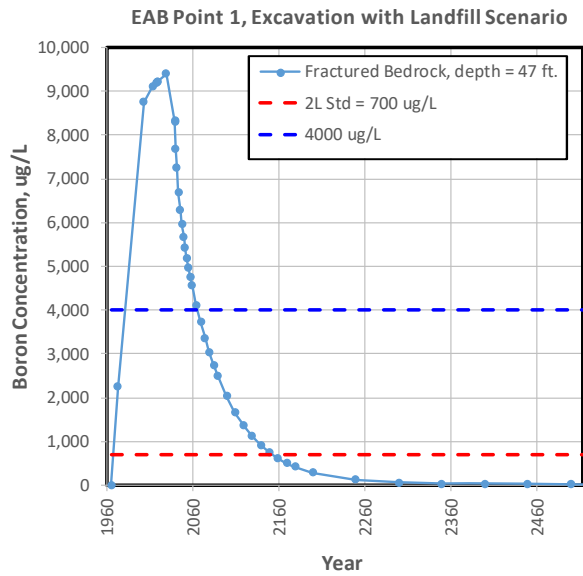


Figure 24. Times series of boron concentrations at six representative locations in the EAB and WAB during the Excavation with Landfill scenario.

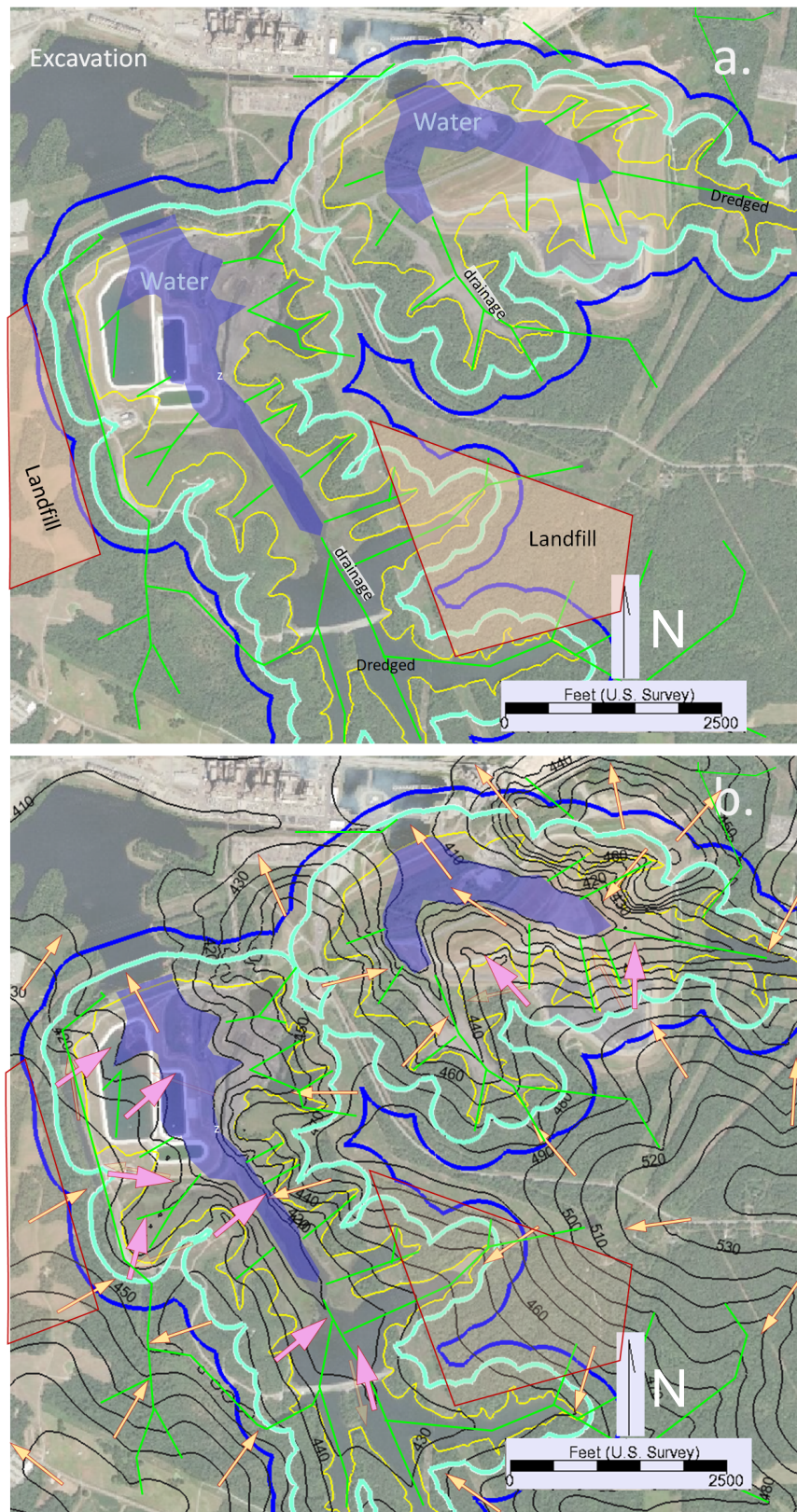


Figure 25. Configuration of features used to represent the Complete Excavation scenario in the model. a.) Green lines are drains and blue area is region that will be covered with surface water. Red shades are new on-site landfills. b.) Hydraulic head contours (feet above NAVD88) and flow directions for the Excavation scenario. Thick pink arrows are flow directions that differ from current conditions, thin orange arrows are flow directions similar to current directions. Existing 500-ft compliance boundary shown as blue line, future 250-ft compliance boundary for the Excavation scenario shown as light blue line, and waste boundary shown as yellow line.

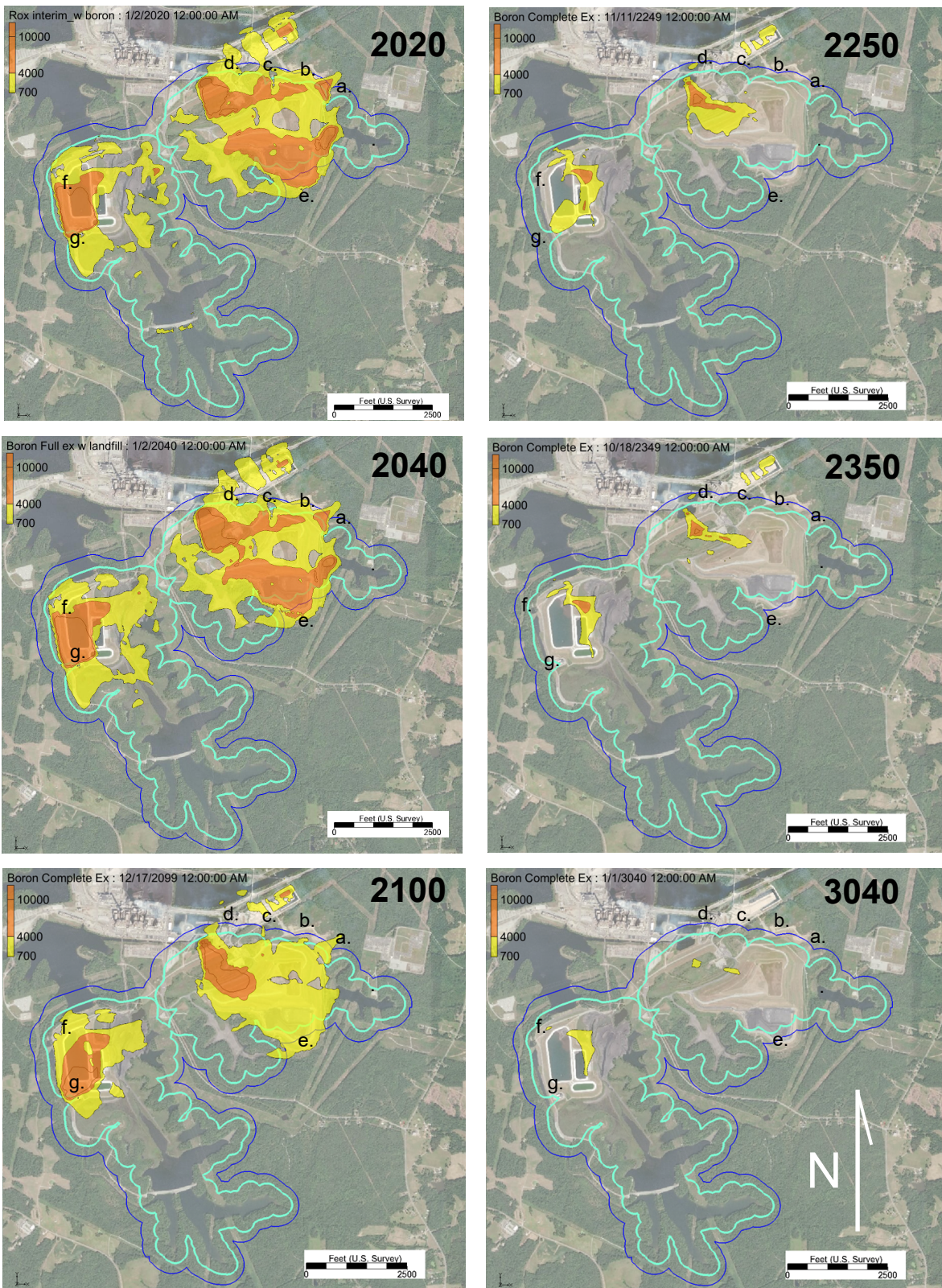


Figure 26. Distribution of boron concentrations ( $\mu\text{g/L}$ ) during Complete Excavation scenario at representative times in the Transition Zone (layer 13). Existing 500-ft compliance boundary shown as blue line, future 250-ft compliance boundary for the Excavation scenario shown as light blue line. Letters are reference locations. a.) northeast EAB; b.) north EAB; c.) gypsum storage area, EAB; d.) northwest EAB; e.) southeast EAB; f.) northwest WAB; g.) west WAB.

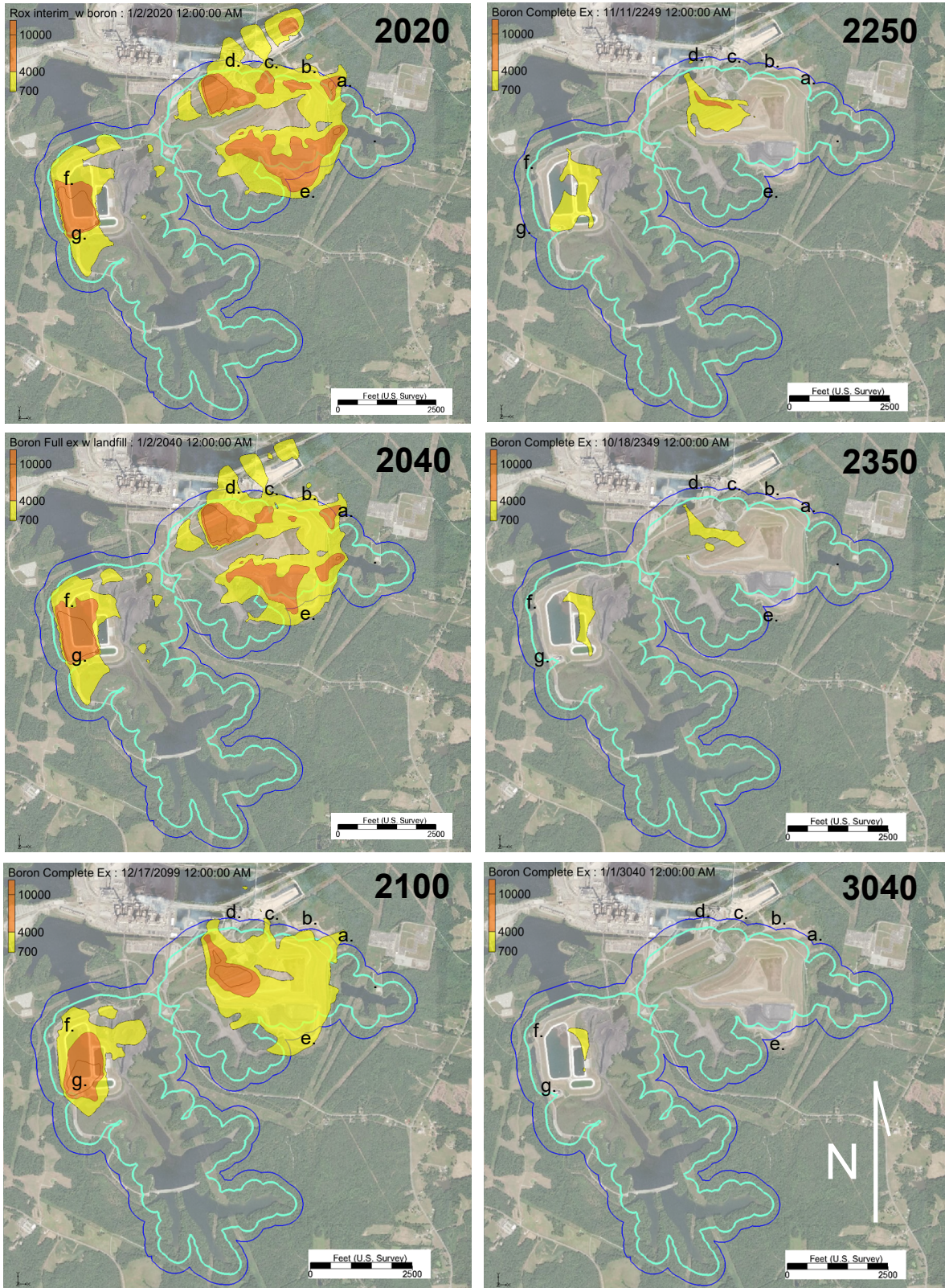
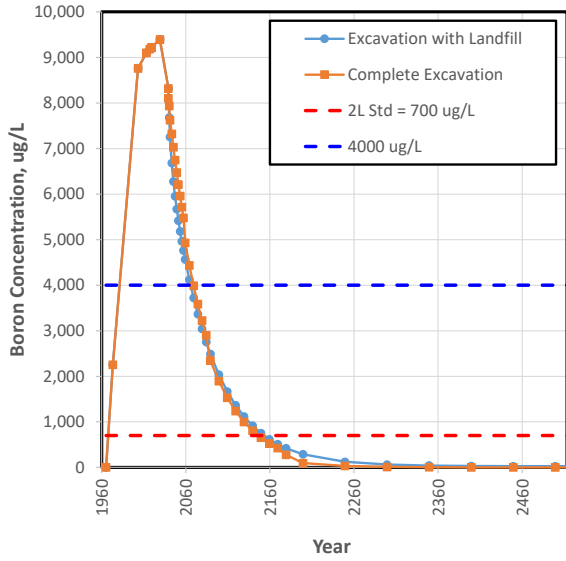
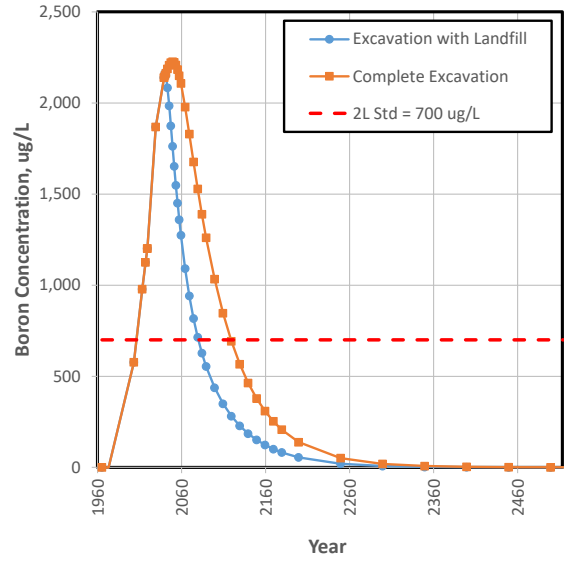


Figure 27. Distribution of boron concentrations ( $\mu\text{g/L}$ ) during Complete Excavation scenario at representative times in the Shallow Rock Zone (layer 15). Existing 500-ft compliance boundary shown as blue line future, 250-ft compliance boundary for the Excavation scenario shown as light blue line. Letters are reference locations. a.) northeast EAB; b.) north EAB; c.) gypsum storage area, EAB; d.) northwest EAB; e.) southeast EAB; f.) northwest WAB; g.) west WAB.

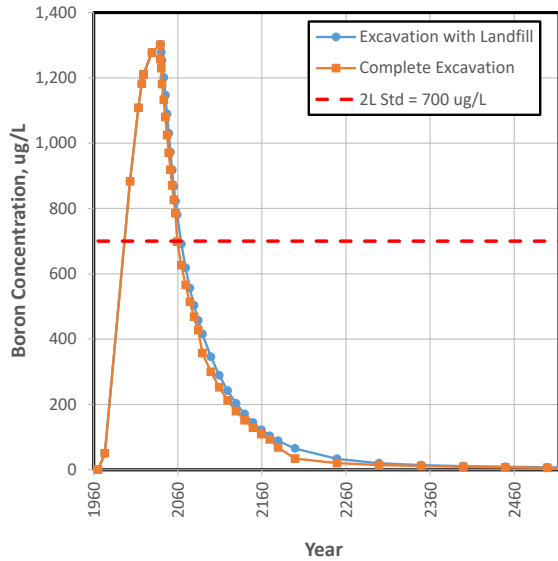
EAB Point 1, Excavation Scenario, Fractured Rock, d = 47 ft.



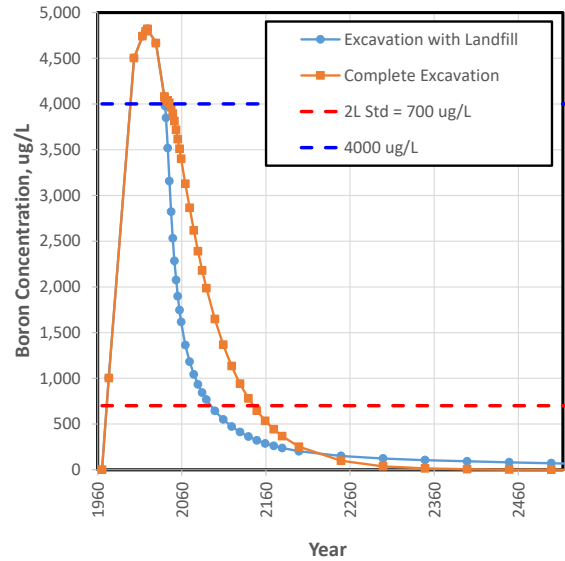
EAB Point 3, Excavation Scenario, Fractured Rock, d = 46 ft.



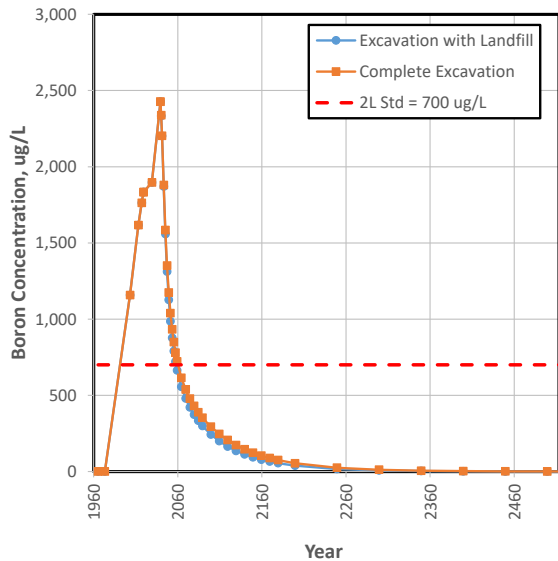
EAB Point 4, Excavation Scenario, Fractured Rock, d = 49 ft.



EAB Point 6, Excavation Scenario, Fractured Rock, d = 52 ft.



WAB Point 9, Excavation Scenario, Fractured Rock, d = 58 ft.



WAB Point 10, Excavation Scenario, Fractured Rock, d = 64 ft.

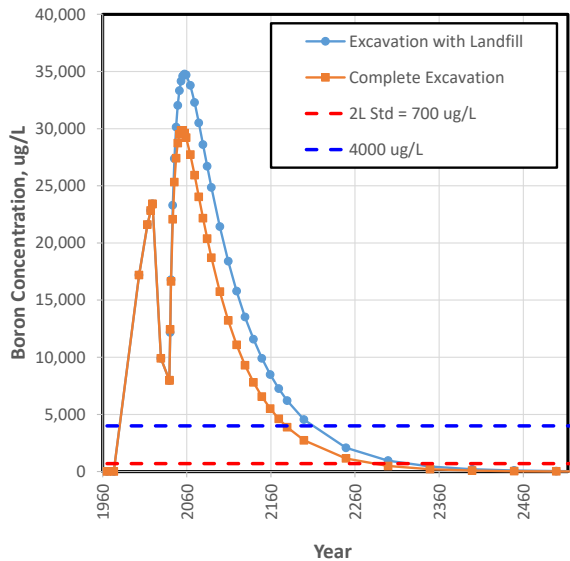


Figure 28. Times series of boron concentrations at six representative locations in the EAB and WAB during the Excavation with Landfill and Complete Excavation scenarios.

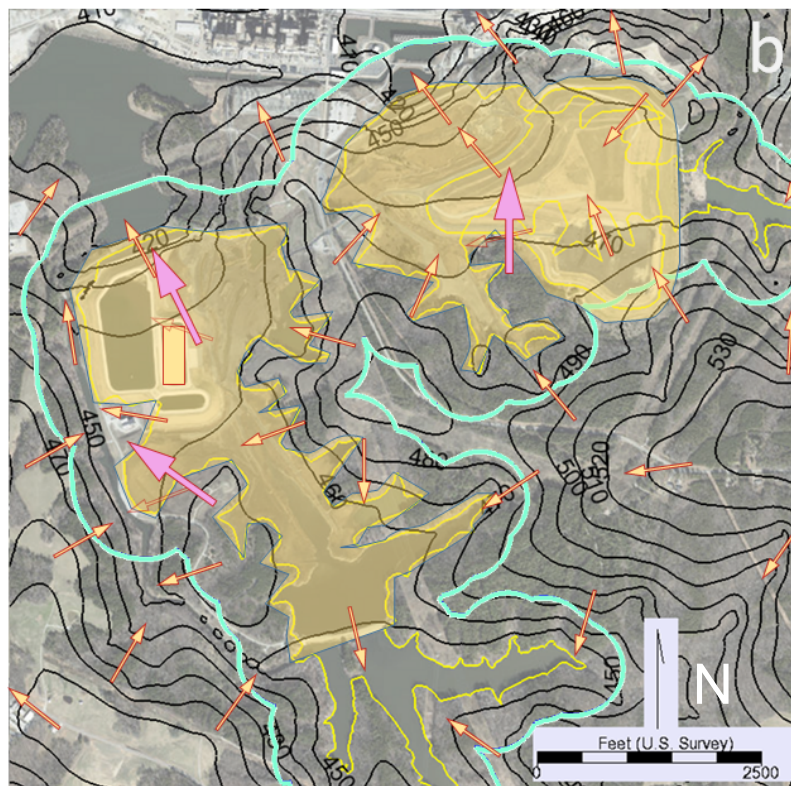
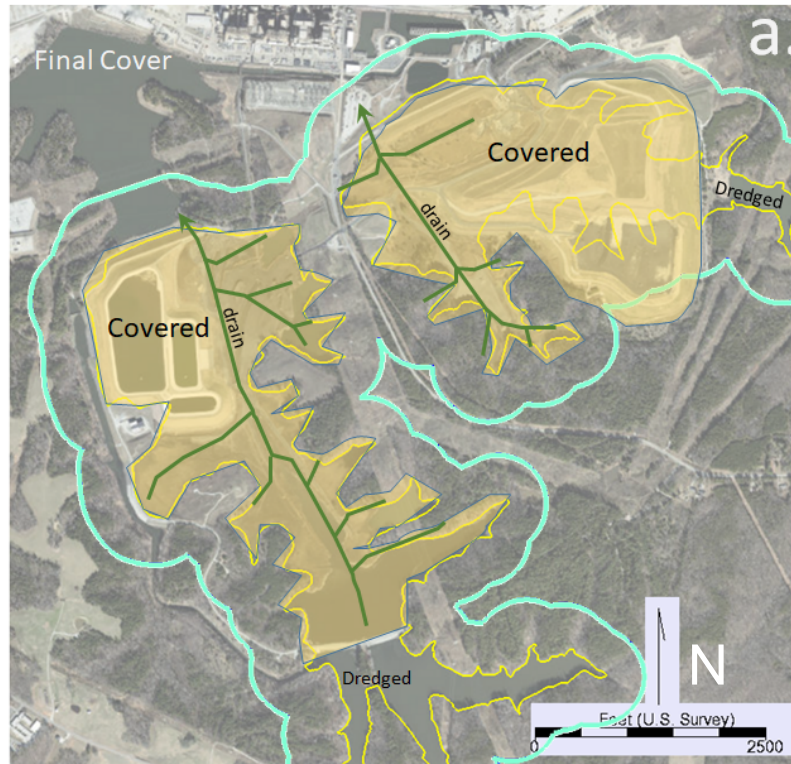


Figure 29. Configuration of features used to represent the Final Cover scenario in the model (a) and simulated hydraulic heads (b). a.) Yellow area is covered with low permeability cap, green lines are swale drains beneath the cover. b.) Hydraulic head contours (feet above NAVD88) and flow directions for the Final Cover scenario. Thick pink arrows are flow directions that differ from current conditions, thin orange arrows are flow directions similar to current directions. Compliance boundary for the Final Cover scenario is the same as the existing 500-ft compliance boundary and is highlighted in light blue, waste boundary shown as yellow line.

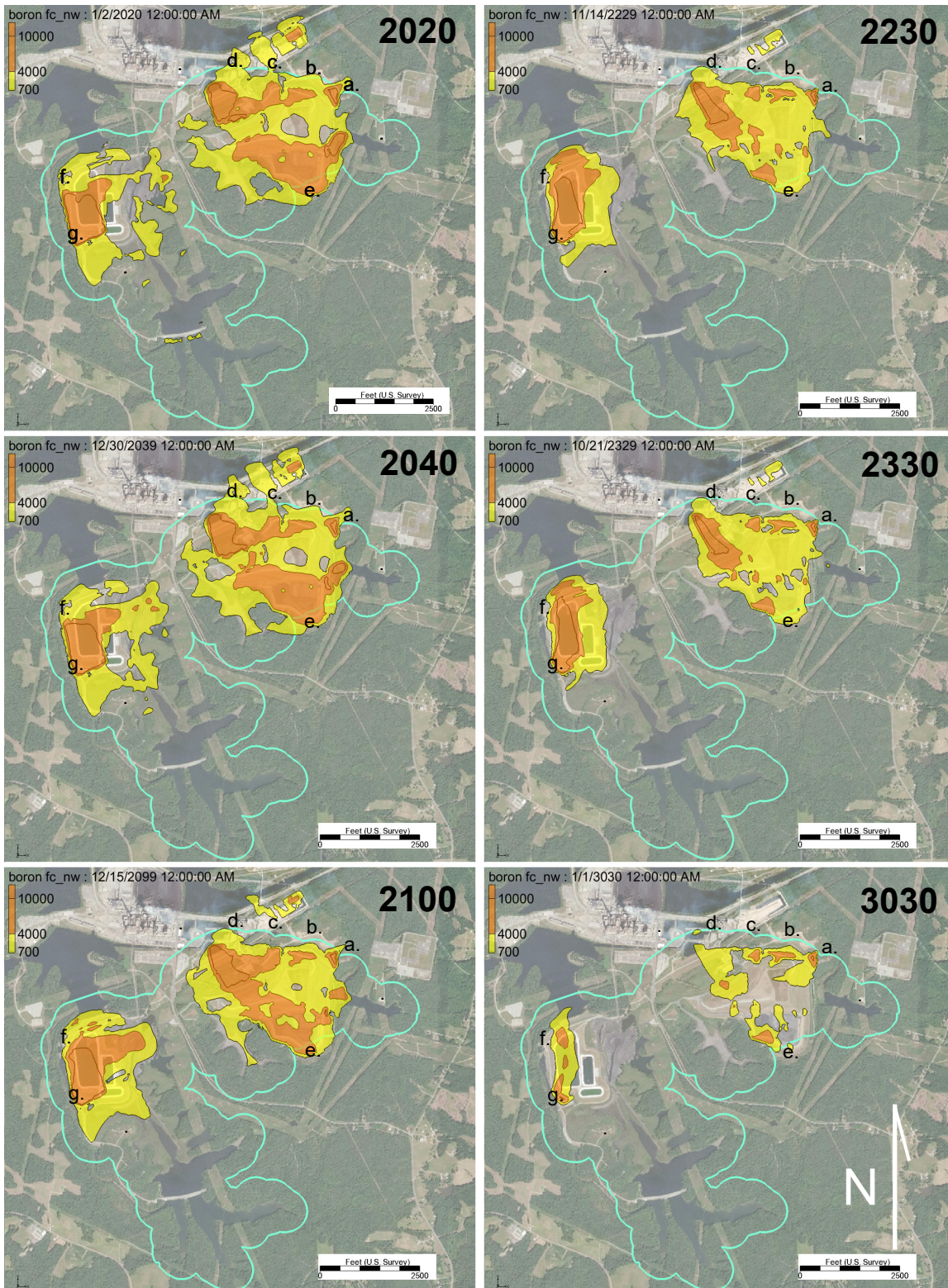


Figure 30. Distribution of boron concentrations ( $\mu\text{g/L}$ ) during the Final Cover scenario at representative times in the Transition Zone (layer 13). Persistent boron concentrations in EAB above the water table. Compliance boundary for the Final Cover scenario is the same as the existing 500-ft compliance boundary and is highlighted in light blue. Letters are reference locations. a.) northeast EAB; b.) north EAB; c.) gypsum storage area, EAB; d.) northwest EAB; e.) southeast EAB; f.) northwest WAB; g.) west WAB.

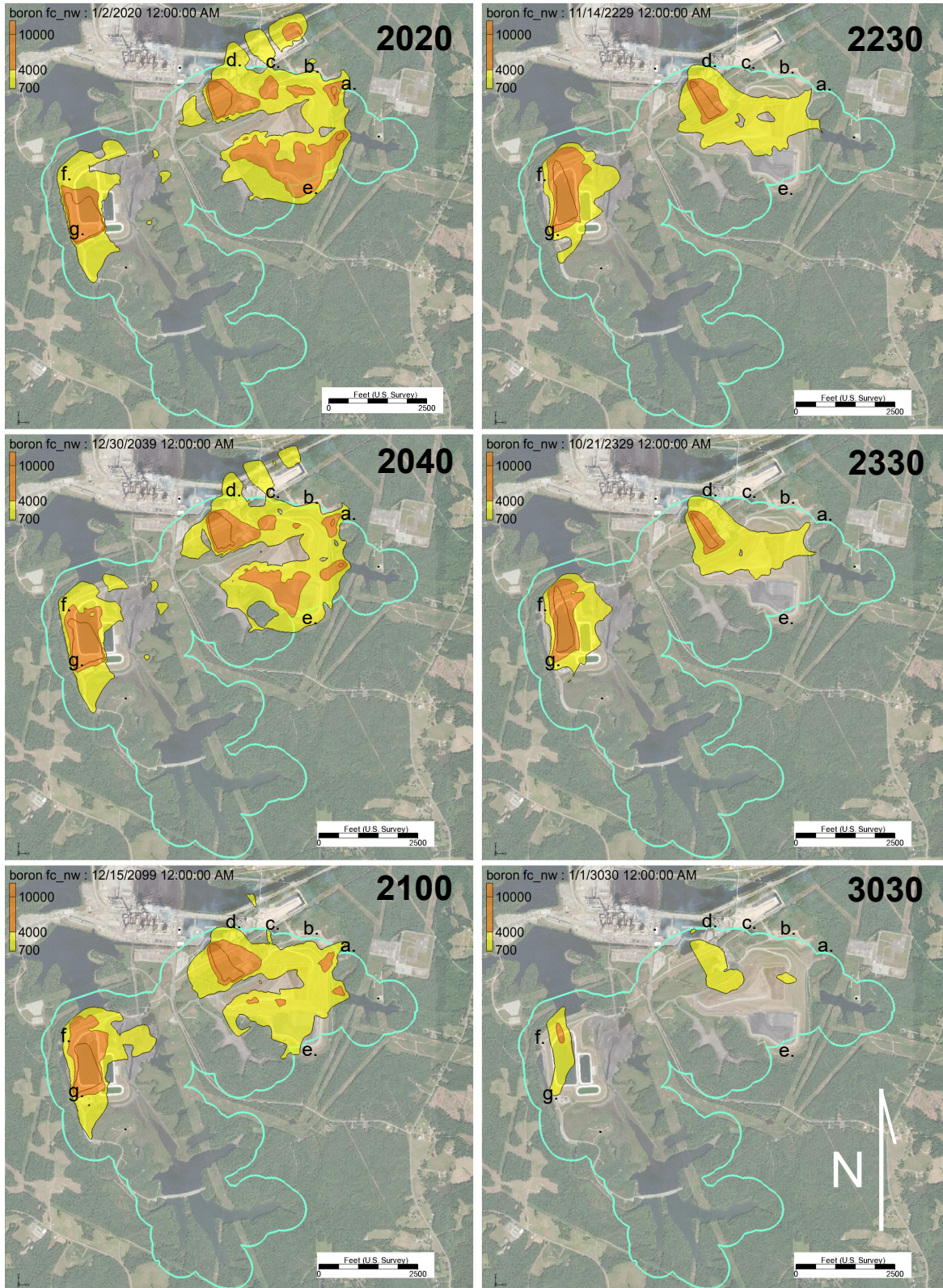


Figure 31. Distribution of boron concentrations ( $\mu\text{g/L}$ ) during the Final Cover scenario at representative times in the Shallow Rock Zone (layer 15). Compliance boundary for the Final Cover scenario is the same as the existing 500-ft compliance boundary and is highlighted in light blue. Letters are reference locations. a.) northeast EAB; b.) north EAB; c.) gypsum storage area, EAB; d.) northwest EAB; e.) southeast EAB; f.) northwest WAB; g.) west WAB.

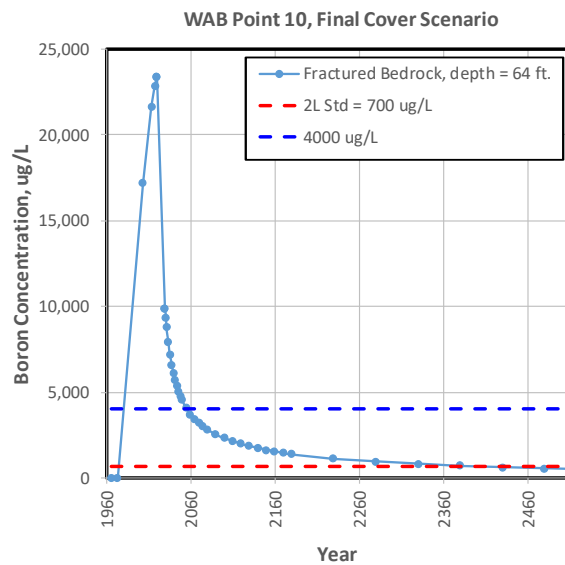
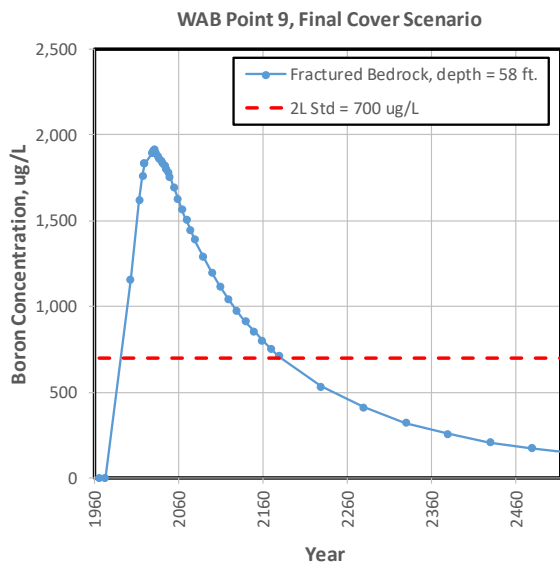
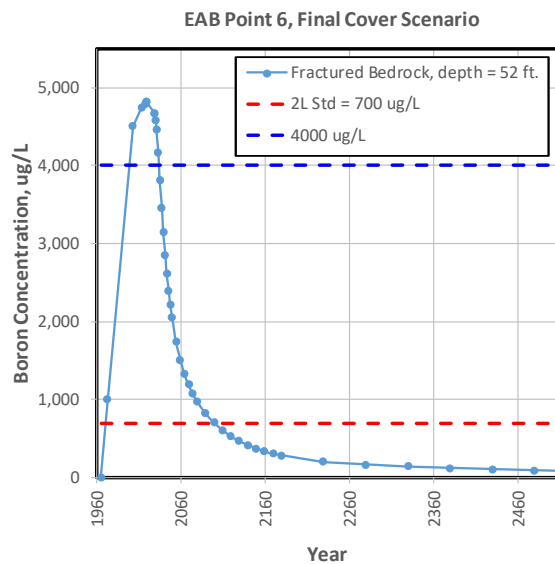
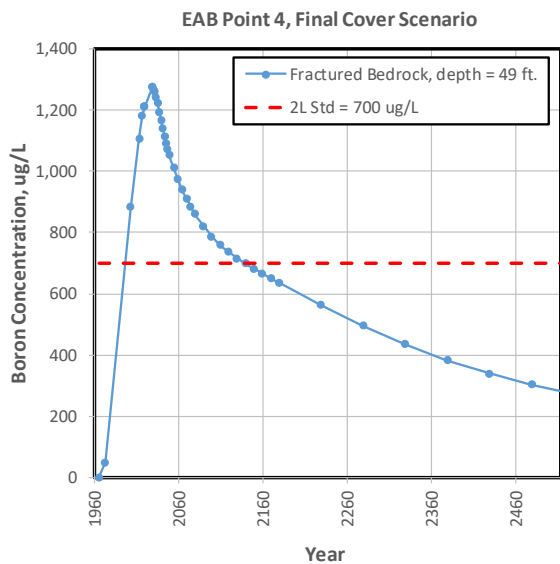
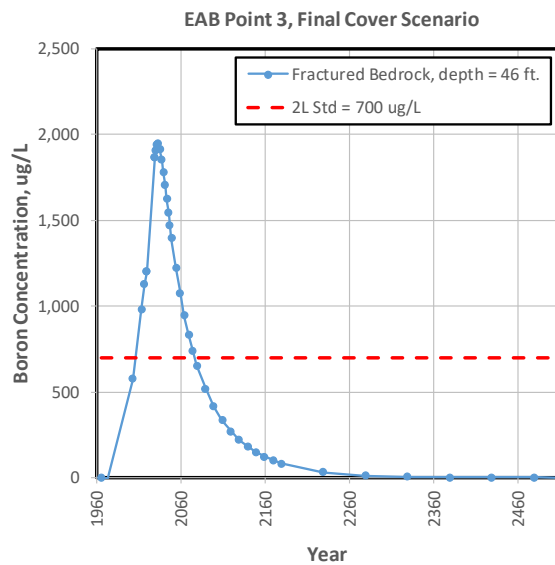
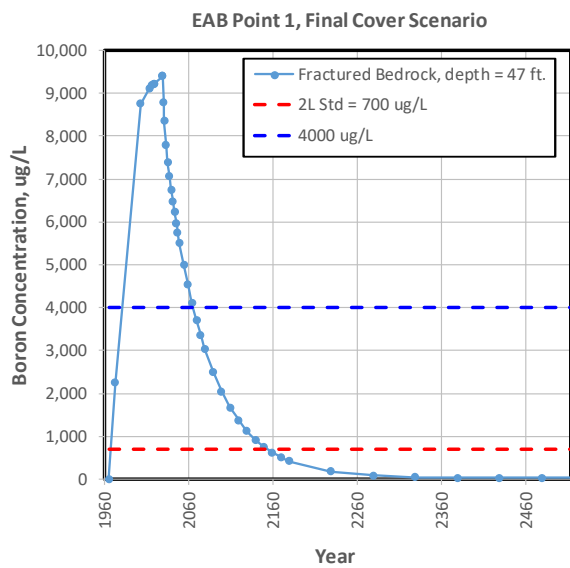


Figure 32. Times series of boron concentrations at six representative locations in the EAB and WAB during the Final Cover scenario.

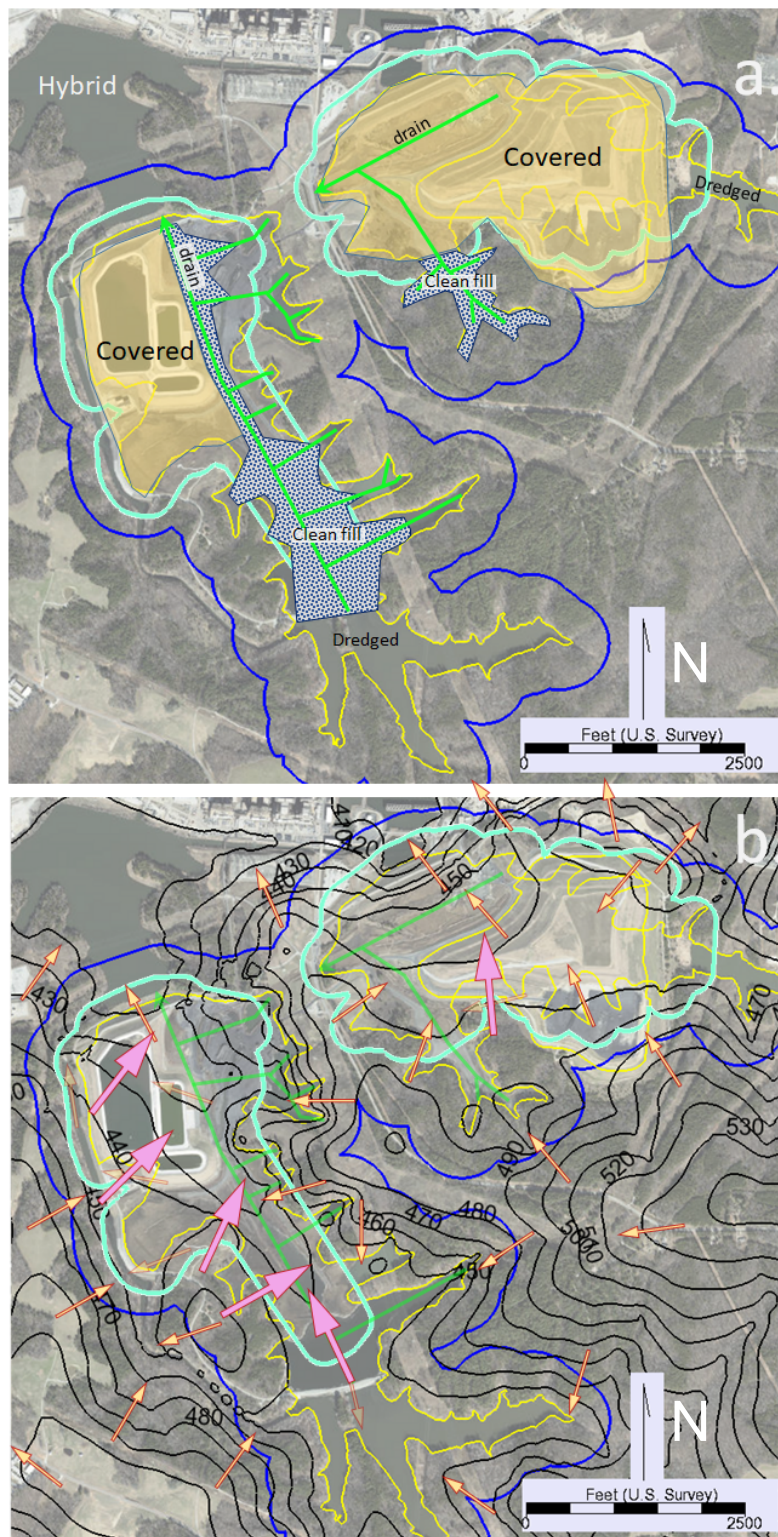


Figure 33. Configuration of features used to represent the Hybrid scenario in the model (a) and simulated hydraulic heads (b). a.) Yellow area is covered with low permeability cap, stippled area is where ash is excavated and replaced with clean fill, and green lines are re-swale drains beneath the cover and clean fill. Existing 500-ft compliance boundary shown as blue line, future 250-ft compliance boundary for the Hybrid scenario shown as light blue line, and waste boundary shown as yellow line. b.) Hydraulic head contours (feet above NAVD88) and flow directions for the Hybrid scenario. Pink arrows are flow directions that differ from current conditions, orange arrows are flow directions similar to current directions. Existing 500-ft compliance boundary shown as blue line, future 250-ft compliance boundary for the Hybrid scenario shown as light blue line, and waste boundary shown as yellow line.

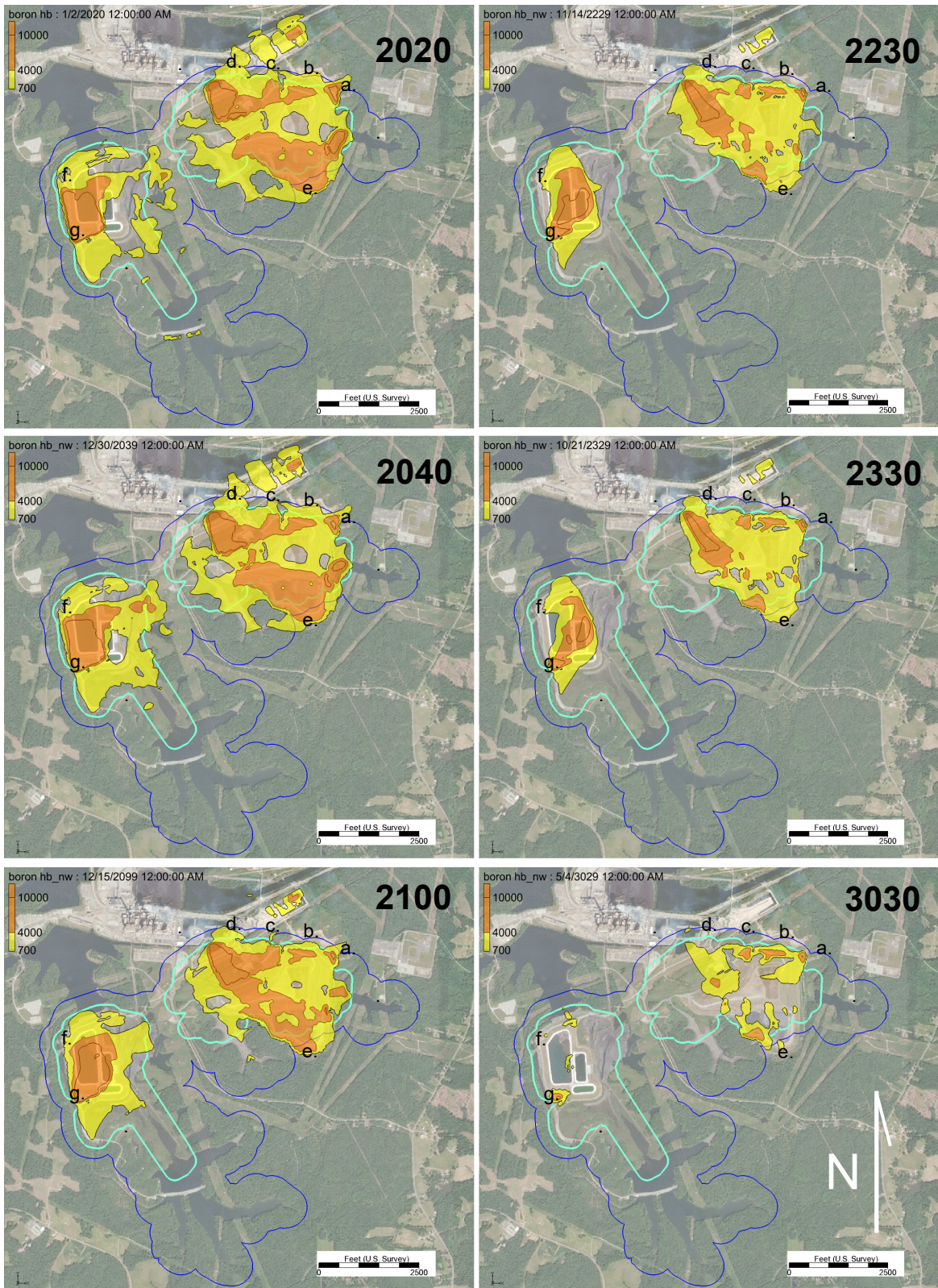


Figure 34. Distribution of boron concentrations ( $\mu\text{g/L}$ ) during the Hybrid scenario at representative times in the Transition Zone (layer 13). Persistent boron concentrations in the EAB are above the water table. Existing 500- ft compliance boundary shown as blue line, future 250-ft compliance boundary for the Hybrid scenario shown as light blue line. Letters are reference locations. a.) northeast EAB; b.) north EAB; c.) gypsum storage area, EAB; d.) northwest EAB; e.) southeast EAB; f.) northwest WAB; g.) west WAB.

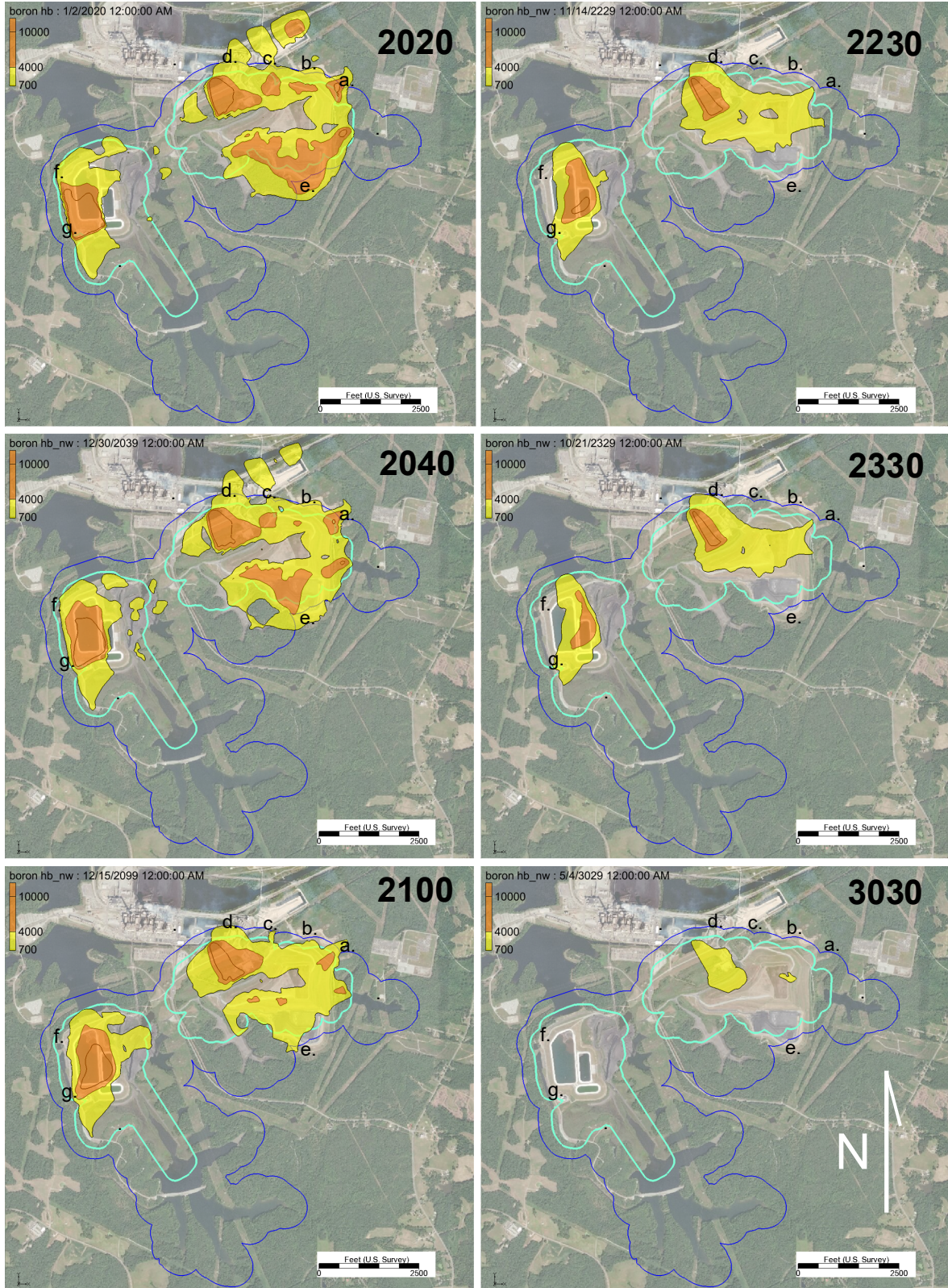


Figure 35. Distribution of boron concentrations ( $\mu\text{g/L}$ ) during the Hybrid scenario at representative times in the Shallow Rock Zone (layer 15). Existing 500-ft compliance boundary shown as blue line, future 250-ft compliance boundary for the Hybrid scenario shown as light blue line. Letters are reference locations. a.) northeast EAB; b.) north EAB; c.) gypsum storage area, EAB; d.) northwest EAB; e.) southeast EAB; f.) northwest WAB; g.) west WAB.

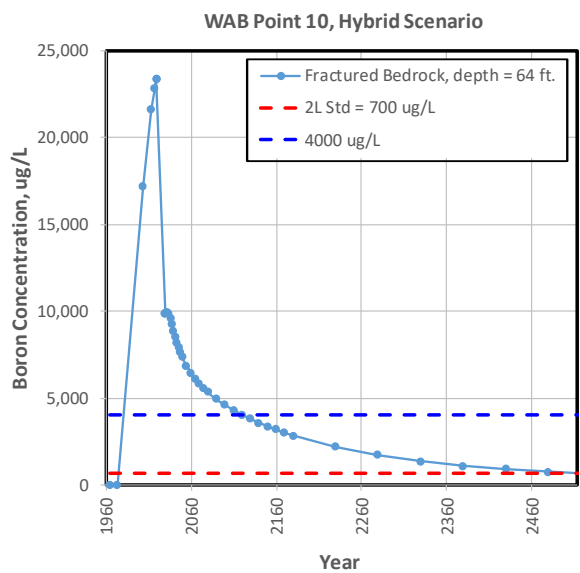
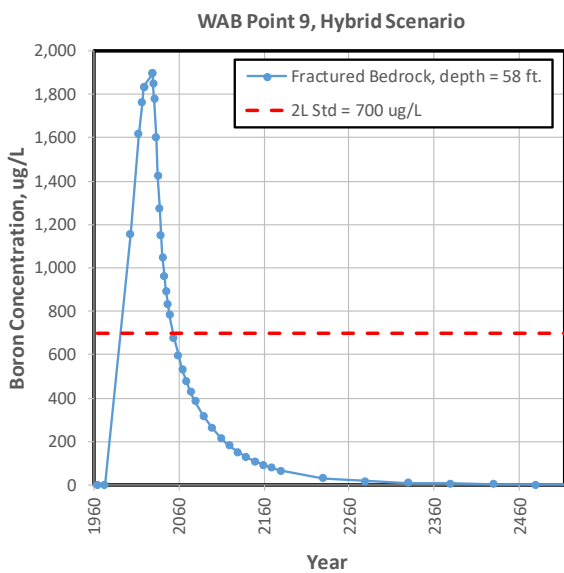
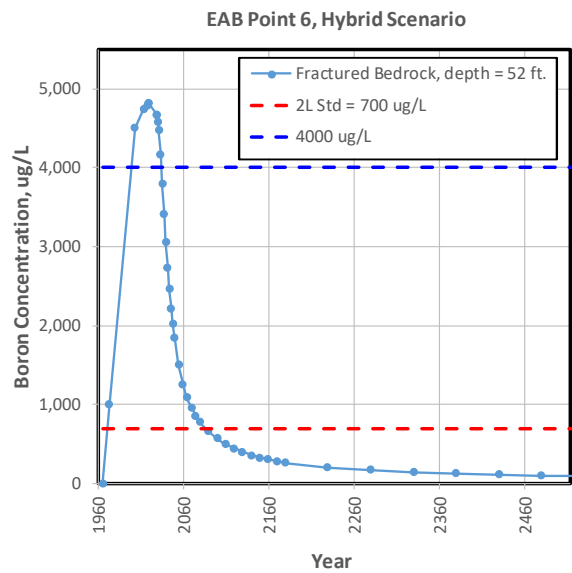
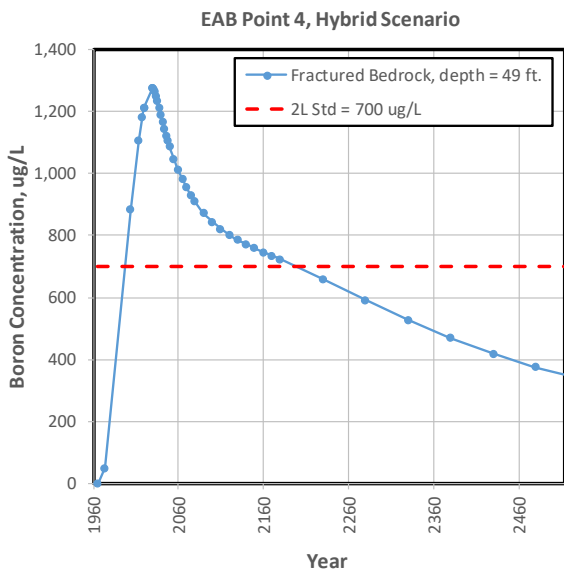
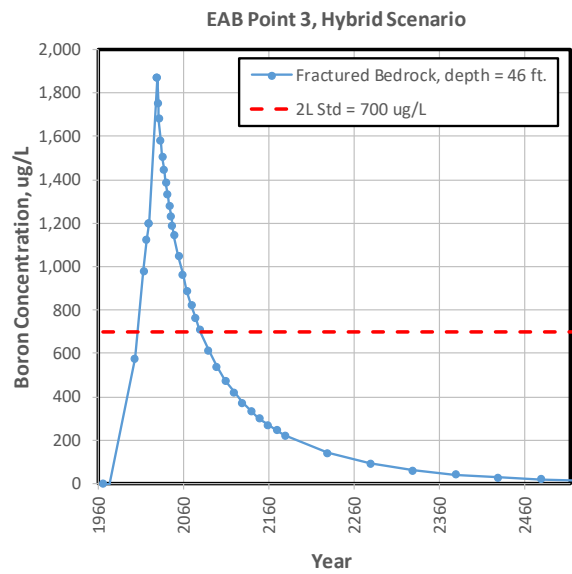
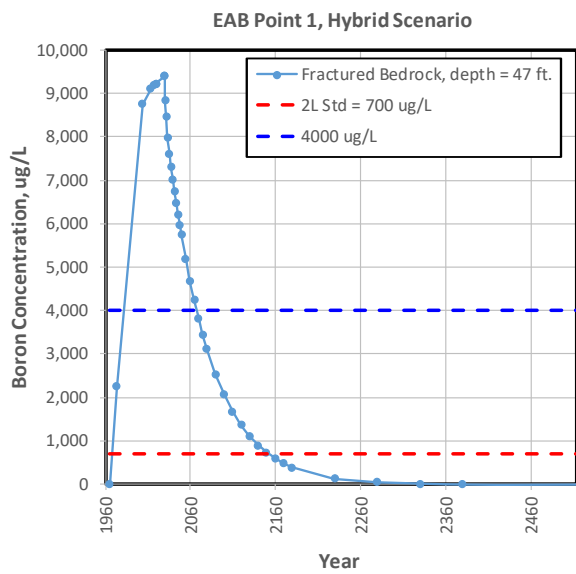


Figure 36. Times series of boron concentrations at six representative locations in the EAB and WAB during the Hybrid scenario.

Year 2240

Transition Zone (Layer 13)

Top of Bedrock (Layer 15)

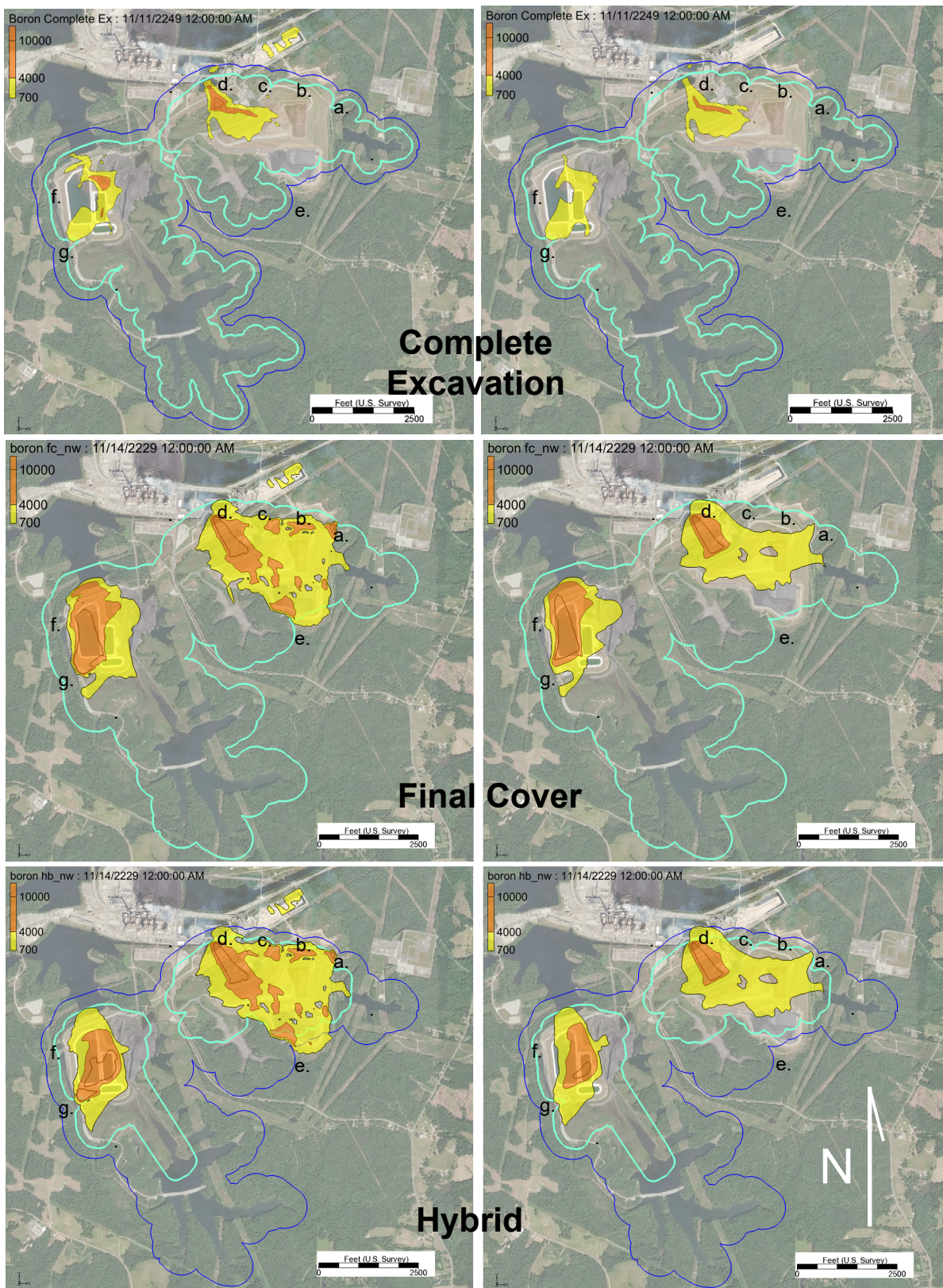


Figure 37. Comparison of simulated boron concentrations ( $\mu\text{g/L}$ ) in the Transition Zone (left) and in the top of bedrock (right) around year 2240 for the three closure scenarios. For the Complete Excavation scenario the existing 500-ft compliance boundary shown as line and future 250-ft compliance boundary shown as light blue line. For the Final Cover scenario the existing 500-ft compliance boundary shown as light blue line. For the Hybrid scenario the existing 500-ft compliance boundary shown as blue line and future 250-ft compliance boundary shown as light blue line. Letters are reference locations. a.) northeast EAB; b.) north EAB; c.) gypsum storage area, EAB; d.) northwest EAB; e.) southeast EAB; f.) northwest WAB; g.) west WAB.

# Year 3040

## Transition Zone (Layer 13)      Top of Bedrock (Layer 15)

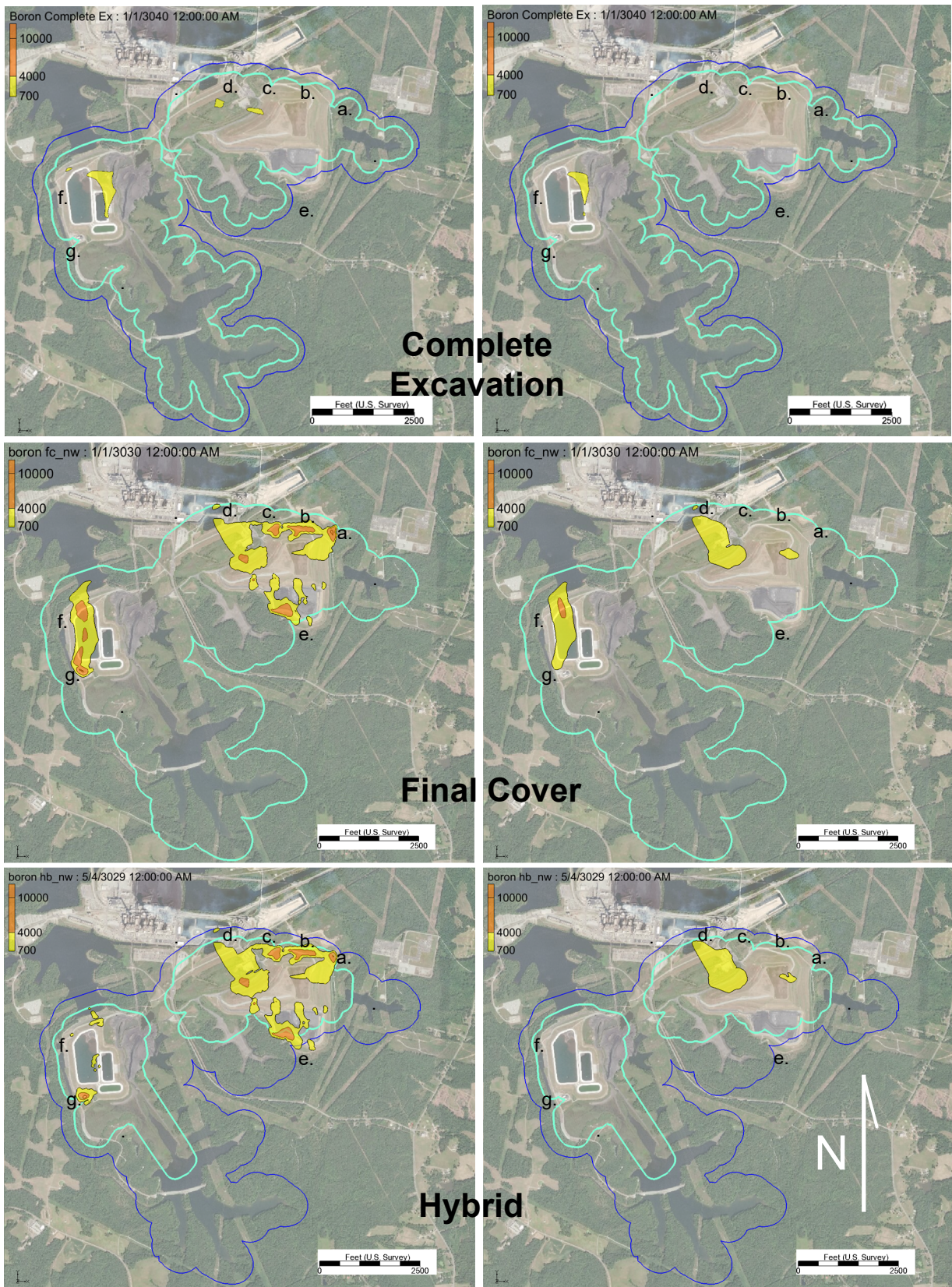


Figure 38. Comparison of simulated boron concentrations ( $\mu\text{g/L}$ ) in the Transition Zone (left) and in the top of bedrock (right) around year 3040 for the three closure scenarios. For the Complete Excavation scenario the existing 500- ft compliance boundary shown as blue line and future 250-ft compliance boundary shown as light blue line. For the Final Cover scenario the existing 500-ft compliance boundary shown as light blue line. For the Hybrid scenario the existing 500-ft compliance boundary shown as blue line and future 250-ft compliance boundary shown as light blue line. Letters are reference locations. a.) northeast EAB; b.) north EAB; c.) gypsum storage area, EAB; d.) northwest EAB; e.) southeast EAB; f.) northwest WAB; g.) west WAB.

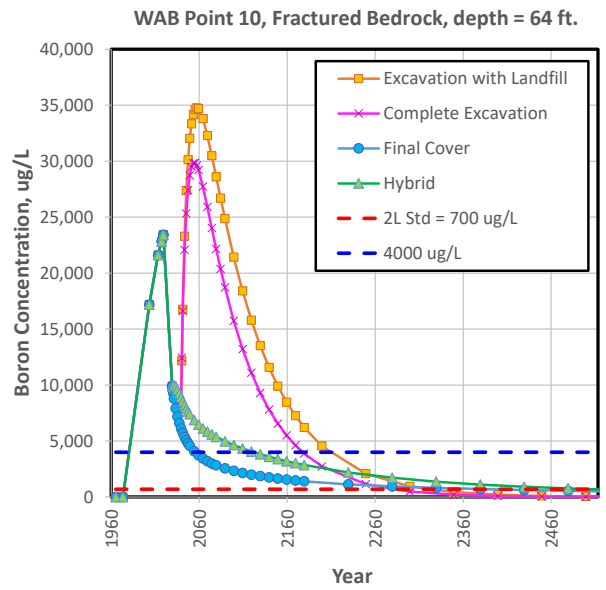
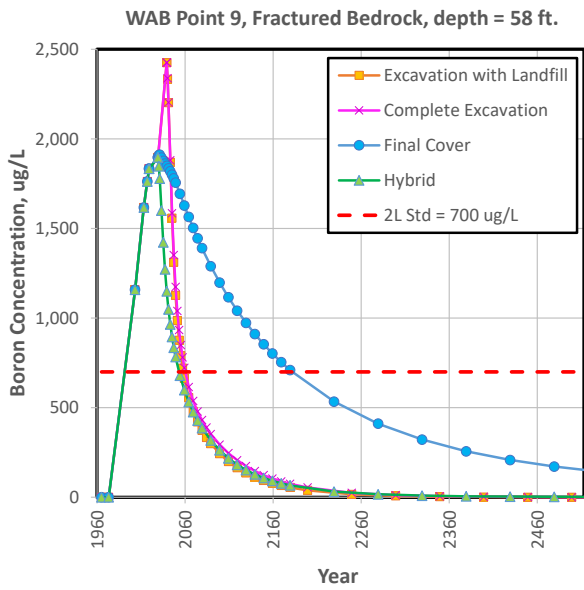
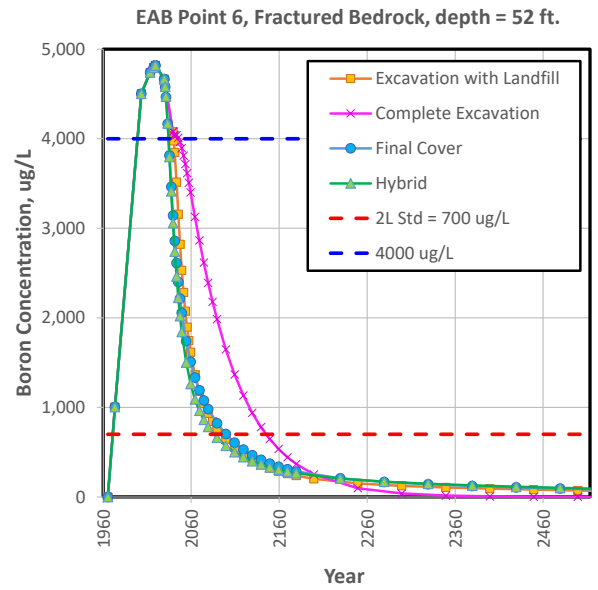
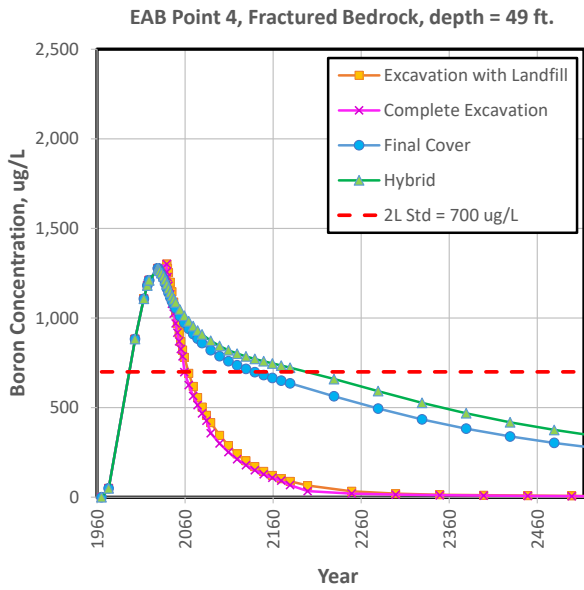
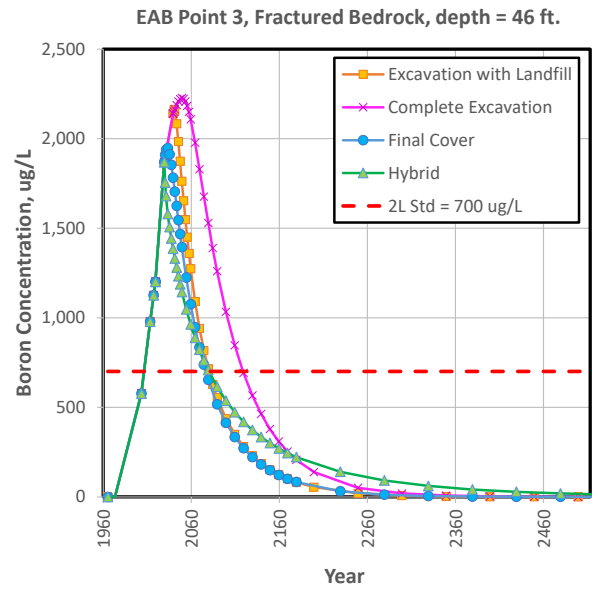
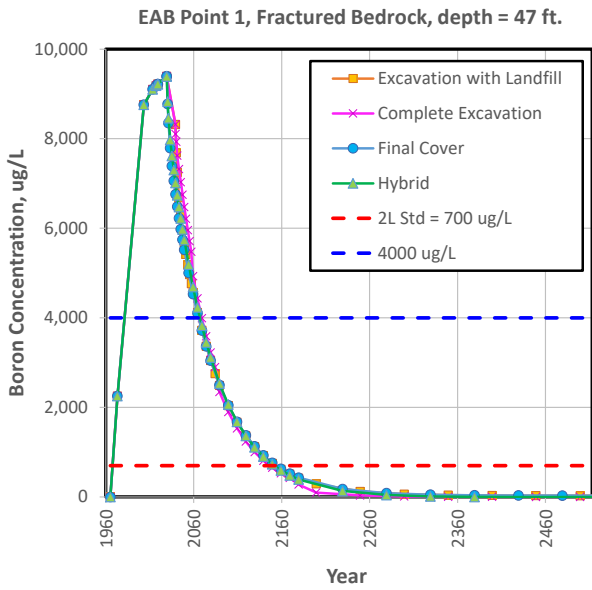
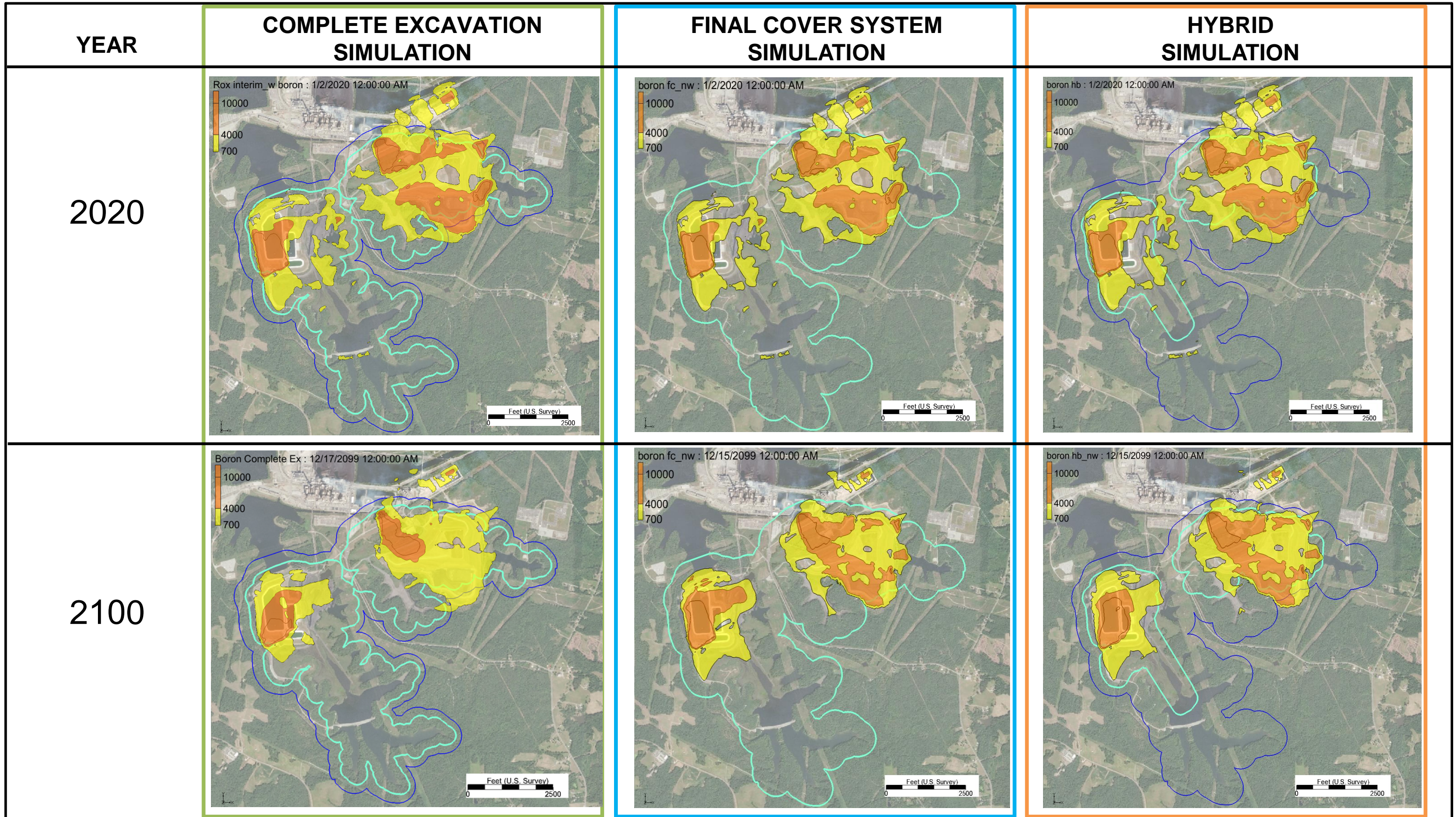


Figure 39. Comparison of boron time series at six representative locations in the EAB and WAB for the Excavation, Final Cover, and Hybrid scenarios.



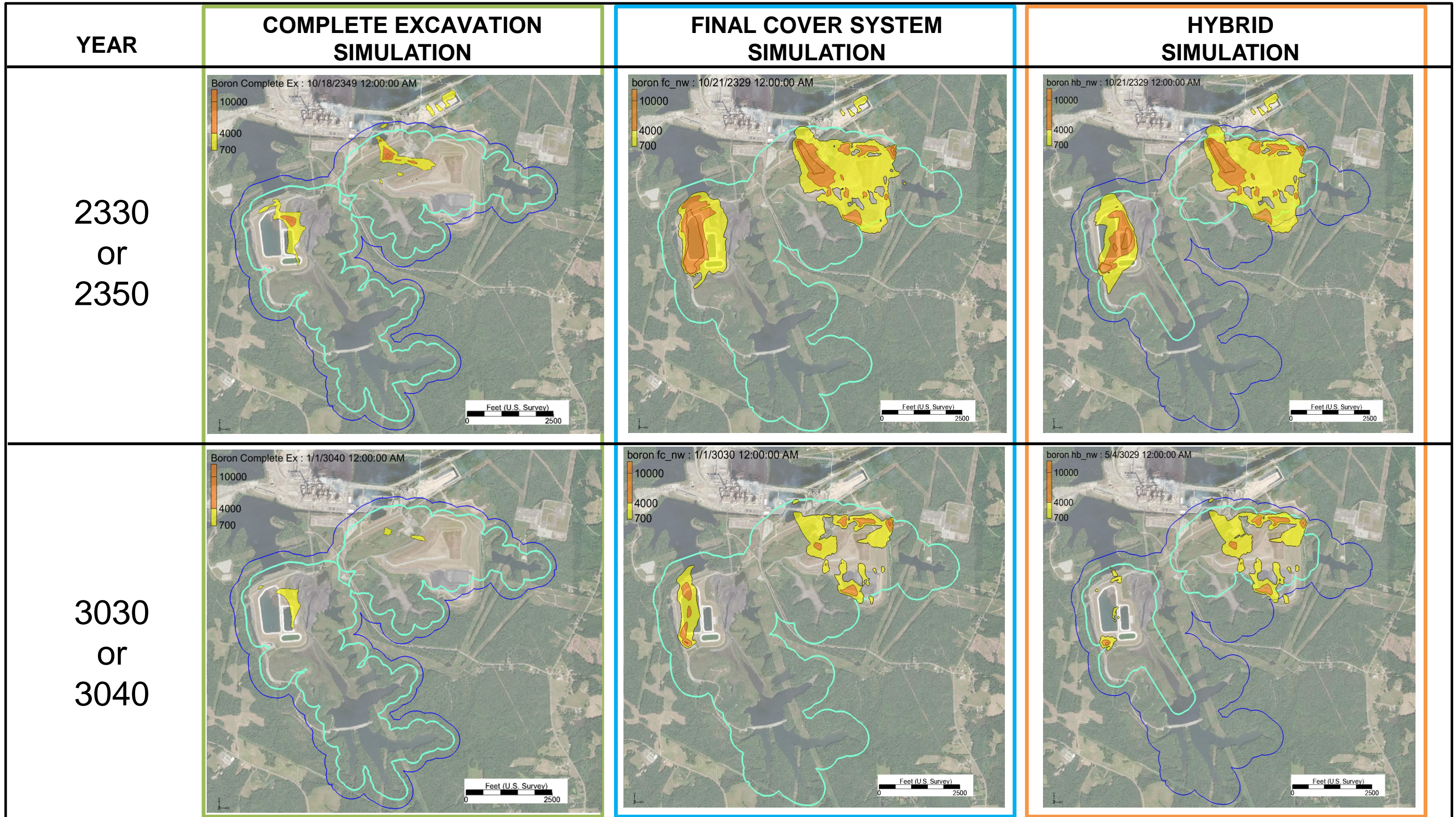
**NOTES:**

THE START DATES FOR THE THREE MODEL SCENARIOS ARE BASED ON THE COMPLETION DATES FOR THOSE ACTIVITIES. THESE DATES ARE:

- EXCAVATION – YEAR 2040
- FINAL COVER SYSTEM – YEAR 2030
- HYBRID – YEAR 2030

EXISTING COMPLIANCE BOUNDARY AS DARK BLUE LINE.  
 FUTURE COMPLIANCE BOUNDARY LIGHT BLUE LINE ASSOCIATED WITH BASIN CLOSURE OPTION.

**FIGURE 40**  
**COMPARISON OF CLOSURE OPTIONS FOR THE**  
**TRANSITION FLOW ZONE**  
**MODEL YEARS 2020 AND 2100**  
**ROXBORO STEAM ELECTRIC PLANT**  
**DUKE ENERGY PROGRESS, LLC**  
**SEMORA, NORTH CAROLINA**

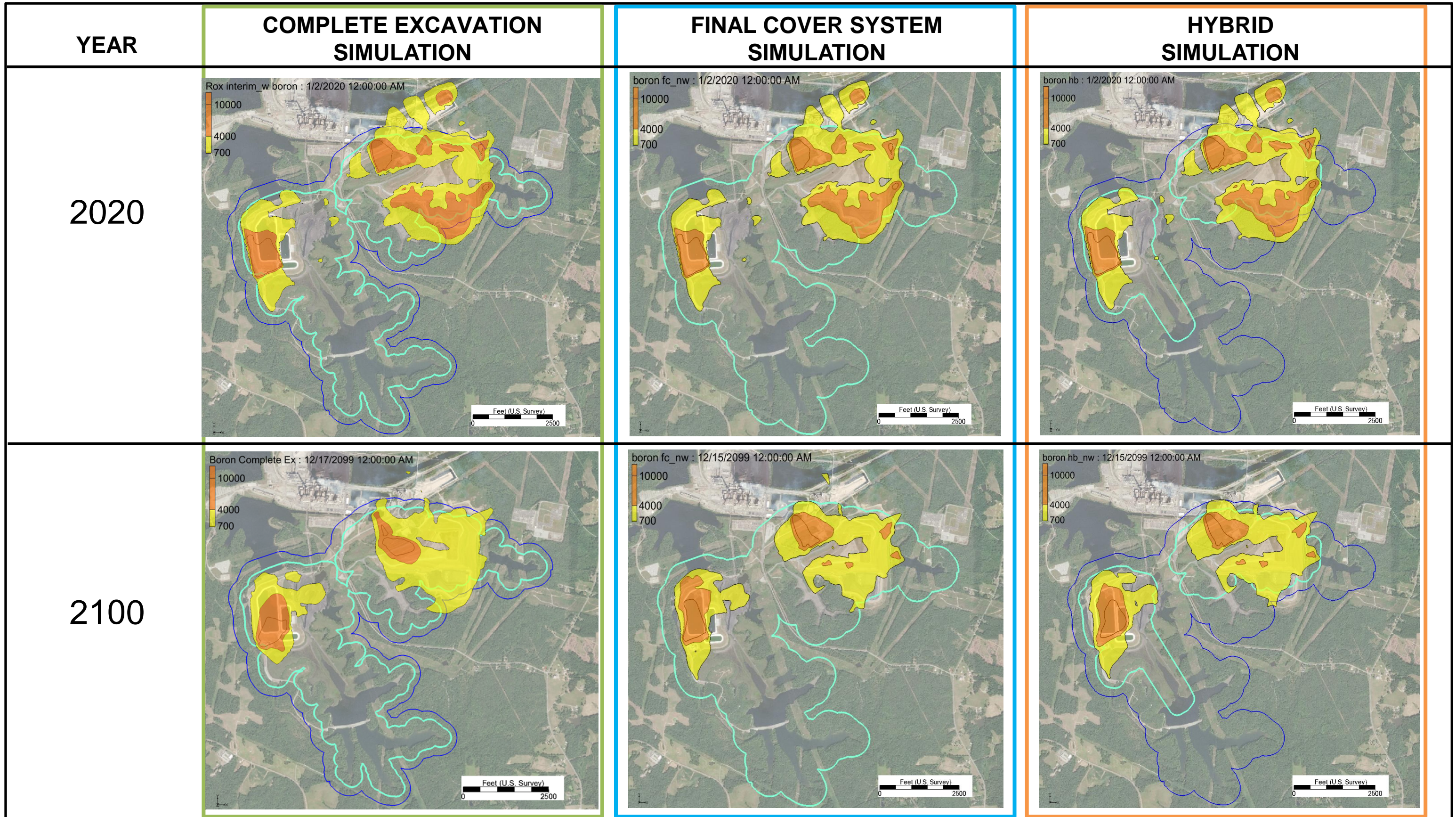


**NOTES:**  
THE START DATES FOR THE THREE MODEL SCENARIOS ARE BASED ON THE COMPLETION DATES FOR THOSE ACTIVITIES. THESE DATES ARE:

- EXCAVATION – YEAR 2040
- FINAL COVER SYSTEM – YEAR 2030
- HYBRID – YEAR 2030

EXISTING COMPLIANCE BOUNDARY AS DARK BLUE LINE.  
FUTURE COMPLIANCE BOUNDARY LIGHT BLUE LINE ASSOCIATED WITH BASIN CLOSURE OPTION.

**FIGURE 41**  
**COMPARISON OF CLOSURE OPTIONS FOR THE**  
**TRANSITION FLOW ZONE**  
**MODEL YEARS 2330/2350 AND 3030/3040**  
**ROXBORO STEAM ELECTRIC PLANT**  
**DUKE ENERGY PROGRESS, LLC**  
**SEMORA, NORTH CAROLINA**

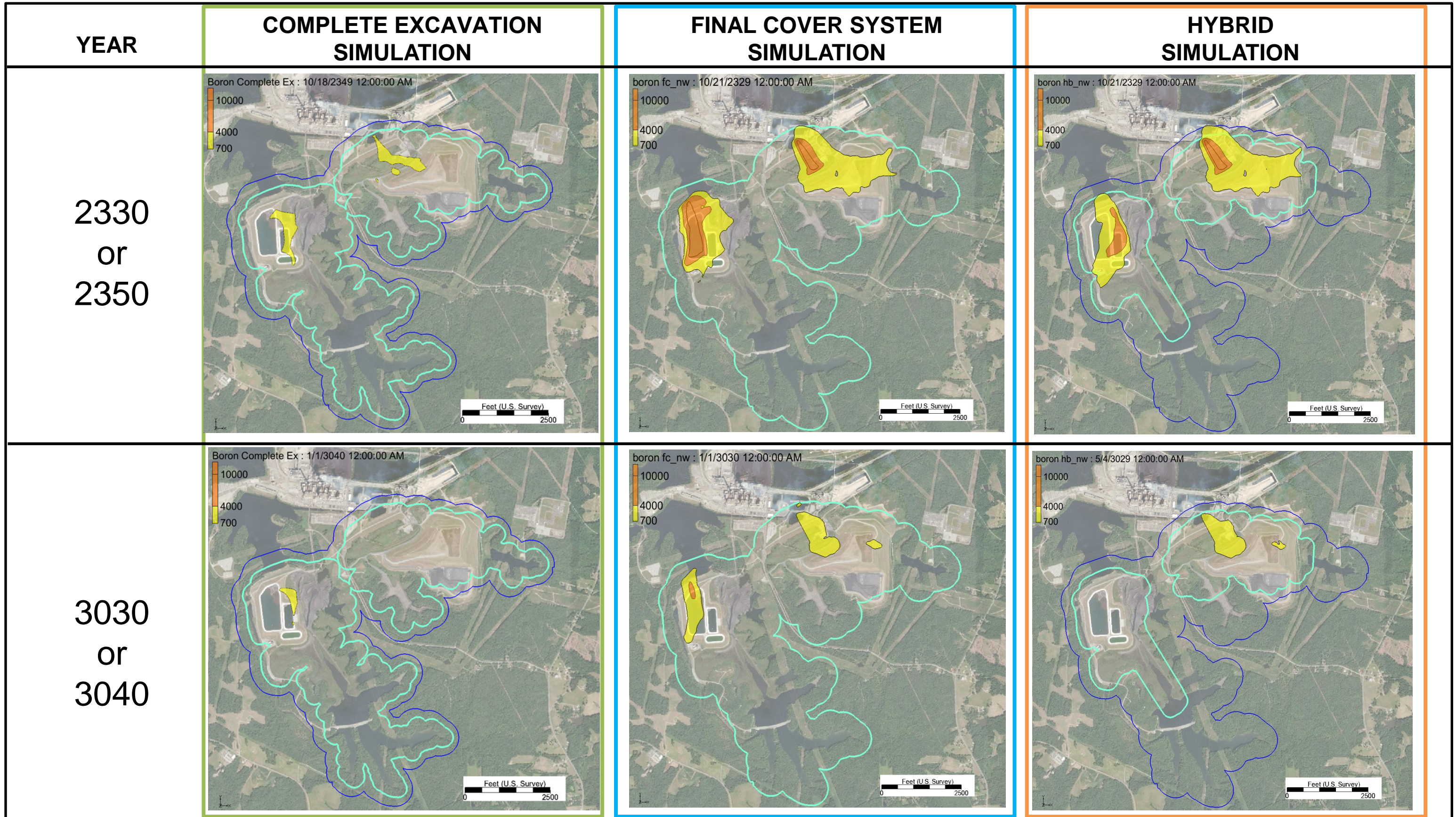


**NOTES:**  
 THE START DATES FOR THE THREE MODEL SCENARIOS ARE BASED ON THE COMPLETION DATES FOR THOSE ACTIVITIES. THESE DATES ARE:

- EXCAVATION – YEAR 2040
- FINAL COVER SYSTEM – YEAR 2030
- HYBRID – YEAR 2030

EXISTING COMPLIANCE BOUNDARY AS DARK BLUE LINE.  
 FUTURE COMPLIANCE BOUNDARY LIGHT BLUE LINE ASSOCIATED WITH BASIN CLOSURE OPTION.

**FIGURE 42**  
**COMPARISON OF CLOSURE OPTIONS FOR THE**  
**UPPER BEDROCK FLOW ZONE**  
**MODEL YEARS 2020 AND 2100**  
**ROXBORO STEAM ELECTRIC PLANT**  
**DUKE ENERGY PROGRESS, LLC**  
**SEMORA, NORTH CAROLINA**



**NOTES:**

THE START DATES FOR THE THREE MODEL SCENARIOS ARE BASED ON THE COMPLETION DATES FOR THOSE ACTIVITIES. THESE DATES ARE:

- EXCAVATION – YEAR 2040
- FINAL COVER SYSTEM – YEAR 2030
- HYBRID – YEAR 2030

EXISTING COMPLIANCE BOUNDARY AS DARK BLUE LINE.  
FUTURE COMPLIANCE BOUNDARY LIGHT BLUE LINE ASSOCIATED WITH BASIN CLOSURE OPTION.

**FIGURE 43**  
**COMPARISON OF CLOSURE OPTIONS FOR THE**  
**UPPER BEDROCK FLOW ZONE**  
**MODEL YEARS 2330/2350 AND 3030/3040**  
**MAYO STEAM ELECTRIC PLANT**  
**DUKE ENERGY PROGRESS, LLC**  
**ROXBORO, NORTH CAROLINA**